

ACC/AHA PRACTICE GUIDELINES—FULL TEXT

ACC/AHA/ASNC Guidelines for the Clinical Use of Cardiac Radionuclide Imaging

A Report of the American College of Cardiology/American Heart Association Task Force on Practice Guidelines (ACC/AHA/ASNC Committee to Revise the 1995 Guidelines for the Clinical Use of Cardiac Radionuclide Imaging)

COMMITTEE MEMBERS

Francis J. Klocke, MD, MACC, FAHA, *Chair*

Michael G. Baird, MD, FACC, FAHA

Timothy M. Bateman, MD, FACC, FAHA

Daniel S. Berman, MD, FACC, FAHA

Blase A. Carabello, MD, FACC, FAHA

Manuel D. Cerqueira, MD, FACC, FAHA

Anthony N. DeMaria, MD, MACC, FAHA

J. Ward Kennedy, MD, MACC, FAHA

Beverly H. Lorell, MD, FACC, FAHA

Joseph V. Messer, MD, MACC, FAHA

Patrick T. O’Gara, MD, FACC, FAHA

Richard O. Russell, Jr., MD, FACC

Martin G. St. John Sutton, MBBS, FACC

James E. Udelson, MD, FACC

Mario S. Verani, MD, FACC*

Kim Allan Williams, MD, FACC, FAHA

TASK FORCE MEMBERS

Elliott M. Antman, MD, FACC, FAHA, *Chair*

Sidney C. Smith, Jr., MD, FACC, FAHA, *Vice Chair*

Joseph S. Alpert, MD, FACC, FAHA

Gabriel Gregoratos, MD, FACC, FAHA

Jeffrey L. Anderson, MD, FACC

David P. Faxon, MD, FACC, FAHA

Valentin Fuster, MD, PhD, FACC, FAHA

Raymond J. Gibbons, MD, FACC, FAHA†**

Loren F. Hiratzka, MD, FACC, FAHA

Sharon Ann Hunt, MD, FACC, FAHA

Alice K. Jacobs, MD, FACC, FAHA

Richard O. Russell, MD, FACC, FAHA**

*Deceased

**Former Task Force Member

†Former Task Force Chair

ber): Up to 999 copies, call 1-800-611-6083 (US only) or fax 413-665-2671; 1000 or more copies, call 214-706-1466, fax 214-691-6342, or e-mail pub-auth@heart.org.

This document was approved by the American College of Cardiology Foundation Board of Trustees in July 2003, the American Heart Association Science Advisory and Coordinating Committee in July 2003, and the American Society of Nuclear Cardiology Board of Directors in July 2003.

When citing this document, the American College of Cardiology Foundation, the American Heart Association, and the American Society of Nuclear Cardiology request that the following citation format be used: Klocke FJ, Baird MG, Bateman TM, Berman DS, Carabello BA, Cerqueira MD, DeMaria AN, Kennedy JW, Lorell BH, Messer JV, O’Gara PT, Russell RO Jr., St. John Sutton MG, Udelson JE, Verani MS, Williams KA. ACC/AHA/ASNC guidelines for the clinical use of cardiac radionuclide imaging: a report of the American College of Cardiology/American Heart Association Task Force on Practice Guidelines (ACC/AHA/ASNC Committee to Revise the 1995 Guidelines for the Clinical Use of Radionuclide Imaging). (2003). American College of Cardiology Web Site. Available at: http://www.acc.org/clinical/guidelines/radio/rni_fulltext.pdf.

This document is available on the World Wide Web sites of the American College of Cardiology (www.acc.org), the American Heart Association (www.americanheart.org), and the American Society of Nuclear Cardiology (www.asnc.org). Single copies of this document are available by calling 1-800-253-4636 or writing the American College of Cardiology Foundation, Resource Center, at 9111 Old Georgetown Road, Bethesda, MD 20814-1699. Ask for reprint number 71-0266. To obtain a reprint of the Executive Summary published in the October 1, 2003 issue of the *Journal of the American College of Cardiology* and the September 16, 2003 issue of *Circulation*, ask for reprint number 71-0265. To purchase bulk reprints (specify version and reprint num-

TABLE OF CONTENTS

Preamble	2
I. Introduction.....	3
II. Acute Syndromes.....	4
A. Myocardial Perfusion Imaging in the Assessment of Patients Presenting With Chest Pain to the Emergency Department.....	4
B. Detection of AMI When Conventional Measures Are Nondiagnostic.....	6
1. “Hot Spot” Infarct Imaging.....	6
2. Acute Rest Myocardial Perfusion Imaging.....	7
C. Radionuclide Testing in Risk Assessment: Prognosis and Assessment of Therapy After STEMI... 7	
D. Radionuclide Testing in Risk Assessment: Prognosis and Assessment of Therapy After NSTEMI or UA.....	8
III. Chronic Syndromes.....	9
A. Detection (Diagnosis) of CAD.....	9
1. Sensitivity and Specificity.....	9

2. Effect of Referral Bias.....	11	Vasculopathy.....	35
3. Quantitative Analysis.....	12	5. Chagas Myocarditis and/or Cardiomyopathy.....	36
4. ECG-Gated SPECT.....	12	6. Sarcoid Heart Disease.....	36
5. Attenuation Correction.....	13	7. Cardiac Amyloidosis.....	36
6. Positron Emission Tomography.....	14	8. RV Dysplasia.....	36
B. Management of Patients With Known or Suspected Chronic CAD: Assessment of Disease Severity, Risk Stratification, and Prognosis.....	14	9. Hypertrophic Cardiomyopathy.....	37
1. Nongated MPI.....	15	10. Hypertensive Heart Disease.....	37
2. Gated SPECT.....	18	11. Valvular Heart Disease.....	38
3. Radionuclide Angiography.....	18	12. Adults With Congenital Heart Disease.....	40
4. Cost Effectiveness.....	18	Appendix 1: Procedures and Principles.....	40
5. Frequency of Testing.....	19	A. Introduction to Nuclear Cardiology.....	40
6. Evaluation of the Effects of Medical Therapy.....	19	B. Nuclear Cardiology Instrumentation.....	40
C. Specific Patient Populations.....	19	C. Radiopharmaceuticals.....	41
1. African Americans.....	19	1. Single-Photon MPI.....	41
2. Women.....	19	2. Positron Emission Tomography.....	41
3. Normal Resting ECG, Able to Exercise.....	19	3. First-Pass RNA.....	42
4. Intermediate-Risk Duke Treadmill Score.....	20	4. Gated-Equilibrium RNA.....	42
5. Normal Resting ECG, Unable to Exercise.....	20	D. Image Acquisition, Analysis, and Display.....	42
6. LBBB/Pacemakers.....	20	1. SPECT MPI.....	42
7. Left Ventricular Hypertrophy.....	21	2. Planar MPI.....	42
8. Patients With Nonspecific ST-T Wave Changes.....	21	3. PET Perfusion Imaging.....	43
9. Elderly.....	21	4. First-Pass RNA.....	43
10. Asymptomatic Patients.....	21	5. ECG-Gated Planar Equilibrium Blood Pool RNA.....	43
11. Obese Patients.....	22	6. ECG-Gated Tomographic Equilibrium Blood Pool Imaging.....	43
12. Diabetes.....	22	E. Quality Assurance, Artifact Detection, and Correction.....	44
13. After Coronary Calcium Screening.....	22	1. Quality Control.....	44
14. Before and After Revascularization.....	22	2. Attenuation Correction.....	45
15. Radionuclide Imaging Before Noncardiac Surgery.....	23	3. Motion Correction and Depth-Dependent Blurring.....	45
D. Recommendations: Cardiac Stress Myocardial Perfusion SPECT in Patients Able to Exercise.....	24	F. Clinical Procedures.....	45
E. Recommendations: Cardiac Stress Myocardial Perfusion SPECT in Patients Unable to Exercise.....	26	1. Myocardial Perfusion Imaging.....	45
F. Recommendations: Cardiac Stress Myocardial Perfusion PET.....	26	2. Analysis of Ventricular Function.....	50
G. Recommendations: Cardiac Stress Perfusion Imaging Before Noncardiac Surgery.....	27	3. Myocardial Infarct-Avid Imaging.....	51
IV. Heart Failure.....	28	4. Myocardial Ischemia Imaging.....	52
A. Assessment of LV Systolic Dysfunction.....	28	5. Positron Emission Tomography.....	52
B. Assessment of LV Diastolic Dysfunction.....	28	Appendix 2: Abbreviations.....	53
C. Assessment of CAD.....	29	References.....	53
1. Importance of Detecting CAD in Heart Failure Patients.....	29	PREAMBLE	
2. MPI to Detect CAD in Heart Failure Patients.....	29	It is important that the medical profession play a significant role in critically evaluating the use of diagnostic procedures and therapies in the management or prevention of disease states. Rigorous and expert analysis of the available data documenting relative benefits and risks of those procedures and therapies can produce helpful guidelines that improve the effectiveness of care, optimize patient outcomes, and impact the overall cost of care favorably by focusing resources on the most effective strategies.	
D. Assessment of Myocardial Viability.....	29	The American College of Cardiology (ACC) and the American Heart Association (AHA) have jointly engaged in the production of such guidelines in the area of cardiovas- cular disease since 1980. This effort is directed by the ACC/AHA Task Force on Practice Guidelines, whose charge is to develop and revise practice guidelines for important cardiovascular diseases and procedures. Experts in the sub- ject under consideration are selected from both organiza-	
1. Goals of Assessing Myocardial Viability.....	29		
2. General Principles of Assessing Myocardial Viability by Radionuclide Techniques.....	30		
3. Techniques and Protocols for Assessing Myocardial Viability.....	31		
4. Image Interpretation for Myocardial Viability: Quantitative Versus Visual Analysis of Tracer Activities.....	32		
5. Comparison of Techniques.....	33		
E. Etiologies of Heart Failure.....	33		
1. Dilated Cardiomyopathy.....	33		
2. Dilated Cardiomyopathy due to Doxorubicin/ Anthracycline Cardiotoxicity.....	34		
3. Dilated Cardiomyopathy due to Myocarditis.....	35		
4. Posttransplant Rejection and Allograft			

tions to examine subject-specific data and write guidelines. The process includes additional representatives from other medical practitioner and specialty groups when appropriate. Writing groups are specifically charged to perform a formal literature review, weigh the strength of evidence for or against a particular treatment or procedure, and include estimates of expected health outcomes when data exist. Patient-specific modifiers, comorbidities and issues of patient preference that might influence the choice of particular tests or therapies are considered as well as frequency of follow-up and cost effectiveness.

These practice guidelines are intended to assist physicians and other qualified healthcare professionals in clinical decision making by describing a range of generally acceptable approaches for the diagnosis, management, or prevention of specific diseases or conditions. These guidelines attempt to define practices that meet the needs of most patients in most circumstances. The ultimate judgment regarding care of a particular patient must be made by the physician and patient in light of all of the circumstances presented by that patient.

The ACC/AHA Task Force on Practice Guidelines makes every effort to avoid any actual or potential conflicts of interest that might arise as a result of an outside relationship or personal interest of a member of the writing panel. Specifically, all members of the writing panel are asked to provide disclosure statements of all such relationships that might be perceived as real or potential conflicts of interest. These statements are reviewed by the parent task force, reported orally to all members of the writing panel at the first meeting, and updated as changes occur.

Elliott M. Antman, MD, FACC, FAHA
Chair, ACC/AHA Task Force on Practice Guidelines

Sidney C. Smith, Jr., MD, FACC, FAHA
Vice-Chair, ACC/AHA Task Force on Practice Guidelines

I. INTRODUCTION

The ACC/AHA Task Force on Practice Guidelines was formed to make recommendations regarding the appropriate use of testing and technology in the diagnosis and treatment of patients with known or suspected cardiovascular disease. Cardiac radionuclide imaging (nuclear cardiology) is one such important technology.

Guidelines for the Clinical Use of Cardiac Radionuclide Imaging were originally published in 1986 and updated in 1995. Important new developments have continued to occur since 1995, particularly in the areas of acute and chronic ischemic syndromes and heart failure. The Task Force therefore believed the topic should be revisited de novo and invited the American Society for Nuclear Cardiology (ASNC) to cosponsor this undertaking. This report represents a joint effort of the three organizations. The committee that prepared it included acknowledged experts in radionuclide testing, as well as general cardiologists and cardiologists with expertise in other imaging modalities. Committee members

were drawn from both the academic and private practice sectors, with the three sponsoring organizations equally represented.

This document was reviewed by 3 official reviewers nominated by the ACCF, 3 official reviewers nominated by the AHA, 3 official reviewers nominated by the ASNC, the ACC/AHA Task Force on Practice Guidelines, and four additional content reviewers.

The ACC/AHA classifications I, II, and III are used to summarize indications as follows:

Class I: Conditions for which there is evidence and/or general agreement that a given procedure or treatment is useful and effective.

Class II: Conditions for which there is conflicting evidence and/or a divergence of opinion about the usefulness/efficacy of a procedure or treatment.

Class IIa: Weight of evidence/opinion is in favor of usefulness/efficacy.

Class IIb: Usefulness/efficacy is less well established by evidence/opinion.

Class III: Conditions for which there is evidence and/or general agreement that the procedure/treatment is not useful/effective and in some cases may be harmful.

Levels of evidence for individual class assignments are designated as:

- A** = Data derived from multiple randomized clinical trials
- B** = Data derived from a single randomized trial, or from nonrandomized studies
- C** = Consensus opinion of experts

Techniques considered investigational are not further classified.

In considering the use of a specific technique in individual patients, the following factors are important

1. the quality of the available laboratory and equipment used for performing the study and the quality, expertise, and experience of the professional and technical staff performing and interpreting the study
2. the sensitivity, specificity, and predictive accuracy of the technique
3. the cost and accuracy of the technique compared with that of other diagnostic procedures
4. the effect of positive or negative results on subsequent clinical decision making

The present report discusses the usefulness of nuclear cardiological techniques in three broad areas: acute ischemic syndromes, chronic syndromes, and heart failure. Utility is considered for diagnosis, severity of disease/risk assess-

ment/prognosis, and assessment of therapy. Recommendations are summarized within each section. An appendix provides detailed descriptions of the individual nuclear cardiological techniques covered in this report.

The committee conducted comprehensive searching of the scientific and medical literature on radionuclide imaging in heart disease. Because this guideline represents a full revision, no time constraints were applied to the searches and all relevant references were reviewed. In addition to broad-based searching on radionuclide imaging, specific targeted searches were performed on radionuclide imaging and the following subtopics: chest pain, viability, ejection fraction (EF), hypertensive heart failure, hypertrophic heart failure, electron-beam computed tomography (EBCT), adenosine, technetium-99m (Tc-99m), antimyosin, dipyridamole, glucarate, risk stratification, prognosis, non-Q-wave infarction, gamma-camera imaging, positron emission tomography (PET), acute myocardial infarction (AMI), heart failure, ischemia, ventricular volumes, left ventricular (LV) function, and angina. The committee reviewed all compiled reports from computerized searches and conducted additional hand searching. Throughout this literature review, abstracts of unpublished data more than 2 years old were excluded.

Recommendations in this guideline are derived from the literature search results. A complete list of the large number of publications on cardiac imaging is beyond the scope of this report; only selected references are included. The report does not include a discussion of digital subtraction angiography, high speed (cine) computed tomography (CT), or nuclear magnetic resonance imaging (MRI)—although these are not radionuclide-based *per se*, they were included in the original 1986 guideline but not the 1995 update. The present guideline applies to adults but not to children.

This report overlaps with several previously published ACC/AHA guidelines for patient treatment that potentially involve cardiac radionuclide imaging. These include published guidelines for chronic stable angina (SA; 2002), unstable angina and non-ST-elevation myocardial infarction (UA/NSTEMI; 2002), heart failure (2001), perioperative cardiovascular evaluation for noncardiac surgery (2002), exercise testing (2002), valvular heart disease (1998), and AMI (1999). The present report is not intended to include information previously covered in these guidelines, or to provide a comprehensive treatment of the topics addressed in these guidelines.

II. ACUTE SYNDROMES

For the purpose of organization, this chapter will be divided into four parts: (1) evaluation of chest pain in the emergency department for patients with suspected acute coronary syndromes (ACS); (2) detection of AMI when conventional measures are nondiagnostic; (3) assessment of risk, therapy, and prognosis in ST-elevation AMI (STEMI); and (4) diagnosis and assessment of risk, therapy, and prognosis in UA/NSTEMI.

A. Myocardial Perfusion Imaging in the Assessment of Patients Presenting With Chest Pain to the Emergency Department

In the United States, more than 5 million patients present to the emergency department each year with chest pain and approximately 50% are admitted to the hospital, at a cost of \$10 to \$12 billion (1,2). The rate of myocardial infarction (MI) in these patients ranges from 2 to 10%, with an average of 5% (1,2). More than one-half of patients admitted for suspected ischemic chest pain are discharged without a proven diagnosis of MI or UA. Conversely, 5 to 10% of patients discharged from the emergency department have an unrecognized infarction, and others have UA (2).

The differentiation between cardiac and noncardiac chest pain is often difficult. Although a thorough history and physical evaluation, resting electrocardiogram (ECG), and cardiac markers or enzymes are all important elements to be considered when deciding which patients need to be admitted to the hospital, many patients with a normal ECG and negative serum markers and enzymes are admitted because of diagnostic uncertainty. Optimal decision-making in patients seen in the emergency department with chest pain requires triage into risk categories based on the probability of AMI, UA, or both, and the subsequent risk and potential interventional options. Within such an algorithm, radionuclide imaging provides clinically useful information for diagnosis and management. The UA guidelines use four risk levels for chest pain: noncardiac, chronic SA, possible ACS, and definite ACS (3). Radionuclide imaging is most appropriate in patients with possible ACS.

Rest thallium-201 (Tl-201) imaging has been used as an aid in the decision process of patients presenting to the emergency department with chest pain (4,5) and as a risk stratification modality in patients with no evidence of previous MI who were admitted to rule out MI. The sensitivity and specificity for AMI, UA, and overall detection of coronary artery disease (CAD) were high. Nonetheless, Tl-201 is not a practical tracer for imaging of acute chest pain patients in the emergency department because of the need for immediate imaging after injection, as this agent redistributes in the myocardium over time. Thus, images obtained late do not reflect blood flow at the time of injection. For logistical reasons, acute rest chest pain imaging with Tl-201 is not widely used in clinical practice.

The availability of Tc-99m-labeled flow agents, which are trapped in the myocardium and do not redistribute, has offered a new window of opportunity to image acute patients. Tracer injection may be performed at rest in the emergency department, and patients may be transferred to the nuclear medicine or nuclear cardiology laboratory for subsequent imaging as these late images reflect myocardial blood flow (MBF) at the time of injection. Published observational studies using the Tc-99m tracers are listed in Table 1 (1,2,6-10).

In patients with chest pain and receiving resting perfusion imaging, sensitivity and specificity for acute ischemic syndromes or a diagnosis of CAD were better than clinical fac-

Table 1. Published Studies Using Tc-99m Tracers

Year	Author	n	Imaging Modality	Abnormal Test (%)	Outcome Assessed	Outcomes (%)	Sensitivity	Specificity	Positive Predictive Value	Negative Predictive Value
1991	Bilodeau (6)	45	Sestamibi SPECT	29 (64%)	Significant CAD	26 (58%)	96%	79%	94%	86%
1993	Varetto (7)	64	Sestamibi SPECT	30 (46.9%)	AMI	13 (20%) 14 (22%)	100%	92%	90%	100%
1997	Tatum (2)	438*	Sestamibi SPECT	100 (23%)	MI	7 (1.6%)	100%	78%	Not Determined	Not Determined
1998	Heller (1)	357	Tetrofosmin SPECT	153 (43%)	Death	0				99%
1999	Duca (8)	75	Sestamibi or tetrofosmin SPECT	27 (36%)	MI	20 (6%)	90%	59.5%	12%	81%
1999	Kontos (9)	620	Sestamibi SPECT	241 (39%)	CAD	26 (35%)	73%	93%	89%	100%
1994	Hilton (10)	102	Sestamibi SPECT	32 (31%)	MI	9 (12%) 59 (9%) 58 (9%) 12 (12%) 1 (1%)	100%	73%	33%	93%
					Death		92%	67%	47%	
							81%	74%	Not Determined	Not Determined
							94%	83%	Not Determined	Not Determined
							100%	78%	Determined	Determined

AMI indicates acute myocardial infarction; CAD, coronary artery disease; MI, myocardial infarction; SPECT, single-photon emission computed tomography.

*The 438 patients in this study were classified as lower-risk patients prior to perfusion imaging.

tors and the resting ECG (6,7,11). Accuracy was highest when patients were injected while they had chest pain, but positive studies were present in 11 of 14 patients diagnosed with UA who were injected an average of 4.7 hours after the chest pain had resolved (7). As shown in Table 1, the negative predictive value is high in these studies. In the study by Hilton *et al.* (11) only 1 of 70 patients (1.5%) with normal single-photon emission CT (SPECT) results had a significant cardiac event (coronary revascularization), whereas 12 of 17 patients (71%) with abnormal scans had an event and 2 of 15 (13%) with equivocal studies had an event. Similar results have been reported with the use of Tc-99m-tetrofosmin (1).

The question of when, as well as if, the information provided by perfusion imaging decreases in value relative to the presence or absence of symptoms is not resolved. Although some studies suggest that the diagnostic value for detection of CAD is less in the absence of ongoing symptoms (6), other studies indicate that the predictive or prognostic value for cardiac events is maintained up to 6 hours after symptom cessation (2). These issues should be borne in mind when incorporating perfusion imaging results in the absence of ongoing symptoms. When more than 2 to 3 hours have elapsed after symptom cessation, a normal rest perfusion image seems to identify a low-risk patient but does not exclude the presence of CAD.

The diagnostic accuracy of sestamibi SPECT has also been compared with that of cardiac troponin I (cTnI) (9). Among 620 patients studied, 9% had AMI and 13% had a final diagnosis of significant coronary disease. Sensitivity for detecting MI was similar between SPECT imaging (92%) and cTnI (90%). The initial cTnI value, however, had only a sensitivity of 39% and serial determinations were necessary to achieve a high sensitivity. In the 81 patients who had significant coronary disease, but no AMI, 75% had a positive perfusion imaging study. Comparisons have also been made to a wider panel of acute serum markers (8). All patients with an AMI had an abnormal SPECT study. The sensitivity of acute rest SPECT for objective evidence of CAD was 73%. Individual serum markers had a low sensitivity for symptomatic myocardial ischemia alone. Serum troponin-T and TnI were highly specific for AMI but had a low sensitivity at presentation (8).

The observational studies summarized in Table 1 suggest a high negative predictive value for ruling out an acute ischemic syndrome in the emergency department setting. This view is now supported by two randomized multicenter controlled clinical trials performed to assess whether incorporating imaging information favorably influences decision making in emergency department patients with suspected acute ischemia. An initial study enrolled 46 chest pain patients who all had resting Tc-99m-tetrofosmin scans (12). The patients were then randomly assigned to have, or not have, scan results provided to the emergency department physicians. Patients whose evaluations included the scan results had a 50% reduction in length of stay and hospital costs and similar rates of in-hospital and 30-day follow-up events. In a much larger study, 2475 patients with symptoms

suspicious for acute ischemia but normal or nondiagnostic ECGs were randomized to a strategy of usual care emergency department evaluation (without imaging) or a strategy incorporating perfusion imaging (rest Tc-99m-sestamibi SPECT) (13). The imaging strategy was associated with a favorable effect on decision-making (ie, patients randomized to the imaging strategy were less often unnecessarily admitted to the hospital or held for observation and were more often discharged home directly from the emergency department). In the decision-making process, imaging results were incorporated into all available information, including history and physical exam.

Based on the growing body of literature on the use of emergency department imaging of patients with chest pain, and in accordance with the ACC/AHA 2002 Guideline Update for the Management of Patients with Unstable Angina and Non-ST-Segment Elevation Myocardial Infarction (3) and the ACC/AHA Guidelines for the Management of Patients with Acute Myocardial Infarction (14), the following conclusions can be reached:

1. The sensitivity of acute rest imaging for MI appears very high and is maximal at the onset of acute infarction, in contrast with the sensitivity of serum enzyme markers, which require several hours to become maximally positive. Patients discharged home with negative scans have a very low likelihood for cardiac events (high negative predictive value), whereas patients with positive scans are at higher risk for events.
2. After initial triage based on symptoms, ECG, and history, rest SPECT imaging in the emergency department appears to be useful for identifying patients at high risk (those with perfusion defects), who should be admitted, and patients with low-risk (those with normal scans), who in general may be discharged home with a low-risk for subsequent ischemic events.
3. Whether the addition of exercise stress imaging in patients with a negative rest scan on the same day versus delayed stress imaging would be a preferable approach is presently under study.

Table 2 identifies the recommendations for rest radionuclide imaging in the evaluation of chest pain in the emergency department for patients with suspected ACS.

B. Detection of AMI When Conventional Measures Are Nondiagnostic

1. “Hot Spot” Infarct Imaging

In the past, cardiac “hot spot” scintigraphy with Tc-99m pyrophosphate or indium-111 antimyosin antibody was used to diagnose AMI. These techniques were most useful in patients with conduction system abnormalities on the resting ECG that limited an ECG diagnosis and in patients who presented late after symptom onset when cardiac enzymes

Table 2. Recommendations for Emergency Department Imaging for Suspected Acute Coronary Syndromes

Indication	Test	Class	Level of Evidence
1. Assessment of myocardial risk in possible ACS patients with nondiagnostic ECG and initial serum markers and enzymes, if available.	Rest MPI	I	A
2. Diagnosis of CAD in possible ACS patients with chest pain with nondiagnostic ECG and negative serum markers and enzymes or normal resting scan.	Same day rest/stress perfusion imaging	I	B
3. Routine imaging of patients with myocardial ischemia/necrosis already documented clinically, by ECG and/or serum markers or enzymes.	Rest MPI	III	C

ACS indicates acute coronary syndrome; CAD, coronary artery disease; ECG, electrocardiogram; MPI, myocardial perfusion imaging.

(See Figure 6 of the ACC/AHA 2002 Guideline Update for the Management of Patients with Unstable Angina and Non-ST-Segment Elevation Myocardial Infarction at www.acc.org/clinical/guidelines/unstable/unstable.pdf and Figure 1 of the ACC/AHA Guidelines for the Management of Patients with Acute Myocardial Infarction at www.acc.org/clinical/guidelines/nov96/1999/jac1716f01.htm.)

might not be definitive. Because of the limited patient population in which these studies were clinically useful for diagnosis and management and the availability of better serum markers and imaging techniques, hot spot infarct imaging is used infrequently and has a limited role in diagnosing ACS. Pyrophosphate imaging still has a role in the diagnosis of amyloidosis and for the detection of myocardial contusion after chest wall trauma.

2. Acute Rest Myocardial Perfusion Imaging

Rest myocardial perfusion imaging (MPI) with Tl-201, Tc-99m-sestamibi, or Tc-99m-tetrofosmin has a high sensitivity for diagnosing AMI. Tc-99m tracers are uniquely suited to accurately measure myocardium at risk in patients with AMI (15-17). Because there is minimal redistribution of the radiopharmaceutical over time, imaging can be delayed for a few hours after the injection and still provide accurate information about myocardial perfusion at the time of injection, which reflects the area of myocardium at risk. However, such defects do not distinguish among acute ischemia, acute infarction, or previous infarction. Serial changes on follow-up perfusion imaging suggest an acute process but cannot definitely distinguish ischemia from infarction although the changes allow measurement of myocardial salvage, which is the area initially at risk minus the final infarct size. Myocardium at risk is a major determinant of final infarct size. The final infarct size assessed by perfusion tomography is a major determinant of subsequent patient survival (18,19). Measurement of final infarct size with sestamibi tomography is closely correlated with the left ventricular ejection fraction (LVEF), regional wall motion score, and creatine kinase release, and the size also predicts patient outcomes.

Despite this well-validated body of experimental and clinical knowledge for diagnosis, assessment of myocardium at risk, and management of AMI, the availability of alternative methods and the logistics and time demands of performing MPI in the setting of AMI has limited its widespread clinical application. This technique has value in clinical trials for treatment of acute infarction as it can sometimes reduce the

number of patients required for significant results between treatment groups.

C. Radionuclide Testing in Risk Assessment: Prognosis and Assessment of Therapy After STEMI

The prognosis of STEMI is primarily a function of EF, infarct size, and residual myocardium at risk. Thus, acute or late measurement of EF, infarct size, and myocardium at risk provides important prognostic management information (14). Radionuclide techniques are also useful for assessing the presence and extent of stress-induced myocardial ischemia, which are useful for immediate and long-term management of patients. Imaging is also useful in patients referred for coronary angiography as it identifies the “culprit” lesion and the hemodynamic significance of a moderate stenosis.

In the prethrombolytic era, several planar studies demonstrated the value of exercise and pharmacologic myocardial perfusion scintigraphy for risk stratification (20-26). In the thrombolytic therapy and direct angioplasty era, submaximal exercise SPECT imaging continued to provide important prognostic indicators (22,27). It was demonstrated that MPI was more effective than was exercise ECG testing to predict patient outcomes. The perfusion data provide incremental information over clinical factors and the LVEF. When clinical data, resting LVEF, and stress scintigraphic data are combined, coronary angiography may not provide additional incremental value in predicting prognosis (27).

Pharmacologic perfusion tomography using adenosine (28,29) or dipyridamole (30) is also very useful for risk stratifying patients after an AMI. The advantage of pharmacologic stress compared with dynamic exercise is that studies can be performed earlier after acute infarction. In the multicenter study by Brown *et al.* (30) a pre-discharge dipyridamole tomographic study afforded better stratification of patients into low-, intermediate-, and high-risk groups compared with stratification provided by a submaximal exercise perfusion imaging study. This may be a result of enhanced sensitivity for detection of reversible ischemia in patients undergoing pharmacologic stress versus submaximal exercise testing.

Pharmacologic perfusion scintigraphy has the advantage of allowing early risk stratification (between 2 and 5 days after the infarction) with a very good safety record (22,24,27-30). The presence and extent of myocardial ischemia, the number and extent of myocardial perfusion defects, transient stress-induced LV dilation, and increased tracer lung uptake (especially useful with Tl-201) are all markers of a poor prognosis.

Patients with small fixed perfusion defects have an excellent prognosis, and it is unlikely they will benefit from invasive investigation or revascularization. Conversely, patients with markers of increased risk by stress perfusion tomography may be preferentially referred for coronary angiography and revascularization. Although such a strategy is intuitively appealing, no prospective data are available that establish the superiority of revascularization in this setting, as opposed to aggressive medical therapy. A small pilot prospective study has suggested that aggressive medical therapy and revascularization are equally beneficial in reducing a patient's risk, provided that either therapy is capable of producing a substantial decrease in perfusion defect size (31). A larger prospective randomized trial, the INSPIRE trial—AdenosINE Sestamibi SPECT Post InfaRction Evaluation, is currently being performed to determine the value of sequential perfusion imaging to assess not only the initial postinfarction risk but also its subsequent change after medical and revascularization therapy.

Prospective randomized trials that assessed the value of routine coronary angiography followed by revascularization within a few days of the acute infarction have not shown improved outcomes in patients with Q-wave infarction. Hence, a noninvasive stratification may be used initially in most stable postinfarction patients. Unstable patients, as well as those with markers of high clinical or scintigraphic risk, may be directly referred to catheterization.

Although there are no published trials showing that the use of ECG-gated SPECT imaging provides incremental information over conventional SPECT perfusion studies in this patient population, it is believed that the improvement in

diagnostic accuracy and recognition of artifacts with the use of gating makes this an important part of perfusion imaging, and ECG-gated assessment of function should be performed whenever possible.

The recommendations for radionuclide testing in risk assessment, prognosis, and assessment of therapy after STEMI are shown in Table 3.

D. Radionuclide Testing in Risk Assessment: Prognosis and Assessment of Therapy After NSTEMI or UA

In the United States coronary angiography is often performed in patients with NSTEMI or UA either as an initial method for evaluation and treatment or as a later method after a variable delay.

The ACC/AHA 2002 Guideline Update for the Management of Patients with Unstable Angina and Non-ST-Segment Elevation Myocardial Infarction (3) (<http://www.acc.org/clinical/guidelines/unstable/incorporated/index.htm>) recommends an early invasive strategy in patients with any of several high-risk indicators and no serious comorbidities. High-risk findings on noninvasive stress testing (eg, MPI) are one such indication. In the absence of high-risk findings, the guidelines endorse either an early conservative or early invasive strategy in patients without contraindications for revascularization. The guidelines recommendations are based on several publications (32-36).

MPI has been shown to be particularly useful in the pre-discharge risk stratification of patients with UA. In the study by Brown *et al.* (37), 52 patients with medically stabilized UA underwent exercise planar Tl-201 imaging within 1 week of admission. At an average follow-up of 39 months, cardiac death or nonfatal MI occurred in 6 of 23 (26%) patients with thallium redistribution versus 1 of 29 (3%) of those without redistribution (*P* less than 0.05). The number of segments with thallium redistribution and a history of prior MI were the only significant predictors of all events. However, thallium redistribution was the only predictor of cardiac death or nonfatal MI on follow-up. In this study,

Table 3. Recommendations for Use of Radionuclide Testing in Diagnosis, Risk Assessment, Prognosis, and Assessment of Therapy After Acute ST-Segment Elevation Myocardial Infarction

Patient Subgroup(s)	Indication	Test	Class	Level of Evidence
All	1. Rest LV function	Rest RNA or ECG-gated SPECT MPI	I	B
Thrombolytic therapy without catheterization	2. Detection of inducible ischemia and myocardium at risk	Stress MPI with ECG-gated SPECT whenever possible	I	B
Acute STEMI	3. Assessment of infarct size and residual viable myocardium	MPI at rest or with stress using gated SPECT	I	B
	4. Assessment of RV function with suspected RV infarction	Equilibrium or FPRNA	IIa	B

ECG indicates electrocardiogram; FPRNA, first-pass radionuclide angiogram; LV, left ventricular; MPI, myocardial perfusion imaging; RNA, radionuclide angiogram; RV, right ventricular; SPECT, single-photon emission computed tomography; STEMI, ST-segment elevation myocardial infarction.

coronary anatomy was not a good predictor of future events.

In a similar study, patients with UA stabilized on medical therapy underwent a symptom-limited exercise thallium SPECT. Reversible thallium defects occurred in 20 of 22 patients (91%) who developed cardiac events versus 5 of 17 patients (29%) of those who did not develop events (*P* less than 0.0001), over a mean follow-up of 39 months (38).

In another study by Strattman *et al.* (39), patients underwent a sestamibi stress myocardial perfusion SPECT study before hospital discharge. The event-free survival was approximately 90% over a follow-up of 18 months in patients with normal scans versus 55% in those with abnormal scans. Patients with reversible defects in this study had a less favorable prognosis, with an event-free survival of only 30% over 18 months. Death or MI in this study was rare in patients with a normal scan but occurred in 20% of those with abnormal scans and in 40% of those with reversible defects over 18 month follow-up. Several other studies give support to the use of MPI either with Tl-201, Tc-99m-sestamibi, exercise, or dipyridamole imaging in patients with UA (40-45).

Thus, the presence and extent of reversible perfusion defects on stress testing after the patient is stabilized are highly predictive of future events. In some studies (43,44), a fixed defect was also predictive of future events. Radionuclide angiography (RNA) can assess improved LV function in patients who have undergone revascularization and have evidence of ventricular dysfunction between episodes of UA. Likewise, MPI can document improvement in rest perfusion to areas of rest ischemia (46).

Table 4 lists the uses of radionuclide testing in patients for prognosis and assessment of therapy in patients with NSTEMI and UA. ECG gating of the perfusion images is recommended whenever possible.

III. CHRONIC SYNDROMES

A. Detection (Diagnosis) of CAD

The basis for the diagnostic application of nuclear testing lies in the concept of sequential Bayesian analysis of disease probability. Integrated predictive models based on clinical history and physical examination parameters have been developed from large patient registries and have been published in the form of nomograms for estimating the pretest likelihood of angiographically significant coronary disease as well as cardiac survival (47-51). A thorough discussion of the concepts of likelihood of CAD is provided in the ACC/AHA 2002 Guideline Update for the Management of Patients With Chronic Stable Angina (52) ([http:// www. acc.org/clinical/guidelines/stable/update_explantext.htm](http://www.acc.org/clinical/guidelines/stable/update_explantext.htm)), accompanied by a simplified table for estimating pretest probability ranges. MPI is most useful in patients with an intermediate likelihood of angiographically significant CAD based on age, sex, symptoms, risk factors, and the results of stress testing (for patients who have undergone prior stress testing).

1. Sensitivity and Specificity

In patients with suspected or known chronic stable coronary disease, the largest accumulated experience in MPI has been with the tracer Tl-201, but available evidence suggests that the newer tracers Tc-99m-sestamibi and Tc-99m-tetrofosmin yield similar diagnostic accuracy (53-63). Thus, for the most part, Tl-201, Tc-99m-sestamibi, or Tc-99m-tetrofosmin can be used interchangeably for diagnosing CAD.

Tables 5 and 6 present sensitivities and specificities of myocardial perfusion SPECT for the detection of angiographically significant (more than 50% stenosis) CAD. Only studies reporting both sensitivity and specificity are included.

Table 4. Recommendations for Use of Radionuclide Testing for Risk Assessment/Prognosis in Patients With Non–ST-Segment Elevation Myocardial Infarction and Unstable Angina

Indication	Test	Class	Level of Evidence
1. Identification of inducible ischemia in the distribution of the “culprit lesion” or in remote areas in patients at intermediate or low risk for major adverse cardiac events.	Stress MPI with ECG gating whenever possible	I	B
2. Identification of the severity/extent of inducible ischemia in patients whose angina is satisfactorily stabilized with medical therapy or in whom diagnosis is uncertain.	Stress MPI with ECG gating whenever possible	I	A
3. Identification of hemodynamic significance of coronary stenosis after coronary arteriography.	Stress MPI	I	B
4. Measurement of baseline LV function.	Rest RNA or gated SPECT MPI	I	B
5. Identification of the severity/extent of disease in patients with ongoing suspected ischemia symptoms when ECG changes are nondiagnostic.	Rest MPI	IIa	B

ECG indicates electrocardiogram; LV, left ventricular; MPI, myocardial perfusion imaging; RNA, radionuclide angiogram; SPECT, single-photon emission computed tomography.

Table 5. Sensitivity and Specificity of Exercise Myocardial Perfusion Single-Photon Emission Computed Tomography for Detecting Coronary Artery Disease (Greater Than or Equal to 50% Stenosis)—Generally Without Correction for Referral Bias

Year	Author	Radiopharmaceutical	Prior MI (%)	Sensitivity		Specificity	
				Pts. with CAD	%	Pts. w/out CAD	%
2001	Elhendy (65)	Sestamibi/Tetrofosmin	0	183/240	76	67/92	73
1999	Azzarelli (66)	Tetrofosmin	66	199/209	95	20/26	77
1998	San Roman (67)	Sestamibi	0	54/62	87	21/30	70
1998	Budoff (68)	Sestamibi	0	12/16	75	12/17	71
1998	Santana-Boado (69)	Sestamibi	0	91/100	91	57/63	90
1998	Acampa (70)	Sestamibi	47	23/25	92	5/7	71
1998	Acampa (70)	Tetrofosmin	47	24/25	96	6/7	86
1998	Ho (71)	Tl-201	22	19/24	79	15/20	75
1997	Iskandrian (72)	Tl-201	21	717/820	87	120/173	69
1997	Candell-Riera	Sestamibi	0	53/57	93	32/34	94
1997	Yao (74)	Sestamibi	55	34/36	94	14/15	93
1997	Heiba (75)	Sestamibi	31	28/30	93	2/4	50
1997	Ho (76)	Tl-201	33	29/38	76	10/13	77
1997	Taillefer (77)	Sestamibi	17	23/32	72	13/16	81
1997	Van Eck-Smit (78)	Tetrofosmin	NR	46/53	87	6/7	86
1996	Hambye (79)	Sestamibi	0	75/91	82	28/37	75
1995	Palmas (80)	Sestamibi	30	60/66	91	3/4	75
1995	Rubello (81)	Sestamibi	57	100/107	93	8/13	61
1994	Sylven (82)	Sestamibi	37	41/57	72	5/10	50
1994	Van Train (83)	Sestamibi	19	91/102	89	8/22	36
1993	Berman (84)	Sestamibi/Tl-201	0	50/52	96	9/11	82
1993	Forster (85)	Sestamibi	0	10/12	83	8/9	89
1993	Chae (86)	Tl-201	42	116/163	71	52/80	65
1993	Minoves (87)	Sestamibi/Tl-201	42	27/30	90	22/24	92
1993	Van Train (88)	Sestamibi	16	30/31	97	6/9	67
1992	Quinones (89)	Tl-201	NR	65/86	76	21/26	81
1991	Coyne (90)	Tl-201	NR	38/47	81	39/53	74
1991	Pozzoli (91)	Sestamibi	19	41/49	84	23/26	88
1990	Kiat (92)	Sestamibi	45	45/48	94	4/5	80
1990	Mahmarián (93)	Tl-201	43	192/221	87	65/75	87
1990	Nguyen (94)	Tl-201	NR	19/25	75	5/5	100
1990	Van Train (95)	Tl-201	35	291/307	95	30/64	47
1989	Iskandrian (96)	Tl-201	45	145/164	88	36/58	62
	Total			2971/3425		772/1055	
	Average				87		73

MI indicates myocardial infarction; NR, not reported; Sestamibi, Tc-99m-sestamibi; Tetrofosmin, Tc-99m-tetrofosmin; Tl-201, thallium-201.

Based on English language manuscripts providing data with greater than or equal to 50% stenosis criterion.

ed. A meta-analysis of diagnostic test performance has summarized evidence documenting that the sensitivity of exercise electrocardiography is significantly lower than that of myocardial perfusion SPECT (64). Less-than-100% values for sensitivity and specificity may reflect physiologic and technical factors (eg, the visually estimated angiographic severity of coronary stenoses does not always correlate with functional severity as assessed by coronary flow reserve after maximal pharmacologic coronary vasodilation) (109). As discussed below, the specificity in more recent studies is affected adversely by referral bias (110,111). In addition, a true physiologic decrease in blood flow may be seen in the absence of a fixed coronary stenosis (112). At times apparent abnormalities on myocardial perfusion SPECT are due to

artifacts such as soft-tissue attenuation; the use of gated SPECT, prone imaging, and/or attenuation correction can improve the specificity of SPECT.

Since the introduction of dipyridamole-induced coronary vasodilation as an adjunct to Tl-201 MPI (113-115), pharmacologic interventions have become an important tool in noninvasive diagnosis of CAD (90,94,107,108,114-123). Dipyridamole SPECT imaging with Tl-201 or Tc-99m-sestamibi appears to be as accurate as is exercise SPECT (124-126). Results of MPI during adenosine infusion are similar to those obtained with dipyridamole and exercise imaging (90,94,120,122). A single 81-patient study has reported enhanced detection of reversible perfusion defects by Tc-99m-sestamibi compared to Tc-99m-tetrofosmin during

Table 6. Sensitivity and Specificity of Vasodilator Stress Single-Photon Emission Computed Tomography for Detecting Coronary Artery Disease (Greater Than or Equal to 50% Stenosis)—Without Correction for Referral Bias

Year	Author	Vasodilator	Radiopharmaceutical	Prior MI (%)	Sensitivity		Specificity	
					Pts. with CAD	%	Pts. w/out CAD	%
2000	Smart (97)	Dipyridamole	Sestamibi	NR	95/119	80	47/64	73
1998	Takeishi (98)	Adenosine	Tetrofosmin	17	39/44	89	17/21	81
1997	Watanabe (99)	Adenosine	Tl-201	19	40/46	87	21/24	88
1997	Watanabe (99)	Dipyridamole	Tl-201	23	34/41	83	21/29	72
1997	Taillefer (77)	Dipyridamole	Sestamibi	11	23/32	72	5/5	100
1997	He (100)	Dipyridamole	Tetrofosmin	52	41/48	85	6/11	55
1997	Cuocolo (101)	Adenosine	Tetrofosmin	23	22/25	88	1/1	100
1997	Amanullah (102)	Adenosine	Sestamibi/ Tl-201	0	159/171	93	37/51	73
1997	Miller (103)	Dipyridamole	Sestamibi	34	186/204	91	11/40	28
1997	Iskandrian (72)	Adenosine	Tl-201	28	452/501	90	41/49	84
1995	Aksut (104)	Adenosine	Tl-201	24	358/398	90	38/45	84
1995	Miyagawa (105)	Adenosine	Tl-201	15	67/76	88	35/44	80
1993	Marwick (106)	Adenosine	Sestamibi	0	51/59	86	27/38	71
1991	Coyne (90)	Adenosine	Tl-201	NR	39/47	83	40/53	75
1991	Nishimura (107)	Adenosine	Tl-201	13	61/70	87	28/31	90
1990	Verani (108)	Adenosine	Tl-201	NR	24/29	83	15/16	94
1990	Nguyen (94)	Adenosine	Tl-201	37	49/53	92	7/7	100
	Total				1740/1963		397/529	
	Average					89		75

Based on English language manuscripts providing data with greater than or equal to 50% stenosis criterion.

MI indicates myocardial infarction; NR, not reported; Sestamibi, Tc-99m-sestamibi; Tetrofosmin, Tc-99m-tetrofosmin; Tl-201, thallium-201.

dipyridamole vasodilator stress in patients with mild to moderate CAD (127). Further information regarding the comparative sensitivity and specificity of the tracers when used with pharmacologic stress, as well as the ability of the tracers to identify disease in individual arteries and to assess the overall extent of disease, would be of interest.

Although dobutamine perfusion imaging has reasonable diagnostic accuracy (128), there has been far less experience with this approach than with exercise, dipyridamole, or adenosine myocardial perfusion SPECT. Dobutamine stress does not provoke as great an increase in coronary flow (129,130) as does dipyridamole or adenosine stress and is, therefore, less ideal for stress MPI. Its use should generally be restricted to patients with contraindications to dipyridamole and adenosine. Stress RNA is now performed infrequently and is therefore not included in the recommendations.

2. Effect of Referral Bias

In estimating the true sensitivity and specificity of noninvasive testing, referral or work-up bias needs to be taken into account (110,111). In cardiology, once a noninvasive test is accepted as being clinically effective for diagnosis and risk stratification, its results strongly influence the performance of subsequent coronary angiography. Referral bias results in an overestimation of test sensitivity and an underestimation of test specificity. Sensitivity is the proportion of patients with disease who are correctly detected as abnormal by the

test, and specificity is the proportion of patients without disease who are correctly detected as normal by the test. In the extreme case, once the test becomes used as the absolute “gatekeeper” to catheterization, sensitivity and specificity can no longer be accurately measured. For example, even if the test in question had a true sensitivity of 90% and a true specificity of 90%, the observed sensitivity and specificity would still by definition be 100% and 0%, respectively, because only positive test responders are catheterized. This extreme example illustrates the care with which current medical literature needs to be interpreted with respect to sensitivity and specificity rates. Table 7 illustrates the effect of referral bias in the limited number of studies that have corrected for it.

Because of the profound impact of referral bias on specificity, the concept of the normalcy rate has been developed and applied in multiple different clinical studies. The normalcy rate applies to patients with a low likelihood of CAD, based on sequential Bayesian analysis of age, sex, symptom classification, and the results of noninvasive stress testing (other than the test in question) (131,132). The term normalcy rate is used to describe the frequency of normal test results in patients with a low likelihood of CAD, to differentiate it from specificity, which as noted above refers to the frequency of normal test results in patients with normal coronary angiograms. Patients with a low likelihood of CAD are chosen in preference to normal volunteers because they are closer in age and risk factors to patients with CAD undergoing

Table 7. Noninvasive Tests Before and After Adjustment for Referral Bias

Year	Author	Modality	Total Patients	Sensitivity		Specificity	
				Biased	Adjusted	Biased	Adjusted
2002	Miller et al. (108a)	Exercise SPECT sestamibi/Tl-201	Overall: 1853	98	65	13	67
1998	Santana-Boado et al. (69)	Exercise/dipyridamole and SPECT sestamibi	Men: 100 Women: 63	93	88	89	96
1996	Cecil et al. (108b)	Exercise SPECT Tl-201	Overall: 2688	98	82	14	59
1993	Schwartz et al. (282)	Tl-201	Men: 845	67	45	59	78
1986	Diamond (108c)	Exercise planar Tl-201	Overall: 2269	91	68	34	71

Sestamibi indicates Tc-99m-sestamibi; SPECT, single-photon emission computer tomography; Tl-201, thallium-201.

Modified from Gibbons et al. ACC/AHA 2002 Guideline Update on the Management of Patients With Chronic Stable Angina (52).

testing, and because they are part of a population with clinically suspected CAD before their referral. Reported normalcy rates for myocardial perfusion SPECT are listed in Table 8. There may be a small difference in normalcy rate between Tc-99m and Tl-201 tracers, but the literature is not definitive in this regard.

3. Quantitative Analysis

Quantitative analysis of myocardial perfusion SPECT has been developed by using a variety of approaches (83,88,95,137-147) and, in general, has similar sensitivities and specificities compared with those of expert visual analysis. Quantitative analysis has also been shown to be equal to expert visual interpretation in the assessment of prognosis (148). These quantitative approaches decrease inter- and intraobserver variability and facilitate serial assessment of myocardial perfusion and function.

4. ECG-Gated SPECT

The current state of the art is ECG-gated myocardial perfusion SPECT (gated SPECT), which in 2000 was estimated to be performed in approximately 80% of myocardial perfusion SPECT studies in the United States. The ability to observe myocardial contraction in segments with apparent fixed perfusion defects permits the nuclear test reader to discern attenuation artifacts from true perfusion abnormalities. Taillefer et al. (77) reported the result of a study comparing the accuracy of Tl-201 and gated Tc-99m-sestamibi in a cohort of 115 women (85 with suspected CAD, 30 normal volunteers). Although no significant differences between the radiopharmaceuticals were found with respect to test sensitivity, specificity tended to be greater with Tc-99m-sestamibi when gated SPECT was analyzed. These findings supported previous work by DePuey et al. (149). Choi et al. (150) also confirmed this finding and extended it to include gated SPECT studies performed with Tc-99m-tetrofosmin.

The use of gating may also result in increased reader confidence in scan interpretation. Although this phenomenon is difficult to verify and quantify, it is reasonable to expect that it would result in a reduction in the number of "equivocal" scans reported. This hypothesis has been examined by Smanio et al. (151). In 285 consecutive patients (143 women, 142 men) who underwent stress SPECT imaging with Tc-99m-sestamibi, gated SPECT reduced the frequency of borderline studies (borderline normal or borderline abnormal) from 31 to 10%. The number of patients with a less than 10% likelihood of CAD whose scans were interpreted as normal was increased (74 to 93%, *P* less than 0.0001), and patients with documented CAD tended to be appropriately reclassified from equivocal to abnormal. The ability of gated SPECT to provide measurement of LVEF, segmental wall motion, and LV absolute volumes also adds to the prognostic information that can be derived from a SPECT perfusion study.

Table 8. Normalcy Rate of Stress SPECT in Patients With a Low Likelihood of CAD

Year	Author	Stress	Stress Radiopharmaceutical		No. of Pts	%	Likelihood of CAD
1999	Azzarelli (66)	Exercise	Tetrofosmin		61	93	Less than 5%
1997	Heo (133)	Exercise	Sestamibi		61	95	Less than 5%
1996	Amanullah (38)	Adenosine	Sestamibi		71	93	Less than 10%
1996	Nicolai (134)	Adenosine	Sestamibi		22	86	Less than 5%
1995	Zaret (63)	Exercise	Tetrofosmin		58	97	Less than 3%
1994	Heo (135)	Exercise	Sestamibi/Tl-201		34	97	Less than 5%
1994	Van Train (83)	Exercise	Sestamibi		37	81	Less than 5%
1993	Berman (84)	Exercise	Sestamibi/Tl-201		107	95	Less than 5%
1992	Kiat (136)	Exercise	Tl-201		55	89	Less than 5%
1990	Kiat (92)	Exercise	Sestamibi		8	88	Less than 5%
1990	Van Train (95)	Exercise	Tl-201		76	82	Less than 5%
1989	Iskandrian (54)	Exercise	Tl-201		131	94	Less than 5%
	Total				721	91	

CAD indicates coronary artery disease; Sestamibi, Tc-99m-sestamibi; SPECT, single-photon emission computed tomography; Tetrofosmin, Tc-99m-tetrofosmin; Tl-201, thallium-201.

Based on English language manuscripts.

5. Attenuation Correction

Although attenuation correction is not yet widely used, there have been several published reports comparing the diagnostic accuracy of attenuation-corrected and nonattenuation-corrected SPECT, by use of a variety of commercially available approaches (152-158). In general, these have demonstrated improved specificity with no change in overall sensitivity (Table 9). Results from a multicenter blinded read of stress-only attenuation-corrected images versus nonattenuation-corrected images suggest that this method can increase reader confidence and obviate the need for rest images in many patients (159,160). A similar conclusion has been reached in a study of 729 patients with a low to medium pretest probability of CAD being evaluated for chest pain (161). Several studies indicate that optimal results require attention to quality-control steps such as high-count transmission scans, avoidance of truncation, and awareness of the differences in appearance between attenuation-corrected and uncorrected images. Inadequate quality control and lack of experience probably account for some of the interpretive limitations described when this method of acquiring and reconstructing image data was first implemented.

The relative capabilities of gated SPECT and attenuation correction to improve diagnostic specificity are still under study. In a small series of patients with intermediate likelihood of CAD, Lee et al. (162) reported no improvement in either sensitivity or specificity with gated or attenuation-corrected images compared with nongated images. However, a report from a 10-center blinded read of nongated, gated, and attenuation-corrected SPECT in 90 patients (49 with low likelihood for CAD and 41 with angiographically-proved disease) showed that the percentage of studies interpreted unequivocally as normal or abnormal was 37%, 42%, and 84%, respectively. This study was powered to compare the incremental value of attenuation correction to gating, and the results were a statistically significant improvement in both diagnostic accuracy and interpretive confidence (159,160). In an additional study, Links et al. (163) have similarly concluded that gating and attenuation correction are complementary and synergistic.

The field of attenuation correction continues to evolve rapidly, with some available systems having undergone more detailed and successful clinical validation than others. Based on current information and the rate of technology improve-

Table 9. Comparative Diagnostic Accuracy of Attenuation-Corrected and Nonattenuation-Corrected Single-Photon Emission Computed Tomography

Author	Sensitivity		Specificity		Normalcy	
	NC	AC	NC	AC	NC	AC
Ficaro (152)	78%	84%	46%	82%	88%	98%
Hendel (164)	76%	78%	44%	50%	86%	96%
Links* (157)	84%	88%	69%	92%	69%	92%
Gallowitsch (155)	89%	94%	69%	84%	NA	NA
Ficaro† (152)	93%	93%	84%	88%	78%	85%

*Includes motion correction and depth dependent blur correction.

†Includes scatter correction.

AC indicates attenuation-corrected SPECT; NA, not available; NC, nonattenuation-corrected SPECT; Single-photon emission computed tomography, SPECT.

Table 10. Sensitivity and Specificity of Positron Emission Tomography for Detecting Coronary Artery Disease (Greater Than or Equal to 50% Stenosis)

Year	Author	Stress	Radiopharmaceutical	Prior MI (%)	Sensitivity		Specificity	
					Pts. with CAD	%	Pts. w/out CAD	%
1992	Marwick (176)	Dipyridamole	Rubidium-82	49	63/70	90	4/4	100
1992	Grover-McKay (173)	Dipyridamole	Rubidium-82	13	16/16	100	11/15	73
1991	Stewart (165)	Dipyridamole/ Exercise	Rubidium-82	42	50/60	83	18/21	86
1990	Go (172)	Dipyridamole	Rubidium-82	47	142/152	93	39/50	78
1989	Demer (171)	Dipyridamole	Rubidium-82/ N-13-ammonia	34	126/152	83	39/41	95
1988	Tamaki (169)	Exercise	N-13-ammonia	75	47/48	98	3/3	100
1986	Gould (167)	Dipyridamole	Rubidium-82/ N-13-ammonia	NR	21/22	95	9/9	100
Total					465/520	89	123/143	86

CAD indicates coronary artery disease; MI, myocardial infarction; NR, not reported.

Based on English language manuscripts providing data with greater than or equal to 50% stenosis criterion.

ment, a Society of Nuclear Medicine and American Society of Nuclear Cardiology joint statement concluded that attenuation correction has become a method for which the weight of evidence/opinion is in favor of its usefulness (164).

6. Positron Emission Tomography

A number of studies, involving a total of several hundred patients, indicate that perfusion imaging with PET using dipyridamole and either rubidium-82 or N-13-ammonia is a sensitive and specific clinical method to diagnose CAD (165-173). Sensitivities with either tracer range from 83 to 100%, with specificities from 73 to 100% as shown in Table 10. Only studies in which both the sensitivity and specificity of PET were reported are included. Although rubidium-82 is the only PET perfusion tracer currently approved by the Food and Drug Administration (FDA) for clinical use, N-13-ammonia is also used for assessment of myocardial perfusion. The advantage of rubidium-82 is that it is obtained from a generator, obviating the need for a cyclotron. Three studies have compared the sensitivity and specificity of myocardial perfusion SPECT with that of myocardial perfusion PET. In a study by Tamaki (169) of 48 patients with CAD and 3 without, PET demonstrated a 98% sensitivity and SPECT 96% sensitivity, whereas specificity was 100% in both. In a study of 152 patients with CAD and 50 without CAD, Go *et al.* (172) demonstrated improved sensitivity with PET (93% vs. 76%) with similar specificity (78% for PET vs. 80% with SPECT). In the third study by Stewart *et al.* (165) evaluating 60 patients with CAD and 21 without, the sensitivities of PET and SPECT were similar (84% vs. 83%, respectively), whereas SPECT demonstrated lower specificity (53 vs. 86% by PET). In this latter study the myocardial perfusion SPECT studies were more commonly clinically indicated than were the PET studies, potentially setting up a greater tendency for referral bias to have affected the specificity of SPECT. Overall, because of the higher resolution of PET and the routine application of attenuation correction, it is probable that sensitivity and specificity are slightly higher for PET com-

pared with SPECT, but there is not a robust database of head-to-head comparisons.

B. Management of Patients With Known or Suspected Chronic CAD: Assessment of Disease Severity, Risk Stratification, and Prognosis

Nuclear tests are best applied for risk stratification in patients with a clinically intermediate risk of a subsequent cardiac event, analogous to the optimal diagnostic application of nuclear testing to patients with an intermediate likelihood of having CAD. For prognostic testing, patients known to be at high risk or low risk would not be appropriate patients for cost-effective risk stratification, because they are already risk stratified sufficiently for clinical decision making. In general, low risk has been defined as a less than 1% cardiac mortality rate per year, high risk as a more than 3% cardiac mortality rate per year. Intermediate risk refers to the 1 to 3% cardiac mortality rate per year range (52). In chronic CAD, it has been suggested that a more than 3% per year mortality rate can be used to identify patients with minimal symptoms whose mortality rate can be improved by coronary artery bypass grafting (CABG) (175) and can be considered high risk. Because the mortality risk for patients undergoing either CABG or angioplasty is at least 1% (176), mildly symptomatic patients with a less than 1% mortality rate would not generally be candidates for revascularization to improve survival. These are, however, general thresholds and may vary according to the age of the patient and comorbidities. For example, in the very elderly, both the low- and high-risk levels would be higher (in the range of 2 to 5% for annual cardiac death), reflecting the higher rate of yearly cardiac death in elderly patients undergoing revascularization.

Many of the major determinants of prognosis in CAD can be assessed by measurements of stress-induced perfusion and function. These include the amount of infarcted myocardium, the amount of jeopardized myocardium (supplied by vessels with hemodynamically significant stenosis) and the degree or severity of ischemia (tightness of the indi-

vidual coronary stenosis). Of additional importance in prognostic assessment is the stability (or instability) of the CAD process, a factor that may explain an apparent paradox. Although nuclear tests, in general, are expected to identify only hemodynamically significant stenoses, it has been observed that most MIs occur in regions with less than 50% diameter narrowing (177,178). Normal nuclear scans, however, expected to occur in patients with no CAD or in patients with only mild angiographic CAD, are associated with a very low risk of either cardiac death or nonfatal MI. Several explanations may account for this apparent paradox. Patients with severe multivessel CAD (and extensively abnormal stress perfusion images) also probably have more numerous mild plaques subject to potential instability and acute MI than do patients with no severe stenoses. In the seminal study of Little *et al.* (177), which documents that many acute infarcts occur on previously “mild” stenoses, the vast majority of patients had multivessel severe stenoses as well. Another potential explanation for the apparent paradox involves a differential response to stress of mild stenoses associated with stable and unstable plaque due to abnormal endothelial function (112,179,180). Thus, perfusion imaging identifies *the patient* at risk for events such as acute MI, rather than *the lesion* at risk.

Studies including large patient samples have now demonstrated that factors estimating the extent of LV dysfunction (LVEF, the extent of infarcted myocardium, transient ischemic dilation (TID) of the LV, and increased lung uptake of Tl-201) are excellent predictors of cardiac mortality. In contrast, markers of provocative ischemia (exertional symptoms, electrocardiographic changes, the extent of reversible perfusion defects, and stress induced ventricular dyssynergy) are better predictors of the subsequent development of acute ischemic syndromes (181). Recent reports have indicated that stress myocardial perfusion SPECT yields incremental prognostic value over clinical and exercise data with respect to cardiac death as an isolated endpoint (181-183). To maximally extract the information regarding prognostic determinants in CAD, it is necessary to consider the full extent and severity of abnormality, either quantitatively (145-147) or semiquantitatively (84), rather than simply determining that the nuclear study is normal or abnormal. The evaluation of prognosis can be facilitated by assessing global perfusion abnormalities by using a composite variable incorporating the extent and severity of hypoperfusion during stress. Table 11 summarizes the most commonly used summed scores.

Furthermore, there appears to be incremental value in measuring both perfusion and function for the purposes of

risk stratification, thus leading to increased prognostic utility of gated cardiac SPECT over standard myocardial perfusion SPECT (181).

1. Nongated MPI

Notwithstanding the demonstrated advantages of gated imaging, nongated myocardial perfusion scintigraphy has played a major role in risk stratification of patients with CAD. SPECT (or planar) imaging with Tl-201 or Tc-99m perfusion tracers, with images obtained at stress and at rest or redistribution, provides important information about the severity of functionally significant CAD. The prognostic value of stress MPI in chronic SA is summarized in Table 12 (studies that included more than 100 patients who did not have recent MI, and that included both positive and negative perfusion images; when multiple reports came from a single institution, only the report with the largest number of patients is included). Normal stress myocardial perfusion SPECT results are highly predictive of a benign prognosis, being consistently predictive of a less than 1% annual risk of cardiac death or MI (Table 13). The difference between the studies in Tables 12 and 13 is that Table 13 did not require that the study contain patients with both positive and negative scan results.

In patients with abnormal SPECT studies, the risk of cardiac death in MI increased with increasing degree of scan abnormalities. In a prospective study of 5183 consecutive patients who underwent rest/stress myocardial perfusion studies, patients with normal scans were at low risk (less than 0.5% per year) for cardiac death and MI during 642 plus or minus 226 days of mean follow-up. Rates of both outcomes increased significantly with worsening scan abnormalities as measured by the summed stress score (SSS) (183). In addition, patients with a mildly abnormal SSS had a low risk of cardiac death (0.8% per year) but an intermediate rate of nonfatal MI (2.3%/year). Similar results have been shown in large series with Tl-201. The magnitude of the perfusion abnormality was the single most important prognostic indicator in another study that demonstrated independent and incremental prognostic information from SPECT Tl-201 scintigraphy compared with that obtained from clinical, exercise treadmill, and catheterization data (201).

Findings other than perfusion defects on myocardial perfusion SPECT are also related to severe or extensive CAD and adverse outcome. Lung uptake of Tl-201 or Tc-99m-*sestamibi* on postexercise or pharmacologic stress images is an indicator of stress-induced global LV dysfunction and is

Table 11. Definitions of Summed Perfusion Scores

Summed Stress Score (SSS)*	Sum of the Segmental Scores at Stress	Amount of infarcted, ischemic, or jeopardized myocardium
Summed Rest Score (SRS)*	Sum of the Segmental Scores at Rest	Amount of infarcted or hibernating myocardium
Summed Difference Score (SDS)*	SSS-SRS	Amount of ischemic or jeopardized myocardium

*Reflect the extent and severity of perfusion abnormality (184).

Table 12. Prognostic Value of Stress Myocardial Perfusion Single-Photon Emission Computed Tomography in Definite or Suspected Coronary Artery Disease

Year, Author	n	Agent	Type of Stress	Mean Age (y)	Men (%)	Patient Population	Abnormal SPECT F/U (%)	Mean F/U (mo)	HE (%/y)	HE/Abnormal SPECT (%/y)	HE/Normal SPECT (%/y)	RR
2003, Berman (185)	5333	Sestamibi	Adenosine	71	50	CAD or Suspected CAD	50	27	2.3	3.9	0.8	4.93
2001, Galassi (186)	459	Tetrofosmin	Exercise	58	78	CAD or Suspected CAD	77	37	2.5	3.0	0.9	3.2
1999, Vanzetto (187)	1137	Tl-201	Exercise	55	75	CAD or Suspected CAD	66	72	1.5	2.0	0.6	3.53
1998, Hachamovitch (183)	4104	Sestamibi (Dual)	Exercise	63	66	Suspected CAD	39	19.4	2.2	4.7	0.7	6.67
1998, Olmos (188)	225	Tl-201	Exercise	56	76	Suspected CAD	49	44.4	1.8	2.7	0.9	2.86
1998, Alkeylani (189)	086	Sestamibi	Exercise or Dipyridamole	64	88	Suspected CAD	62	27.6	3.4	5.0	0.6	8.92
1997, Snader (190)	3400	Tl-201	Exercise	58	63	Suspected CAD	21	-24	1.6 (ACM)	-3.8 (ACM)	-1.0 (ACM)	3.75
1997, Boyne (192)	229	Sestamibi	Exercise	58	50	CAD or Suspected CAD	32	19.2	2.2	5.1	0.8	6.23
1996, Geleijnse (192)	392	Sestamibi	Dobutamine-Atropine	60	56	SA	67	22	6.0	8.7	0.8	10.67
1995, Heller (193)	512	Sestamibi	Dipyridamole	67	44	CAD or Suspected CAD	58	12.8	4.6	6.9	1.3	5.29
1994, Machecourt (194)	1926	Tl-201	Exercise or Dipyridamole	57	68	Suspected CAD or Angina, CAD or Suspected CAD	63	33	2.0	2.9	0.5	6.23
1994, Kamal (195)	177	Tl-201	Dipyridamole	64	62	CAD	83	22	4.3	5.2	0	-
1994, Stratmann (196)	534	Sestamibi	Adenosine	65	97	SA	66	13	10.1	14.3	1.6	9.12
1994, Stratmann (197)	521	Sestamibi	Dipyridamole	59	98	SA	60	13	4.2	6.7	0.5	14.60

ACM indicates all-cause mortality; CAD, coronary artery disease; Dual, performed with Tl-201 rest studies; F/U, follow-up; HE, hard event (ie, cardiac death or nonfatal myocardial infarction); RR, relative risk; SA, stable angina; SPECT, single-photon emission computed tomography; y, year.

Table 13. Prognostic Value of Normal Stress Myocardial Perfusion Single-Photon Emission Computed Tomography

Year, Author	n	Agent	Type of Stress	Mean Age (y)	Men (%)	Patient Population	Normal SPECT F/U (%)	Mean F/U (mo)	HE/Abnormal SPECT (%/y)
2003, Hachamovitch (198)	15475	Sestamibi (dual)	Exercise or Adenosine	61	51	CAD or Suspected CAD	48	21.9	0.6
2001, Galassi (186)	459	Tetrofosmin	Exercise	58	78	CAD or Suspected CAD	23	37	0.9
2000, Groutas (199)	236	Tetrofosmin (dual)	Exercise or Adenosine	61	43	Normal SPECT	100	25	0.4
1999, Gibbons (182)	4473	Tl-201 or Sestamibi	Exercise	61	46	Normal or near normal SPECT	100	36	0.6
1999, Soman (200)	473	Sestamibi	Exercise or Dipyridamole	56	58	Normal SPECT	100	30	0.2
1999, Vanzetto (187)	1137	Tl-201	Exercise	55	75	CAD or Suspected CAD	34	72	0.6
1998, Olmos (188)	225	Tl-201	Exercise	56	76	CAD or Suspected CAD	51	44.4	0.9
1998, Alkeylami (189)	1086	Sestamibi	Exercise or Dipyridamole	64	88	SA	38	27.6	0.6
1997, Snader (190)	3400	Tl-201	Exercise	58	63	Suspected CAD	79	~24	~1.0 (ACM)
1997, Boyne (191)	229	Sestamibi	Exercise	58	50	CAD or Suspected CAD	68	19.2	0.8
1996, Geleijnse (192)	392	Sestamibi	Dobutamine-Atopine	60	56	SA	33	22	0.8
1995, Heller (193)	512	Sestamibi	Dipyridamole	67	44	CAD or Suspected CAD	42	12.8	1.3
1994, Macheourt (194)	1926	Tl-201	Exercise or Dipyridamole	57	68	Angina, CAD or Suspected CAD	37	33	0.5
1994, Kamal (195)	177	Tl-201	Adenosine	64	62	CAD	17	22	0
1994, Stratmann (196)	534	Sestamibi	Dipyridamole	65	97	SA	34	13	1.6
1994, Stratmann (197)	521	Sestamibi	Exercise	59	98	SA	40	13	0.5
Total	27855						48	26.8	0.6

ACM indicates all-cause mortality; CAD, coronary artery disease; dual, performed with Tl-201 rest studies; F/U, follow-up; HE, hard event (ie, cardiac death or nonfatal myocardial infarction); mo, months; RR, relative risk; SA, stable angina; Sestamibi, Tc-99m-sestamibi; SPECT, single-photon emission computed tomography; Tetrofosmin, Tc-99m-tetrofosmin; y, years.

associated with pulmonary venous hypertension in the presence of multivessel CAD (202-206). Increased lung uptake of thallium induced by exercise or pharmacologic stress is also associated with a high risk for cardiac events (207). One study has reported that Tc-99m-sestamibi lung uptake after stress is a marker of severe and extensive CAD (205). Transient poststress ischemic LV dilation, often referred to as TID, and noted by comparison of the LV size from ungated poststress and rest acquisitions, also correlates with severe (greater than 90% stenosis) proximal left anterior descending or two- or three-vessel CAD (208-212). This finding is frequently seen in patients with severe and/or extensive CAD with either exercise or vasodilator stress.

2. Gated SPECT

The information contained in the combined assessment of perfusion and function with gated myocardial perfusion SPECT is likely to enhance its prognostic and diagnostic content. The most common current approach combines poststress and/or rest LV function by gated SPECT with rest and/or stress perfusion measurements.

Because gated SPECT has become routine only recently, there are few reports of the incremental value of combined assessment of perfusion and function over perfusion alone in assessing prognosis. Sharir *et al.* (213), studying 1680 patients, demonstrated that both poststress LVEF and end-systolic volume provided significant information over the extent and severity of perfusion defect as measured by the SSS in prediction of cardiac death. Furthermore, these investigators also demonstrated that LV end-systolic volume provided added information over poststress LVEF in prediction of cardiac death. In a subsequent study of 2686 consecutive patients undergoing stress Tc-99m myocardial perfusion SPECT, Sharir *et al.* (181) demonstrated that poststress EF and the extent of stress induced ischemia as assessed by the summed difference score (SDS) provide complementary information in the prediction of risk of cardiac death. EF was the strongest predictor of mortality, whereas the SDS was the strongest predictor of MI. The combined variables were more effective in risk stratification of patients than were the stress nuclear variables or poststress EF alone. With gated SPECT, it is important to distinguish the poststress LVEF from the resting EF, because in patients with severe CAD stress induced stunning can result in prolonged depression of LVEF (214).

3. Radionuclide Angiography

Rest LVEF is universally recognized as one of the most important determinants of long-term prognosis in patients with chronic stable CAD (215,216). RNA can also be helpful in evaluating dyspnea by establishing the state of right ventricle (RV) and LV performance. LV function during exercise reflects disease severity and provides prognostic information. Jones and colleagues from the Duke databank have studied rest and exercise first-pass RNA (FPRNA) extensively during the past two decades. Patients with sus-

pected CAD could be risk stratified for subsequent cardiac death by using a diagnostic threshold of 50% EF (217-222). A decline in LVEF in response to exercise is an important indicator of CAD severity and is associated with a poorer 3-year survival than if LVEF increases during exercise (223). In patients with mild symptoms, rest LV dysfunction and one-, two-, or three-vessel CAD, an abnormal peak exercise LVEF or a decrease in LVEF during exercise identifies patients with a poorer prognosis (218,224,225). Patients with preserved LV function at rest, but with enough inducible ischemia to severely reduce LVEF during exercise, also appear to be at greater risk of death (226). Event rates in those with a normal rest LVEF are low, however, and one study indicates that exercise data do not confer independent prognostic information in such patients (227).

4. Cost Effectiveness

The ACC/AHA 2002 Guideline Update for the Management of Patients With Chronic Stable Angina (52) encourages the use of cardiac imaging as a gatekeeper to cardiac catheterization in order to minimize the rate of normal catheterizations and to enrich the angiographic population with a greater proportion of patients with significant, yet treatable disease. To test the principle of selective resource use, Hachamovitch *et al.* (183) reported that when catheterization was limited to patients with moderate-severe perfusion abnormalities (ie, SSS greater than 8), significant cost savings were achieved for 5183 patients undergoing dual isotope stress SPECT imaging. The results revealed a 17% reduction in the rate of cardiac catheterization and cost savings ranging from 22 to 55% for high- to low-risk pretest patients. The SSS appeared to identify patients who benefited from revascularization; in comparing the patients undergoing early revascularization to those undergoing medical therapy, a reduction in mortality with revascularization was observed only in those with very abnormal SSS. O'Keefe *et al.* (228) have reported similar excellent outcomes with medical versus invasive strategies in patients without high-risk stress nuclear findings.

Shaw *et al.* (229) have evaluated a population of 11 249 consecutive SA patients, gathered in a large multicenter trial comprising many U.S. laboratories. In a matched cohort study comparing direct catheterization to myocardial perfusion SPECT with selective catheterization in patients with chronic SA, for all levels of pretest clinical risk, there was a substantial reduction (31 to 50%) in costs when using the SPECT plus selective catheterization approach. This reduction was seen in both the diagnostic (early) and follow-up (late) costs, and included costs of revascularization. Rates of subsequent nonfatal MI and cardiac death were virtually identical in all patient risk subsets. The rate of revascularization, however, was reduced by nearly 50% in the MPI with selective catheterization cohort.

5. Frequency of Testing

Considerations for follow-up testing are summarized in the ACC/AHA 2002 Guideline Update for the Management of Patients With Chronic Stable Angina (52). If patients develop new signs or symptoms that suggest a worsened clinical state, repeat testing at the time of worsening would be appropriate. In the absence of a change in clinical state, the estimated patient risk after initial testing (high, intermediate, or low, as defined earlier) should play an important role in individual recommendations. These recommendations may, of course, also vary with additional factors (eg, age, degree of control of risk factors, and overall clinical state) (198).

6. Evaluation of the Effects of Medical Therapy

For purposes of assessment of medical therapy, either exercise or pharmacologic vasodilator stress might be considered for use with myocardial perfusion SPECT. Mahmarian *et al.* (230), Eichstadt *et al.* (231), and Lewin *et al.* (232) have demonstrated that exercise myocardial perfusion SPECT can be used to document reductions in ischemia with medical therapy. With vasodilator stress, it is important that the patients are not under the influence of caffeine at the time of testing, because caffeine can block the vasodilator effects of adenosine and dipyridamole. Although the available evidence suggests that the efficacy of therapy can be assessed with repeat SPECT procedures while the patient is under the effects of the medical treatment, information about the effects of medical therapy on outcomes is limited. Thus, the clinical utility of radionuclide testing for this purpose remains to be defined.

C. Specific Patient Populations

1. African Americans

The role of noninvasive imaging has rarely been studied or discussed in African Americans or other minorities (189,233-235). In two published studies to date, a normal rest and stress SPECT perfusion study was associated with a 2% per year rate of AMI and/or cardiac death, rather than the less than 1% that has been reported in other populations. Both of those studies, however, included higher than usual cardiac risk patients: those with prior MI (233) (despite normal Tl-201 SPECT) and those with typical angina pectoris (189). In addition, neither study accounted for the incidence of LV hypertrophy (LVH) on SPECT (234) before describing the study as normal. Hypertensive LVH has been recognized as a risk factor in sudden cardiac death and is more prevalent among African Americans. This increases the predisposition to arrhythmias and potentially lethal ischemic events. In one report of survival among African Americans with LVH and CAD, hypertrophy accounted for 40% of the attributive risk of cardiac death (235).

2. Women

The use of radionuclide testing in women is influenced importantly by the later presentation of CAD in women than

in men and by sex-related limitations in exercise stress testing. CAD presents 10 to 15 years later in women than in men. Prevalence begins to increase with the onset of menopause and achieves equivalence at age 70 years (236). The likelihood of coronary disease is exceedingly low in nondiabetic women less than 45 years of age. Limitations of exercise testing have been reviewed in the ACC/AHA 2002 Guideline Update for Exercise Testing (237) (http://www.acc.org/clinical/guidelines/exercise/exercise_clean.pdf).

These issues have provoked interest in the potential additive benefit of stress perfusion imaging in women, particularly those with at least an intermediate likelihood of coronary disease. Initial studies using Tl-201 encountered specificity limitations, often the result of soft-tissue (breast) attenuation, usually in the anterior and anterolateral segments (72,77,238). The recent use of Tc-99m perfusion agents and gated SPECT have enhanced image quality, resulting in reported sensitivities and specificities for detecting coronary disease similar to those in men. In a small randomized trial comparing the diagnostic accuracy of Tl-201 and gated Tc-99m-sestamibi in women, specificities were 67% versus 92%, respectively (77). A retrospective analysis of more than 4000 patients (2/3 men, 1/3 women) who underwent rest Tl-201/exercise Tc-99m-sestamibi SPECT imaging reported incremental prognostic value of MPI as compared to clinical and exercise variables in women as well as men (239). Studies using adenosine Tc-99m-sestamibi SPECT perfusion imaging are now also available. Pharmacologic stress testing deserves particular consideration in women likely to exercise only submaximally (237,240). Amanullah *et al.* (241) reported 91% sensitivity and 86% specificity for detecting coronary disease (greater than 50% diameter stenosis) in 130 women without prior MI, and documented a normalcy rate of 93% in 71 women with a low likelihood of coronary disease. They subsequently found that a moderately to severely abnormal perfusion scan in women (SSS greater than 8) was associated with a 91% sensitivity and 70% specificity for detecting multivessel coronary disease (242). They have also reported that adenosine myocardial perfusion SPECT has similar prognostic value in women with suspected coronary disease as in men (185). PET, similar to Tc-99m-sestamibi (or tetrofosmin) imaging, is advantageous in terms of minimizing soft-tissue attenuation artifacts, and is also under active study in women.

With a perception on the part of clinicians of diminished accuracy of test results in women, the possibility of sex-related referral bias in using noninvasive testing to select patients for coronary arteriography has been raised (243). However, 3 published studies argue against this possibility (246).

3. Normal Resting ECG, Able to Exercise

Patients with a normal resting ECG constitute a large and important subgroup. Most patients who present with multiple risk factors with or without cardiac symptoms have a normal resting ECG (247). Such patients are likely (92 to 96%) to

have normal LV function (248-250) and to have an excellent prognosis (247).

Several studies have examined the incremental value of exercise myocardial perfusion SPECT compared with the exercise ECG in patients with a normal resting ECG who are not taking digoxin (251-255). The exercise ECG has a higher specificity in the absence of rest ST-T changes, LVH, and digoxin. In an analysis that included clinical and exercise ECG parameters for the prediction of left main or three-vessel disease, the modest incremental benefit of imaging did not appear to justify its cost, which has been estimated at \$20550 per additional patient correctly classified (254,256). Mattera *et al.* (255) did report some incremental value, but only for the prediction of hard and soft events (including UA) and only if the exercise ECG was abnormal. The investigators still favored a stepwise strategy that used the exercise ECG as the initial test, such as that proposed by others (253,257). For these reasons, a stepwise strategy is generally recommended in which an exercise ECG, and not a stress imaging procedure, is performed as the initial test in patients with an intermediate pretest likelihood of CAD who are not taking digoxin, have a normal resting ECG, and are able to exercise (52).

A stress imaging technique should be used for patients with widespread rest ST depression (more than 1 mm), complete left bundle-branch block (LBBB), ventricular paced rhythm, pre-excitation, or LVH (52). Although exercise capacity can be assessed in such patients, exercise-induced ischemia cannot be reliably assessed with the stress ECG. Patients unable to exercise because of physical limitations such as reduced exercise capacity, arthritis, amputations, severe peripheral vascular disease, or severe chronic obstructive pulmonary disease should undergo pharmacologic stress testing in combination with imaging.

4. Intermediate-Risk Duke Treadmill Score

The Duke treadmill score combines various forms of information from stress testing and provides a simple way to calculate risk (258,259). The Duke treadmill score equals {exercise time (in minutes) – [5 times the ST-segment deviation, during or after exercise (in millimeters)] – [4 times the angina index (which has a value of 0 if there is no angina, 1 if angina occurs, and 2 if angina is the reason for stopping the test)]}. The annual mortality rate according to risk groups based on the Duke treadmill score is illustrated in Table 20 of the ACC/AHA 2002 Chronic Stable Angina Guideline Update (52). Among outpatients with suspected CAD, two thirds of those with scores indicating low risk had a 4-year survival rate of 99% (average annual mortality rate 0.25%), whereas the 4% who had scores indicating high risk had a 4-year survival rate of 79% (average annual mortality rate 5%). The score has been reported to work well for both inpatients and outpatients, and data suggest that the score works equally well for men and women (258,260,261). However, only a small number of elderly patients has been studied. Comparable scores have been developed by others (262).

Although many patients can be risk stratified on the basis of the Duke treadmill score, many may also fall into a group with an intermediate score associated with an intermediate risk of cardiac death (1.25% per year; see Table 4: Pretest Probability of CAD by Age, Gender, and Symptoms from the ACC/AHA 2002 Guideline Update for Exercise Testing [237]). In these patients several studies have demonstrated the value of myocardial perfusion scintigraphy in further risk assessment (182,261,263). In one study of 2203 patients, rates of cardiac death or nonfatal MI were related to the results of myocardial perfusion SPECT within each risk category of the Duke treadmill score (261,264). In addition, in all patient groups, subsequent catheterization rates more closely paralleled the nuclear score results than the Duke treadmill score results. Similar data have been demonstrated in a large multicenter data set analyzed by Shaw *et al.* (263). In a study of 4649 patients with an intermediate Duke treadmill score and normal or near normal myocardial perfusion SPECT studies, gathered by using multiple SPECT protocols in multiple centers, Gibbons *et al.* (182) demonstrated that the seven-year mortality rate was 1.5%, less than the 1% per year threshold; furthermore, these investigators demonstrated that the test results were appropriately affecting patient management: Over 7 years the cumulative frequency of catheterization in these patients was only 17%.

5. Normal Resting ECG, Unable to Exercise

In patients with an intermediate to high likelihood of CAD who have a normal resting ECG but are unable to exercise, pharmacologic myocardial perfusion SPECT with adenosine or dipyridamole has been shown to be highly effective in diagnosis and risk stratification. The risk of cardiac death, however, in these patients appears to be higher than that associated with patients who are able to exercise (ie, in large prognostic series, the requirement of pharmacologic stress has been an independent prognostic variable in multivariate analyses) (183). The higher risk of patients undergoing pharmacologic stress is most likely related to an increased underlying risk of this population compared to patients who are able to exercise.

6. LBBB/Pacemakers

Pharmacologic stress perfusion imaging is preferable to exercise perfusion imaging for purposes of both diagnosis and risk stratification. Several studies have observed an increased prevalence of myocardial perfusion defects during exercise imaging, in the absence of angiographic coronary disease, in patients with LBBB (265-267). These defects often involve the interventricular septum, may be reversible or fixed and are often absent during pharmacologic stress. Thus, perfusion imaging with pharmacologic vasodilation appears to be more accurate for identifying CAD in patients with LBBB (268-270).

Nonetheless, there are certain clinical circumstances in which exercise stress testing with MPI may provide clinically relevant information even given the likelihood of inducing

a false-positive septal reversible defect in a patient with LBBB. For example, in a patient with an exertional chest pain syndrome, observing the induction of similar chest pain at a low treadmill workload in conjunction with multiple perfusion defects (well beyond the septal area) would identify that the clinical symptoms are likely secondary to multivessel CAD. In contrast, a patient referred for imaging for detection of underlying CAD because of the finding of LBBB on an ECG would be most appropriately tested using pharmacologic stress imaging.

Regarding risk stratification, 245 patients with LBBB underwent SPECT imaging with Tl-201 or Tc-99m-sestamibi during dipyridamole or adenosine stress testing (271). The 3-year overall survival rate was 57% in patients classified as high risk by SPECT compared with 87% in those classified as low risk (P equals 0.001). Patients with a low-risk scan had an overall survival rate that was not significantly different from that of the U.S.-matched population (P equals 0.86). The value of pharmacologic perfusion imaging for prognostication has been confirmed in three other studies (272-274), which included more than 300 patients followed for a mean of nearly 3 years. Given that ECG testing is non-diagnostic in patients with ventricular pacing in a manner similar to that observed with LBBB, it is likely that the considerations regarding the use of radionuclide techniques for diagnostic and risk stratification purposes in patients with ventricular pacemakers are the same as those applied to patients with LBBB. A single study has reported that dobutamine stress is accurate in CAD detection in combination with myocardial perfusion scintigraphy in patients with LBBB (275). Another small study has further described the use of myocardial perfusion SPECT for the risk stratification of patients with implantable cardioverter-defibrillators (276).

7. Left Ventricular Hypertrophy

In patients with LVH, with or without resting ST-segment abnormality, ST depression during exercise is frequently present in the absence of significant CAD. In these patients, stress nuclear techniques have been shown to have similar diagnostic sensitivity and specificity to those observed in patients without LVH (65). It has also been shown that the diagnostic value of myocardial perfusion SPECT is not generally degraded by the presence of hypertension without evidence of LVH (65), although an increased frequency of false-positive studies has been reported in healthy athletes (277). Similarly, although the number of reports is small, the prognostic value of myocardial perfusion SPECT in patients with LVH appears to be equal to that observed in patients without LVH (278).

8. Patients With Nonspecific ST-T Wave Changes

Patients with nonspecific ST-T wave changes, such as might occur with digoxin, Wolff-Parkinson-White syndrome (WPW), or other conditions, are considered to have nondiagnostic stress ECG responses with respect to ST-segment depression. Although there are limited data regarding the

diagnostic and prognostic information for myocardial perfusion SPECT in these patients, those with intermediate to high likelihood of coronary disease can perhaps be effectively assessed for detection and risk stratification with myocardial perfusion SPECT.

9. Elderly

Prognostic value of perfusion scintigraphy in elderly patients has been reported (279). In an exercising population more than 70 years of age, an abnormal exercise thallium imaging was accurate in identifying a high-risk population (279). Because of the higher mortality rate of the general population in this age group, upward adjustment of the intermediate-risk group to levels more than the 1 to 3% as used for general populations may be appropriate. In a preliminary communication, Hayes *et al.* (280) demonstrated that gated SPECT provided incremental prognostic value over nongated SPECT in patients more than 70 years of age.

10. Asymptomatic Patients

MPI has been studied in asymptomatic populations both to detect underlying angiographic CAD and to predict future clinically manifest cardiac events such as revascularization, MI, and cardiac death. As an example, Blumenthal *et al.* (281) found that among asymptomatic siblings of patients with manifest CAD (a group known to be at increased risk of developing CAD), the relative risk (RR) of a cardiac event was 4.7 for those with an abnormal scan, which was a more pronounced risk than having an abnormal exercise ECG. Moreover, the siblings with a concordant abnormal exercise ECG and abnormal perfusion scan had a RR of 14.5.

In any more general asymptomatic population, however, the relatively low prevalence of CAD or risk of future events will affect the performance of any test in a manner predictable by Bayesian principles. Although relative risks will be high with an abnormal test compared to a normal test, the positive predictive value will usually be low. This has been demonstrated by using MPI both to detect CAD (282) and to predict future events (283). It is not clear that detecting asymptomatic, preclinical CAD will lead to therapeutic intervention that will reduce risk beyond that indicated by risk factor profiling and currently recommended strategies to reduce risk (47). The finding of occult CAD may dictate more aggressive risk factor reduction, however.

Persons whose occupations may affect public safety (eg, airline pilots, truckers, bus drivers), or who are professional or high-profile athletes, commonly undergo periodic exercise testing for assessment of exercise capacity and prognostic evaluation of possible CAD (237). Although there are insufficient data to justify this approach, these evaluations are performed for statutory reasons in some cases (237). In some asymptomatic subjects, testing may be appropriate when there is a high-risk clinical situation (eg, diabetes or multiple risk factors) (281). National Cholesterol Education Program guidelines advocated the approach of using a 10-year risk of developing coronary heart disease in determining the aggres-

siveness of treatment for asymptomatic subjects (47). Patients with a greater than 20% 10-year risk are considered to have high risk of developing CAD. Based on the data of Blumenthal *et al.* (281), the use of MPI could theoretically be used to stratify these patients into more precise risk categories.

11. Obese Patients

Very obese patients constitute a special problem because most imaging tables used for SPECT have weight-bearing limits (often 300 lb [135 kg]) that preclude imaging very heavy subjects. These subjects can still be imaged by planar scintigraphy. Obese patients often have suboptimal perfusion images, especially with Tl-201, owing to the marked photon attenuation by soft tissue. In these patients, either Tc-99m-sestamibi or tetrofosmin is probably most appropriate and should yield images of better quality. Image quality can be improved by performing rest and stress imaging on separate days, using a high dose of the Tc-99m-labeled agent in both cases. PET imaging may be superior to conventional MPI in very obese subjects.

12. Diabetes

The increasing recognition of diabetes mellitus as a major risk factor for cardiovascular disease (284) has heightened interest in MPI for CAD diagnosis and risk stratification. Available studies are based on retrospective analyses of patients referred to the nuclear cardiology laboratory. Prospective information in asymptomatic diabetic patients drawn from the general diabetic population is awaited (285).

Kang *et al.* (286) have demonstrated in a large population that Tc-99m-sestamibi myocardial perfusion SPECT has comparable sensitivity, specificity, and normalcy rate for the diagnosis of CAD in diabetic and nondiabetic patients. In a study of 1271 with diabetes and 5862 without diabetes, a normal scan was similarly predictive of low cardiac event rates in both groups. Risk-adjusted event-free survival in patients with mildly and moderately to severely abnormal scans, as defined by the SSS, was worse in patients with diabetes than in nondiabetics (286).

In a multicenter observational study comparing 929 patients with diabetes with 3826 patients without diabetes, Giri *et al.* (287) demonstrated that the presence and extent of myocardial perfusion SPECT abnormality was an independent predictor of cardiac death alone or cardiac death and MI in patients with and without diabetes. Women with diabetes had the worst outcome for any given extent of reversible myocardial defect. The presence of multivessel ischemia was the strongest predictor of total cardiac events and a multivessel fixed defect was a greater predictor of cardiac death in diabetic patients. Risk stratification by stress and SPECT MPI was incremental to that provided by clinical risk assessment. Although survival during the first two years of follow-up in patients with normal SPECT results was similar between patients with and without diabetes, after 2 years the rates increased in patients with diabetes but not in patients without diabetes. Based on these data, the investigators sug-

gested that retesting of diabetic patients with normal studies should occur earlier than in a nondiabetic population.

In a preliminary report, Hayes *et al.* (288) demonstrated that assessment of LVEF from gated SPECT provides incremental value over perfusion SPECT parameters in predicting death in diabetic patients. Of 714 consecutive diabetic patients undergoing gated myocardial perfusion SPECT, the poststress EF added incremental value to the SSS for the prediction of cardiac death.

13. After Coronary Calcium Screening

Various CT techniques, including EBCT and multislice helical CT, are now being used to measure coronary artery calcium scores for the early detection of coronary atherosclerosis. Although some patients can benefit from nuclear stress testing after EBCT, it would clearly not be cost-effective for all patients with atherosclerosis measured by EBCT to go on to the more expensive nuclear cardiology testing. He *et al.* (289) evaluated the frequency of stress-induced ischemia by myocardial perfusion SPECT in 292 men and 78 women who had undergone EBCT testing. Only one of more than 100 patients who demonstrated coronary calcium scores (CCS) of 100 or less had an abnormal myocardial perfusion scan. Twelve percent of patients with moderate CCS (101 to 399) and 47% of patients with extensive CCS (more than 400) had abnormal myocardial perfusion SPECT. In general, when the EBCT score is more than the 75th percentile for age and sex, stress nuclear testing may sometimes be appropriate for purposes of risk stratification.

14. Before and After Revascularization

a. Radionuclide Imaging Before Revascularization Interventions

The high degree of variability in the relationship between visually assessed angiographic degree of stenosis and coronary flow reserve (109) is well recognized. When there is uncertainty regarding the appropriate choice of therapy after coronary angiography, stress nuclear testing can risk-stratify 25 to 75% lesions usefully (290,291). Patients with no ischemia measured by nuclear testing have relatively low risk for cardiac events (292,293). Even in patients with left main or 3-vessel disease on angiography, those with a low-risk SPECT study show an excellent event-free survival rate with medical therapy. Cost-effectiveness analyses further indicate a role for MPI in reducing the rate of revascularization in patients with symptoms of SA, with no implications as to patient outcome (229). Although less critical in CABG, in which typically all suitable vessels with significant angiographic stenoses (more than or equal to 50%) are bypassed, perfusion imaging is particularly helpful in determining the functional importance of single or multiple stenoses in the case of percutaneous interventions targeted to a "culprit lesion" (ie, the ischemia-provoking stenosis). For this application, it is important that patients achieve 85% of maximal-predicted heart rate (MPHR), in order to "unmask" more than just the most severely ischemic region that could lead to

early exercise termination. If a patient cannot achieve this level of exercise, pharmacologic stress may be superior for identifying all regions of stress-induced abnormal perfusion.

b. Radionuclide Imaging After Percutaneous Coronary Intervention

The published ACC/AHA 2002 Guideline Update for Exercise Testing summarizes the available information on exercise testing after percutaneous coronary intervention (PCI) (237). Symptom status is an unreliable index of development of restenosis, with 25% of asymptomatic patients documented as having ischemia on exercise testing (237,294-296). Sensitivities of the exercise ECG for detecting restenosis range from 40 to 55%, less than have been reported with SPECT (294,295,297-299) or exercise echocardiography (299-301). MPI can be helpful in appropriately selected patients. Abnormal perfusion patterns may also reflect periprocedural myocardial injury, side-branch compromise due to plaque shift or stent overlap, new disease, or functional significance of angiographically recognized disease in nonrevascularized vessels. Differentiation among these causes of an abnormal perfusion scan is facilitated if the preintervention anatomy and the procedural details are available.

Neither exercise testing nor radionuclide imaging is indicated in the first month or two after PCI without a specific indication. McPherson *et al.* (302) reported that a minority (30%) of patients with recurrent chest pain within 30 days of PCI had restenosis angiographically. Because myocardial ischemia, whether painful or silent, worsens prognosis (303), some have advocated routine stress myocardial perfusion SPECT testing 3 to 12 months after PCI. The ACC/AHA 2002 Guideline Update for Exercise Testing (237), however, favors only selective stress imaging in patients considered at particularly high risk (eg, patients with decreased LV function, multivessel CAD, proximal left anterior descending disease, previous sudden death, diabetes mellitus, hazardous occupations, and suboptimal PCI results).

The major indication for perfusion imaging in patients late after successful PCI is to evaluate symptoms suggesting new disease. Although some would consider retesting in asymptomatic patients with worrisome arteriographic disease patterns, the role of nuclear testing in risk stratification late after PCI requires further study. Ho *et al.* (304) studied 211 low-risk patients between 1 and 3 years after percutaneous transluminal coronary angioplasty and monitored them for 7.3 years. Despite a low overall annual event rate of 1% per year, an abnormal SSS was significantly predictive of cardiac death or MI, whereas a normal SSS was associated with low risk.

c. Radionuclide Imaging After CABG

Abnormal perfusion patterns after CABG may reflect bypass graft disease, disease in the native coronary arteries beyond the distal anastomosis, nonrevascularized coronaries or side-branches, or new disease. Myocardial perfusion scintigraphy can be useful in determining the location, extent, and severi-

ty of ischemia (305). Its prognostic value has been demonstrated both early (306) and late (307) after CABG. Although atypical chest pains are common early postoperatively and are usually nonischemic in origin, perfusion scintigraphy can be helpful in the presence of a suggestive ECG or symptoms. When ischemia occurs 1 to 12 months after surgery, the etiology is usually peri-anastomotic graft stenosis. Ischemia developing more than 1 year postoperatively usually reflects the development of new stenoses in graft conduits and/or native vessels (312). Miller *et al.* (306) studied 411 patients, 55% of whom were symptomatic, a mean of 11 months after CABG. Exercise SPECT was strongly predictive of events, with perfusion defect extent being the only variable predictive of outcome. Ischemia in regions proximal to bypass insertion was not predictive of events. A recent study by Zellweger *et al.* (310) that used stress SPECT reported annual cardiac mortalities of 1.3% and 1.4%, respectively, in asymptomatic and symptomatic patients within 5 years of CABG. Patients with perfusion defects were at higher risk (2.1 vs. 0.4%), and the risk of death increased in relation to higher SSS. A significant increase in global chi-square occurred with respect to cardiac death after adding nuclear data to prescan information.

Four independent studies have addressed the role of SPECT MPI in patients more than 5 years after CABG. Palmas *et al.* (80) demonstrated in 294 patients that a summed reversibility score and the presence of abnormal lung uptake of thallium added incremental information to clinical variables in predicting outcome. Nallamothu *et al.* (308) found similar results. In 250 patients, the extent of the perfusion defect, multivessel defects, and increased thallium lung uptake were independent predictors of events. Lauer *et al.* (309) monitored almost 9000 asymptomatic patients for 4 years after SPECT testing. Patients with ischemia were at greater risk for hard events than were those without ischemia. Importantly, the mortality rate was 3% annually in these asymptomatic patients. In the subset of patients more than 5 years after CABG in the Zellweger study (310), the number of nonreversible segments was the strongest predictor of cardiac death, independent of symptom status.

15. Radionuclide Imaging Before Noncardiac Surgery

The cardiovascular consultant is frequently asked to provide an assessment of perioperative risk and recommendations for treatment in anticipation of noncardiac surgery in patients with known or suspected cardiovascular disease. Concerns regarding the risks of perioperative myocardial ischemia, infarction, and death in patients with CAD drive the performance of noninvasive and invasive testing and frequently provoke discussions concerning the indications for revascularization. Recent guidelines and studies have re-emphasized the importance of clinical, demographic, and surgical indicators of risk (313,314). In general, noninvasive preoperative testing is best directed at patients considered to be at intermediate clinical risk (diabetes, stable CAD, compensated heart failure) who are scheduled to undergo intermediate or

high-risk surgery (eg, transplantation for end-stage renal disease) (315). According to the 2002 ACC/AHA Guideline Update for Perioperative Cardiovascular Evaluation for Noncardiac Surgery (313) (http://www.acc.org/clinical/guidelines/perio/update/periupdate_index.htm), vascular procedures and prolonged, complicated thoracic, abdominal, and head and neck procedures are considered high risk (313,316). A thorough evaluation of appropriately selected patients will also afford an assessment of cardiac prognosis over the long term. The demonstrated efficacy of beta-adrenoreceptor blockade in reducing the perioperative incidence of MI and death in high-risk patients undergoing vascular surgery may reduce the utilization of noninvasive testing and angiography before noncardiac surgery (317). To date, there are no prospective randomized trial data to support the use of prophylactic coronary revascularization. The indications for PCI or CABG before noncardiac surgery are the same as those that pertain in the nonoperative setting (313).

The assessment of ischemic jeopardy before noncardiac surgery should follow the same principles enumerated above for the evaluation of patients with chronic CAD. On occasion, however, patients who require noncardiac surgery will present with active ischemia or decompensated heart failure for which immediate medical stabilization and risk stratification are indicated. The need for emergency noncardiac surgery will always take precedence. In the more elective setting, exercise stress is preferred in all patients capable of achieving adequate workloads; radionuclide techniques should be reserved for those patients whose baseline ECGs render exercise interpretation invalid or who require pharmacologic stress because of the inability to exercise. Functional status, defined either by history or by objective exercise testing, is a major determinant of perioperative and long-term outcomes (313).

a. Myocardial Perfusion Imaging

Table 14, reprinted from the ACC/AHA Guideline Update for Perioperative Cardiovascular Evaluation for Noncardiac Surgery, summarizes studies of MPI for preoperative assessment of cardiac risk (313). The majority of studies examining the utility of MPI to assess perioperative risk have used TI-201 or Tc-99m and pharmacologic stress with dipyridamole or adenosine. Relatively fewer studies have been reported with exercise or dobutamine stress. For patients with radionuclide evidence of ischemia, the positive predictive value of such testing is uniformly low, in the range of 4 to 20%. The negative predictive value of a normal scan, however, is very high (96 to 100%). Patients with reversible defects are at greater risk for perioperative ischemia than are those with fixed defects; the latter defects may in turn be a marker for longer-term risk. The positive predictive value of perfusion imaging can be improved when testing is applied selectively to patients with a higher pretest likelihood of CAD and when the results are integrated into a clinical risk assessment (25,345,346). In addition, several investigators have reported further improvements with the use of quantita-

tive analytic techniques (328,329,331). As reviewed above for patients with chronic CAD, the results of perfusion imaging studies will drive subsequent decisions regarding the need for further investigation (eg, coronary angiography in patients with high-risk clinical and noninvasive markers) and/or therapy.

If a noninvasive assessment of ischemic jeopardy before noncardiac surgery is necessary, the choice between radionuclide stress perfusion imaging and dobutamine stress echocardiography should be made on the basis of institutional expertise, as well as certain patient specific attributes. These include ability to exercise, predicted response to a chosen pharmacologic agent, body size, and chest configuration. As examples, patients with severe bronchospasm should not receive dipyridamole or adenosine; large body size may limit transthoracic echocardiographic windows and predispose to soft tissue attenuation artifacts in radionuclide imaging; and patients with LBBB should preferentially undergo dipyridamole or adenosine radionuclide imaging. A meta-analysis has shown comparable predictive values among dipyridamole TI-201 scanning, dobutamine stress echocardiography, radionuclide ventriculography, and ambulatory ECG before to vascular surgery (347). The ACC/AHA Guidelines for Perioperative Cardiovascular Evaluation for Noncardiac Surgery have been updated (313).

b. Radionuclide Ventriculography

Exercise radionuclide ventriculography is rarely performed to assess ischemic jeopardy before noncardiac surgery. The evaluation of resting LV function, however, is an important component of the preoperative assessment of patients with symptoms and/or signs of heart failure. LV systolic function is now routinely assessed with gated SPECT techniques at the time of MPI. Not unexpectedly, the risk of perioperative complications is highest among patients with a resting LVEF less than 0.35 (348-355). Reduced LV systolic function is a predictor of perioperative heart failure but bears no consistent correlation with the risk of perioperative ischemia.

D. Recommendations: Cardiac Stress Myocardial Perfusion SPECT in Patients Able to Exercise

Recommendations for Diagnosis of Patients With an Intermediate Likelihood of CAD and/or Risk Stratification of Patients With an Intermediate or High Likelihood of CAD Who Are Able to Exercise (to at least 85% of MPHR)

Class I

- 1. Exercise myocardial perfusion SPECT to identify the extent, severity, and location of ischemia in patients who do not have LBBB or an electronically-paced ventricular rhythm but do have a baseline ECG abnormality which interferes with the interpretation of exercise-induced ST segment changes (ventricular pre-excitation, LVH, digoxin therapy, or more than 1 mm ST depression). (*Level of Evidence: B*)**

Table 14. Myocardial Perfusion Imaging for Preoperative Assessment of Cardiac Risk

Year	Author	n*	Patients w/ Ischemia (%)	Events MI/Death (%)	Perioperative Events		Comments
					Positive/PPV	Normal/NPV	
Vascular Surgery							
1985	Boucher (318)	48	16 (33)	3 (6)	19% (3/16)	100% (32/32)	First study to define risk of thallium redistribution
1987	Cutler (319)	116	54 (47)	11 (10)	20% (11/54)	100% (60/60)	Only aortic surgery
1988	Fletcher (320)	67	15 (22)	3 (4)	20% (3/15)	100% (56/56)	
1988	Sachs (321)	46	14 (31)	2 (4)	14% (2/14)	100% (24/24)	
1989	Eagle (322)	200	82 (41)	15 (8)	16% (13/82)	98% (61/62)	Defined clinical risk
1990	McEnroe (323)	95	34 (36)	7 (7)	9% (3/34)	96% (44/46)	Fixed defects predict events
1990	Younis (324)	111	40 (36)	8 (7)	15% (6/40)	100% (51/51)	Includes long-term follow-up
1991	Mangano (325)	60	22 (37)	3 (5)	5% (1/22)	95% (19/20)	Managing physicians blinded to scan result
1991	Strawn (326)	68	n/a	4 (6)	n/a	100% (21/21)	
1991	Watters (327)	26	15 (58)	3 (12)	20% (3/15)	100% (11/11)	Includes echo (TEE) studies
1992	Hendel (328)	327	167 (51)	28 (9)	14% (23/167)	99% (97/98)	Included long-term follow-up
1992	Lette (329)	355	161 (45)	30 (8)	17% (28/161)	99% (160/162)	Used quantitative scan index
1992	Madsen (330)	65	45 (69)	5 (8)	11% (5/45)	100% (20/20)	
1993	Brown (331)	231	77 (33)	12 (5)	13% (10/77)	99% (120/121)	Prognostic utility enhanced by combined scan and clinical factors
1993	Kresowik (332)	170	67 (39)	5 (3)	4% (3/67)	98% (64/65)	
1994	Baron (333)	457	160 (35)	22 (5)	4% (7/160)	96% (195/203)	Did not analyze for cardiac deaths; no independent value of scan
1994	Bry (334)	237	110 (46)	17 (7)	11% (12/110)	NFMI only	
1995	Koutelou (335)	106	47 (44%)	3 (3%)	6% (3/47)	100% (97/97)	Cost-effectiveness data included
1995	Marshall (336)	117	55 (47%)	12 (10%)	16% (9/55)	100% (49/49)	Used adenosine/SPECT thallium imaging
1997	Van Damme (337)	142	48 (34%)	3 (2%)	n/a	97% (33/34)	Used adenosine thallium and sestamibi. Size of ischemic defect enhanced prognostic utility
Nonvascular Surgery[†]							
1990	Camp (338)	40	9 (23)	6 (15)	67% (6/9)	100% (23/23)	Diabetes mellitus, renal transplant
1991	Iqbal (339)	31	11 (41)	3 (11)	27% (3/11)	100% (20/20)	Exercise 86%, diabetes mellitus, pancreas transplant
1992	Coley (340)	100	36 (36)	4 (4)	8% (3/36)	98% (63/64)	Define clinical risk factors in patients with known or suspected CAD
1992	Shaw (341)	60	28 (47)	6 (10)	21% (6/28)	100% (19/19)	Used adenosine
1993	Takase (342)	53	15 (28)	6 (11)	27% (4/15)	100% (32/32)	Patients with documented or suspected CAD include rest echocardiogram
1994	Younis (343)	161	50 (31)	15 (9)	18% (9/50)	98% (87/89)	Intermediate- to high-risk CAD
1996	Stratmann (344)	229	67 (29%)	10 (4%)	6% (4/67)	99% (1/92)	Used dipyridamole sestamibi and noted fixed defect had more prognostic utility than transient defect

[†]Studies utilizing pharmacologic and/or exercise thallium testing.

All studies except those by Coley (340) and Shaw (341) acquired patient information prospectively. Only in reports by Mangano (325) and Baron (333) were scan results blinded from attending physicians.

Patients with fixed defects were omitted from calculations of positive and negative predictive value.

CAD indicates coronary artery disease; MI, myocardial infarction; n*, number of patients who underwent surgery; n/a, not applicable; NFMI, nonfatal myocardial infarction; NPV, negative predictive value; PPV, positive predictive value; SPECT, single-photon emission computed tomography; TEE, transesophageal echocardiography.

Reprinted from Eagle K et al. ACC/AHA Guideline Update for Perioperative Cardiovascular Evaluation for Noncardiac Surgery: a report of the American College of Cardiology/American Heart Association Task Force on Practice Guidelines (313).

2. Adenosine or dipyridamole myocardial perfusion SPECT in patients with LBBB or electronically-paced ventricular rhythm. (*Level of Evidence: B*)
3. Exercise myocardial perfusion SPECT to assess the functional significance of intermediate (25 to 75%) coronary lesions. (*Level of Evidence: B*)
4. Exercise myocardial perfusion SPECT in patients with intermediate Duke treadmill score. (*Level of Evidence: B*)
5. Repeat exercise MPI after initial perfusion imaging in patients whose symptoms have changed to redefine the risk for cardiac event. (*Level of Evidence: C*)

Class IIa

1. Exercise myocardial perfusion SPECT at 3 to 5 years after revascularization (either PCI or CABG) in selected, high-risk asymptomatic patients. (*Level of Evidence: B*)
2. Exercise myocardial perfusion SPECT as the initial test in patients who are considered to be at high risk (patients with diabetes or patients otherwise defined as having a more than 20% 10-year risk of a coronary heart disease event). (*Level of Evidence: B*)

Class IIb

1. Repeat exercise myocardial perfusion SPECT 1 to 3 years after initial perfusion imaging in patients with known or a high likelihood of CAD, stable symptoms, and a predicted annual mortality of more than 1%, to redefine the risk of a cardiac event. (*Level of Evidence: C*)
2. Repeat exercise myocardial perfusion SPECT on cardiac active medications after initial abnormal perfusion imaging to assess the efficacy of medical therapy. (*Level of Evidence: C*)
3. Exercise myocardial perfusion SPECT in symptomatic or asymptomatic patients who have severe coronary calcification (CT CCS more than 75th percentile for age and sex) in the presence on the resting ECG of pre-excitation (Wolff-Parkinson-White) syndrome or more than 1 mm ST segment depression. (*Level of Evidence: B*)
4. Exercise myocardial perfusion SPECT in asymptomatic patients who have a high-risk occupation. (*Level of Evidence: B*)

E. Recommendations: Cardiac Stress Myocardial Perfusion SPECT in Patients Unable to Exercise

Recommendations for Diagnosis of Patients With an Intermediate Likelihood of CAD and/or Risk Stratification of Patients With an Intermediate or High Likelihood of CAD Who Are Unable to Exercise.

Class I

1. Adenosine or dipyridamole myocardial perfusion SPECT to identify the extent, severity, and location of ischemia. (*Level of Evidence: B*)
2. Adenosine or dipyridamole myocardial perfusion

SPECT to assess the functional significance of intermediate (25 to 75%) coronary lesions. (*Level of Evidence: B*)

3. Adenosine or dipyridamole myocardial perfusion SPECT after initial perfusion imaging in patients whose symptoms have changed to redefine the risk for cardiac event. (*Level of Evidence: C*)

Class IIa

1. Adenosine or dipyridamole myocardial perfusion SPECT at 3 to 5 years after revascularization (either PCI or CABG) in selected, high-risk asymptomatic patients. (*Level of Evidence: B*)
2. Adenosine or dipyridamole myocardial perfusion SPECT as the initial test in patients who are considered to be at high risk (patients with diabetes or patients otherwise defined as having a more than 20% 10-year risk of a coronary heart disease event). (*Level of Evidence: B*)
3. Dobutamine myocardial perfusion SPECT in patients who have a contraindication to adenosine or dipyridamole. (*Level of Evidence: C*)

Class IIb

1. Repeat adenosine or dipyridamole MPI 1 to 3 years after initial perfusion imaging in patients with known or a high likelihood of CAD, stable symptoms, and a predicted annual mortality of more than 1%, to redefine the risk of a cardiac event. (*Level of Evidence: C*)
2. Repeat adenosine or dipyridamole myocardial perfusion SPECT on cardiac active medications after initial abnormal perfusion imaging to assess the efficacy of medical therapy. (*Level of Evidence: C*)
3. Adenosine or dipyridamole myocardial perfusion SPECT in symptomatic or asymptomatic patients who have severe coronary calcification (CT CCS more than the 75th percentile for age and sex) in the presence on the resting ECG of LBBB or an electronically-paced ventricular rhythm. (*Level of Evidence: B*)
4. Adenosine or dipyridamole myocardial perfusion SPECT in asymptomatic patients who have a high-risk occupation. (*Level of Evidence: C*)

F. Recommendations: Cardiac Stress Myocardial Perfusion PET

Recommendations for Diagnosis of Patients With an Intermediate Likelihood of CAD and/or Risk Stratification of Patients With an Intermediate or High Likelihood of CAD

Class I

Adenosine or dipyridamole myocardial perfusion PET in patients in whom an appropriately indicated myocardial perfusion SPECT study has been found to be equivocal for diagnostic or risk stratification purposes. (*Level of Evidence: B*)

Class IIa

1. Adenosine or dipyridamole myocardial perfusion PET to identify the extent, severity, and location of ischemia as the initial diagnostic test in patients who are unable to exercise. *(Level of Evidence: B)*
2. Adenosine or dipyridamole myocardial perfusion PET to identify the extent, severity, and location of ischemia as the initial diagnostic test in patients who are able to exercise but have LBBB or an electronically-paced rhythm. *(Level of Evidence: B)*

G. Recommendations: Cardiac Stress Perfusion Imaging Before Noncardiac Surgery

Class I

1. Initial diagnosis of CAD in patients with intermediate pretest probability of disease and abnormal baseline ECG* or inability to exercise. *(Level of Evidence: B)*
2. Prognostic assessment of patients undergoing initial evaluation for suspected or proven CAD with abnormal baseline ECG* or inability to exercise. *(Level of Evidence: B)*
3. Evaluation of patients following a change in clinical status (eg, ACS) with abnormal baseline ECG* or inability to exercise. *(Level of Evidence: B)*
4. Initial diagnosis of CAD in patients with LBBB and intermediate pretest probability of disease, when used in conjunction with vasodilator stress. *(Level of Evidence: B)*
5. Prognostic assessment of patients with LBBB undergoing initial evaluation for suspected or proven CAD, when used in conjunction with vasodilator stress. *(Level of Evidence: B)*
6. Assessment of patients with intermediate or minor clinical risk predictors† and poor functional capacity (less than 4 METS) who require high-risk noncardiac surgery‡, when used in conjunction with pharmacologic stress. *(Level of Evidence: C)*
7. Assessment of patients with intermediate clinical risk predictors†, abnormal baseline ECGs*, and moderate or excellent functional capacity (greater than 4 METS) who require high-risk noncardiac surgery.

(Level of Evidence: C)

Class IIb

1. Routine assessment of active, asymptomatic patients who have remained stable for up to 5 years after CABG surgery. *(Level of Evidence: C)*
2. Routine evaluation of active, asymptomatic patients who have remained stable for up to 2 years after previous abnormal coronary angiography or noninvasive assessment of myocardial perfusion. *(Level of Evidence: C)*
3. Diagnosis of restenosis and regional ischemia in active, asymptomatic patients within weeks to months after PCI. *(Level of Evidence: C)*
4. Initial diagnosis or prognostic assessment of CAD in patients with right bundle-branch block or less than 1-mm ST depression on resting ECG. *(Level of Evidence: C)*

Class III

1. Routine screening of asymptomatic men or women with low pretest likelihood of CAD. *(Level of Evidence: C)*
2. Evaluation of patients with severe comorbidities that limit life expectancy or candidacy for myocardial revascularization. *(Level of Evidence: C)*
3. Initial diagnosis or prognostic assessment of CAD in patients who require emergency noncardiac surgery. *(Level of Evidence: C)*

*Baseline ECG abnormalities that interfere with interpretation of exercise-induced ST segment changes include LBBB, ventricular pre-excitation, ventricular pacing, LVH with repolarization changes, more than 1-mm ST depression, and digoxin therapy.

†As defined in the ACC/AHA Guideline Update for Perioperative Cardiovascular Evaluation for Noncardiac Surgery (313), intermediate clinical risk predictors include mild angina, prior MI, compensated or prior heart failure, diabetes, and renal insufficiency. Minor clinical risk predictors include advanced age, abnormal ECG, rhythm other than sinus, low functional capacity, history of CVA, and uncontrolled hypertension.

‡High-risk surgery is defined by emergent operations (particularly in the elderly), aortic and other major vascular surgery, peripheral vascular surgery, and other prolonged operations during which major fluid shifts are anticipated (ie, reported cardiac risk often more than 5%).

Table 15. Recommendations for the Use of Radionuclide Imaging in Patients With Heart Failure: Fundamental Assessment

Indication	Test	Class	Level of Evidence
1. Initial assessment of LV and RV function at rest*	Rest RNA	I	A
2. Assessment of myocardial viability for consideration of revascularization in patients with CAD and LV systolic dysfunction who do not have angina	MPI (See Table 17), PET	I	B
3. Assessment of the copresence of CAD in patients without angina	MPI	IIa	B
4. Routine serial assessment of LV and RV function at rest	Rest RNA	IIb	B
5. Initial or serial assessment of ventricular function with exercise	Exercise RNA	IIb	B

*National consensus treatment guidelines are directed by quantitative assessment of LVEF and identification of LVEF less than or equal to 40% (356).

CAD indicates coronary artery disease; LV, left ventricular; MPI, myocardial perfusion imaging; PET, positron emission tomography; RNA, radionuclide angiography; RV, right ventricular.

IV. HEART FAILURE

The clinical syndrome of heart failure in adults is commonly associated with the etiologies of ischemic and nonischemic dilated cardiomyopathy, hypertrophic cardiomyopathy, hypertensive heart disease, and valvular heart disease. Common principles of assessment that influence prognosis and therapy apply to each of these categories. These principles include the assessment of (1) LV function and remodeling, (2) the contribution of myocardial ischemia due to CAD, and (3) myocardial viability. The application of radionuclide imaging to each of these key diagnostic principles is addressed here (Table 15). Second, the role of radionuclide imaging in specific categories of heart failure is addressed.

A. Assessment of LV Systolic Dysfunction

The assessment of LV systolic dysfunction is now an important component of the initial evaluation of all patients with the clinical syndrome of heart failure. LV systolic dysfunction is usually defined by the presence of a LVEF less than 40%. The identification of a depressed LVEF mandates the initiation of a specific treatment pathway that follows national consensus guidelines (356-358). Except for patients with acute myocardial damage, such as patients with acute AMI, secondary dilatation of the LV is usually also present. The absence of LV systolic dysfunction in the patient with clinical symptoms of heart failure raises the possibility of heart failure secondary to valvular heart disease, pericardial disease, predominant diastolic dysfunction (discussed below), or noncardiac conditions including pulmonary disease.

Diagnostic noninvasive imaging techniques have distinct strengths and limitations. In clinical practice, there are differences between the techniques used for quantitative computation versus simple visual estimates of ventricular function and volume. The clinician's choice of noninvasive imaging modality to detect and quantify LV systolic dysfunction in the individual patient with heart failure depends on several variables including cost, ease of access at point-of-care, need for precise computed quantitative measurement, and local expertise. Three issues merit consideration in each individual patient with heart failure:

1. Does the imaging modality permit accurate assignment of the individual patient to the correct functional classification: normal, moderately depressed, or severely depressed LV systolic function (ie, EF less than 40%)?
2. Is a highly reproducible quantitative measurement needed to track changes in systolic function over time (ie, in response to a novel therapy or during surveillance for cardiac toxicity during a therapy such as doxorubicin)?
3. If LV systolic function is preserved, is diastolic dysfunction present?

RNA (ventriculography) can be used to compute quantitative estimates of LV, as well as RV, EF, and absolute volumes.

Visual estimates of function are rarely used. RNA, performed at rest or during exercise stress, is most commonly performed by gated blood pool RNA by use of Tc-99m-pertechnetate bound to red blood cells that is distributed at equilibrium throughout the blood pool (359). First-pass nonequilibrium studies are advantageous for evaluating RV function and can be performed in concert with equilibrium-gated blood pool RNA. First-pass studies can also provide estimates of intracardiac shunts, as discussed below in the section on congenital heart disease. Equilibrium studies can be acquired by either a planar or SPECT approaches, as discussed in Appendix 1. A strength of RNA is that the quantitative computation of EF and chamber volumes does not depend on mathematical assumptions of ventricular geometry. Thus, radionuclide quantitative computations of LV chamber volume and EF are obtainable in nearly 100% of patients. The long biologic half-life of Tc-99m-labeled blood pool agents in gated equilibrium studies also permits serial acquisition of data at rest and during exercise. A potential source of error is selection of a proper region for calculation and subtraction of background activity. Some laboratories use a fixed region of interest (ROI) in which the LV border is identified on the initial end-diastolic frame. Another mode of analysis uses a variable ROI, which is less sensitive to accurate measurement of background activity, in which the computer tracks the LV "contour" of counts throughout the cardiac cycle. The variable-ROI method of EF computation closely correlates with values obtained by contrast ventriculography, measured in the era when the latter was the gold standard (359). In clinical research studies, gated simultaneous measurements of LV volume and pressure can be recorded throughout the cardiac cycle to obtain LV pressure/volume loops applicable to calculation of indices of myocardial contractility which are relatively independent of ventricular loading, such as end-systolic pressure/volume relations.

B. Assessment of LV Diastolic Dysfunction

The objective determination of the presence and severity of diastolic dysfunction is increasingly important in patients with the clinical syndrome of heart failure. In as many as 30 to 40% of patients with heart failure symptoms, the underlying functional abnormality is predominately diastolic dysfunction. In such patients, LV cavity size is usually normal, EF is preserved, and the underlying functional abnormalities of the LV include impaired filling of the ventricle, an increased level of diastolic pressure required to distend the ventricle, or both. Large clinical trials have not yet provided evidence-based data to support the publication of a unified treatment pathway for heart failure patients with diastolic dysfunction. The objective documentation of diastolic dysfunction in heart failure patients can be valuable in clinical practice, however, because it confers prognostic information, promotes detection of common underlying conditions (such as hypertensive hypertrophic heart disease or CAD), and guides therapy. By using commercially available software packages for RNA, the rate of change of counts in diastole

can be analyzed to calculate indices of diastolic filling, including the peak LV filling rate, time to peak filling, and atrial contribution to filling (360). In contemporary practice, Doppler blood flow velocity indices of transmitral flow are more commonly used to assess LV diastolic filling parameters. Large population-based criteria, adjusted for age and sex, for normal versus abnormal diastolic function using RNA have not yet been established. Both age-specific and sex-specific criteria for diagnosing LV diastolic dysfunction by using Doppler blood flow velocity indices of transmitral flow based on large population studies have been defined that are applicable to clinical practice (361).

C. Assessment of CAD

1. Importance of Detecting CAD in Heart Failure Patients

Determining whether LV dysfunction is due predominantly to the consequences of CAD, or to one of the many other etiologies included in the term “nonischemic” cardiomyopathy, is a critical early step in the management of heart failure patients. Decisions regarding the need for cardiac catheterization and coronary angiography will be informed by the initial clinical and noninvasive assessment of these patients and a significant subgroup of patients with heart failure and underlying CAD have a potentially reversible degree of LV dysfunction with revascularization. In addition to identifying the potential for revascularization as a treatment option, the identification of CAD in a patient with heart failure will also have implications regarding secondary prevention strategies, as AMI is a common mechanism of death in patients with heart failure (362).

2. MPI to Detect CAD in Heart Failure Patients

In six published studies examining the role of MPI in detecting CAD in patients with heart failure and LV dysfunction, the sensitivity has been 100% in all studies (363-368). This capability of noninvasive imaging to detect significant CAD in this setting likely results from the pathophysiology of LV dysfunction as a consequence of CAD. That is, LV dysfunction is the consequence of either the presence of large or multiple prior MIs (with subsequent remodeling), or the combination of more moderate infarction extent accompanied by an important degree of inducible ischemia and/or hibernation, states that should be readily identified with perfusion imaging. Hence, in the studies cited, a normal stress perfusion scan in a patient with heart failure and LV dysfunction was associated with a 100% negative predictive value for predicting the absence of CAD. It is not clear how these studies (363-368), some of which involved relatively small numbers of patients and older techniques, may generalize to larger groups of patients and contemporary imaging techniques. Thus, although a normal stress perfusion scan in this setting may obviate the need for invasive coronary angiography, there is still controversy over this issue.

The specificity of perfusion imaging to detect coronary disease is modest, on the average 40 to 50%. The frequent false

positive studies are due to perfusion abnormalities in a significant number of patients with “nonischemic” cardiomyopathy (ie, those patients without epicardial coronary disease). Pathologic studies (369), as well as invasive catheterization studies of coronary blood flow in patients with cardiomyopathy (370,371), have demonstrated that significant territories of myocardial fibrosis may occur in some patients, as well as significant limitations in coronary blood flow reserve to a hyperemic stress, which would result in both fixed and reversible perfusion defects. One study has demonstrated that the magnitude of perfusion abnormalities in patients with nonischemic cardiomyopathy has important prognostic implications (372). Those nonischemic cardiomyopathy patients with a normal perfusion pattern had the most benign outcome during follow-up, whereas those with the most extensive perfusion abnormalities had a significantly higher mortality.

Although the presence of any perfusion abnormality is not highly specific for CAD, the pattern of perfusion abnormality may assist in the differentiation between CAD and nonischemic etiology of heart failure. Thus, more extensive perfusion defects and/or more severe perfusion defects are more likely to be seen in patients with CAD as the etiology of heart failure, whereas smaller and milder defects are more likely to represent patients with nonischemic cardiomyopathy. Data using gated SPECT sestamibi imaging have shown complete discrimination between heart failure patients with ischemic versus nonischemic cardiomyopathy by use of a semiquantitative scoring system of the stress perfusion pattern (367). Hence, comprehensive early evaluation of patients with heart failure and LV systolic dysfunction includes an assessment of the underlying etiology (coronary disease or noncoronary causes), and if coronary disease is determined to be the etiology of the heart failure syndrome, an assessment of the potential for reversible LV dysfunction after revascularization, the latter related to the extent of inducible ischemia and preserved viability within dysfunctional myocardium.

D. Assessment of Myocardial Viability

1. Goals of Assessing Myocardial Viability

In patients with chronic coronary disease and LV dysfunction, there exists an important subpopulation in which revascularization may significantly improve regional or global LV function, as well as symptoms and potentially natural history. The underlying pathophysiology involves reversible myocardial dysfunction (hibernation or stunning), which may exist independently or may coexist within the same patient. These states of potentially reversible LV dysfunction have in common preserved cell membrane integrity and sufficiently preserved metabolic activity to maintain cellular functions and cell membrane integrity in the absence of normal myocyte contractility secondary to resting ischemia or repetitive demand ischemia (“repetitive stunning”). Because the various radionuclide tracers identify preserved cell membrane integrity and aspects of metabolic activity, radionuclide techniques play an important role in the assessment of myocardial viability and, thus, the potential identification of

patients with LV dysfunction and CAD who may benefit significantly from revascularization.

Although the early literature on radionuclide techniques in assessing viability focused on relationships between prevascularization testing and postvascularization changes in physiologic parameters such as perfusion, improvement in regional LV function, or improvement in global function (LVEF), only recently have such studies focused on the ability of the testing modalities to predict improvement in patients' symptoms and natural history. Although it may be expected that improvement in a certain threshold territory of regional LV dysfunction or significant improvement in global EF may be associated with improvements such as symptoms or natural history, it is also possible that symptoms and natural history may improve after revascularization of viable myocardium in the absence of changes in regional and global systolic function. There are many other physiologic parameters that may be affected by revascularization including improvement in diastolic performance, improvement in systolic and diastolic function during stress, stabilization of the arrhythmic milieu, prevention of MI, and potential attenuation of progressive remodeling in a patient with LV dysfunction (373,374). One study has suggested that after revascularization in patients with multivessel coronary disease and LVEF less than 30%, a survival benefit accrued whether or not EF improved (375). Investigations into the relation of the various radionuclide techniques for assessing viability and patient outcomes have more strongly supported the application of these techniques to the clinical decision-making process for revascularization.

A substantial body of literature has emerged regarding the ability of radionuclide tracers in chronic CAD and LV dysfunction to predict improvement in symptoms and natural history after revascularization. Studies have demonstrated that the potential for improved heart failure symptoms and treadmill time following revascularization correlated with the magnitude of the PET "mismatch" pattern (ie, enhanced fluorodeoxyglucose [FDG] uptake relative to perfusion) in such patients (376). In a meta-analysis of 24 published studies involving 3088 patients (average New York Heart Association functional class 2.8), those with evidence of preserved myocardial viability (using different protocols) who underwent revascularization had a substantial reduction in the risk of death during long-term follow-up (annual mortality 16% per year if not revascularized reduced to 3% per year with revascularization, 79.6% RR reduction, *P* less than 0.0001). If nonviability was predominant, the risk of death was intermediate and not affected by revascularization (377). Conclusions that may be drawn are limited by lack of randomization and the fact that observational cohorts analyses are subject to selection biases. The concordance of data and consistency across studies, however, suggest that the radionuclide techniques for assessing viability can play an important role in selecting patients for revascularization with the expectation that natural history will be improved. Thus, the goal of assessing viability is to optimize selection of patients whose symptoms and natural history may improve after revascularization.

2. General Principles of Assessing Myocardial Viability by Radionuclide Techniques

Preservation of myocardial viability exists as a spectrum in a territory with regional ventricular dysfunction, from the possibility of no preserved viability (ie, complete transmural infarction) to completely preserved viability (ie, transmural hibernation or stunning with the potential for full recovery of function). The radionuclide tracers and techniques most often used in this situation have been evaluated for their relation to preserved tissue viability directly, by correlating tracer uptake (of the single-photon tracers TI-201 and sestamibi, and the metabolic tracer FDG) with histologically confirmed extent of tissue viability obtained by a biopsy of the relevant myocardial regions at the time of coronary artery bypass surgery. In these studies, it has been demonstrated that quantitative analysis of tracer uptake correlates directly with the magnitude of preservation of tissue viability (372,378-380). Many studies in the literature evaluate the techniques for assessing viability by assigning a specific threshold or cut-point, often 50 or 60% of maximum tracer uptake, to create dichotomous performance characteristics (sensitivity, specificity, and positive and negative predictive values). An important principle illustrated by the biopsy studies is that tracer uptake represents a continuous variable, with the magnitude of tracer uptake directly reflecting the magnitude of preserved viability. In turn, the magnitude of tracer uptake is linked to the probability of regional functional recovery after revascularization (381,382).

Frequently, studies analyzing radionuclide techniques for assessing viability focus on changes in regional LV function, with the LV subdivided into 17, 20, or even 40 segments. Numerous studies have demonstrated, however, that for global LV function (ie, LVEF) to improve by a clinically significant degree, a certain threshold mass of dysfunctional regions must be viable and successfully revascularized (383). Thus, potential improvement of global LV function is determined by the number of segments or the extent of viable dysfunctional myocardium.

Most studies evaluating the radionuclide techniques for assessing viability have focused on analysis of resting tracer uptake (as with TI-201, sestamibi, or tetrofosmin) or evidence of preserved metabolic activity at rest (by FDG or carbon-11 [C-11] acetate). In some patients, however, nontransmural infarction may have occurred with preservation of some degree of viability in the setting of a noncritically stenosed vessel. In this setting, evidence of uptake of the single-photon tracers or metabolic activity by FDG may result in "intermediate" values, such that the role of revascularization is not clear. When this occurs, assessment of stress-induced ischemia will provide additional important information. One study has demonstrated that the finding of stress-induced ischemia (a reversible perfusion defect) is a more powerful predictor of recovery of function than is a "fixed" defect with similar degree of resting tracer activity (384). When evidence of resting tracer uptake or metabolic activity falls into the intermediate range (in which the probability of recovery of function or improved outcome is itself interme-

diate), addition of stress imaging to assess for the presence of stress-induced ischemia may be helpful for clinical decision making regarding revascularization.

3. Techniques and Protocols for Assessing Myocardial Viability

a. *Thallium-201*

The uptake of Tl-201 is an energy-dependent process requiring intact cell membrane integrity and the presence of Tl-201 implies preserved myocyte cellular viability. The magnitude of Tl-201 uptake (after reinjection in particular) has been correlated with extent of tissue viability by histologic techniques. The redistribution properties of Tl-201 have been used as an important marker of myocardial viability in stress imaging followed by a 3- to 4-hour redistribution image. The presence of a reversible perfusion defect and/or preserved Tl-201 uptake on the 3- to 4-hour redistribution images is an important sign of regional viability. The absence of an important degree of redistribution or Tl-201 uptake on the redistribution images, however, is not a sufficient sign of the absence of regional viability, and iterations of Tl-201 protocols have been investigated to optimize the assessment of regional viability with this tracer.

b. *Tl-201 Reinjection*

The two most widely studied protocols for assessing viability in the presence of an inconclusive result on initial stress/redistribution imaging involve Tl-201 reinjection and late redistribution imaging. In the former protocol, a second dose of Tl-201 (usually 50% of the initial dose) is reinjected into the patient after the redistribution images are complete, and a third set of images is obtained 15 to 20 minutes later. It has been demonstrated that approximately 50% of regions with fixed defects on stress/redistribution imaging will show significant enhancement of Tl-201 uptake after reinjection (385), and this finding is predictive of future improvement in regional LV function after revascularization. The presence of a severe Tl-201 defect after reinjection identifies areas with a very low probability of improvement in function.

c. *Late Redistribution Imaging*

Late redistribution imaging involves obtaining a third set of images 24 to 48 hours after the initial stress Tl-201 injection, essentially allowing more time for redistribution to occur. Although improvement in uptake on late redistribution images has good positive predictive value for identifying regions with potential improvement in function, the negative predictive value is suboptimal in some patients (386). This is likely due to low to very low Tl-201 blood levels, such that redistribution does not take place even after a prolonged time period. The late redistribution image may also be limited by suboptimal image quality due to continued washout and decay of the tracer.

d. *Rest-Redistribution Tl-201*

Rest-redistribution Tl-201 protocols have also been studied extensively. After tracer injection at rest, images are obtained 15 to 20 minutes later, which reflect regional blood flow at rest, and images obtained 3 to 4 hours later after redistribution will generally reflect preserved viability. The finding of a “reversible resting defect” may identify areas of myocardial hibernation, although this finding appears to be an insensitive albeit very specific sign of potential improvement in regional function (387). Quantitative analysis of regional Tl-201 activity on the rest or redistribution images has been shown to correlate with potential improvement in function after revascularization (382,383).

e. *Tc-99m-Sestamibi and Tc-99m-Tetrofosmin*

The Tc-99m-based tracers sestamibi and tetrofosmin do not share the redistribution properties of Tl-201 (although a minor degree of redistribution has been noted); therefore there was initial uncertainty of the ability of these tracers to accurately track myocardial viability. A substantial body of literature, particularly with sestamibi, however, has demonstrated that the performance characteristics for predicting improvement in regional function after revascularization are in general similar to those seen with Tl-201. It would not be expected that there would be any important differences between the tracers in the setting of preserved resting regional blood flow (as might be seen with repetitive stunning). In the setting of hibernation, with potentially diminished blood flow at rest, it might be expected that the redistribution property of Tl-201 would be advantageous. This does not appear to be the case, however, and may be because sestamibi appears to be relatively overextracted at low blood flows, becoming more a tracer of cell membrane integrity than MBF. This has been demonstrated in animal models of reduced resting blood flow, in which sestamibi activity 3 to 4 hours after injection is similar to redistribution Tl-201 uptake (388), and also in human studies, in which sestamibi activity has been found quantitatively similar to redistribution Tl-201 activity after a resting injection in the identification of reversible resting Tl-201 defects (381,389). Thus, quantitative analysis of sestamibi uptake after resting injection appears to provide similar information about myocardial viability as Tl-201. Assessment of sestamibi activity after injection under the influence of nitrates to improve resting blood flow appears to slightly improve the ability of this tracer to detect myocardial viability (390).

Although less extensively studied, tetrofosmin uptake in assessing myocardial viability appears to have similar characteristics as those of sestamibi. There is a good correlation of quantitatively analyzed tetrofosmin uptake with redistribution Tl-201 uptake after resting injection (391), and performance characteristics for predicting recovery of regional function after revascularization appear similar as well, in somewhat more limited data (392). Some studies have demonstrated that by incorporating information about resting function in addition to the perfusion viability data, improve-

Table 16. Radionuclide Imaging Agents Commonly Used to Assess Myocardial Viability

Agent	Mechanism	Validated Protocols
Single-photon TI-201	Requires myocyte cell membrane integrity for uptake (energy-dependent)	Stress/redistribution plus or minus re-injection Stress/late redistribution Rest/redistribution
Tc-99m-sestamibi	Requires myocyte cell membrane integrity for uptake (electrochemical gradient)	QA or SQVA scoring of resting uptake Uptake after nitrates
Positron F18-FDG	Preserved myocyte glucose uptake and phosphorylation	“Mismatch” pattern in conjunction with perfusion imaging QA of resting uptake
N-13-ammonia	Correlates with MBF	Rest MBF image in conjunction with FDG
Rubidium-82	Requires myocyte cell membrane integrity for uptake (energy-dependent)	Early/washout image

FDG indicates flurodeoxyglucose; MBF, myocardial blood flow; QA, quantitative analysis; SQVA, semiquantitative visual analysis; TI-201, thallium-201.

ments in sensitivity and/or specificity for predicting functional recovery after revascularization can be accomplished (393,394).

f. PET Imaging

Positron tracers of blood flow and metabolism have been extensively studied for evaluation of myocardial viability. The ability to label physiologic compounds such as nitrogen, oxygen, carbon and fluorine; the high-energy emissions; and the generally short half-life of the tracers allows examination of numerous physiologic processes. As attenuation correction is more routinely applied with PET than with SPECT, and as count densities are high because of the high-energy positron emitters, absolute quantification of blood flow and metabolic processes is possible, although not widely applied clinically.

The most commonly used PET protocol involves evaluation of myocardial glucose metabolism with 18F-FDG in conjunction with PET or SPECT examination of MBF with 13N-ammonia or Tc-99m-sestamibi, respectively. Meta-analysis of the published data on predicting recovery of regional function after revascularization has suggested that this approach has slightly better overall accuracy than that of single-photon techniques (395). Analysis of clinical outcomes after PET imaging has shown that the magnitude of improvement in heart failure symptoms after revascularization in patients with LV dysfunction correlates with the pre-operative extent of 18F-FDG mismatch pattern (ie, preserved or diminished MBF with enhanced or normal glucose metabolism) (376). Moreover, long-term follow-up studies have suggested that the finding of PET mismatch in patients with CAD and LV dysfunction portends a high risk of cardiac death during medical therapy, whereas that risk is substantially lower after revascularization (396).

The more commonly used PET protocols are summarized in Table 16. Although positron techniques are not as widely used for evaluation of myocardial viability as are SPECT

techniques, several factors suggest that their use will increase over time. These include the increasing availability of 18F-FDG as a result of a growing number of regional cyclotron units; the use of coincidence-detecting SPECT cameras to evaluate 18F-FDG uptake; the availability of mobile PET units, which will increase access; and the increasing availability of standard PET cameras based on expanding oncology applications.

4. Image Interpretation for Myocardial Viability: Quantitative Versus Visual Analysis of Tracer Activities

Since the early 1980s, quantitative analysis of radionuclide tracer uptake has been studied in the attempt to improve detection of CAD as well as in studies for myocardial viability. Gibson *et al.* (397) first demonstrated that among all patients with visually-fixed TI-201 defects, quantitative analysis of the severity of the fixed defect was an important factor in determining regional viability. A similar principle has also been applied to TI-201 reinjection studies, demonstrating that quantitatively severe fixed defects after redistribution are unlikely to improve after TI-201 reinjection. Moreover, whereas visual analysis of sestamibi images appeared to demonstrate an underestimation of myocardial viability, several studies have demonstrated that quantitative analysis of sestamibi uptake results in assessment of viability with similar precision as that of TI-201 techniques (381,389).

Whether quantitative analysis of tracer uptake in radionuclide techniques is required for assessing viability is not definitely established. The initial studies of TI-201 reinjection demonstrated that both visually and quantitatively, TI-201 uptake improved after reinjection in myocardial segments ultimately found to be viable after revascularization (398). Moreover, recent data have demonstrated that when SPECT images are analyzed visually according to a semiquantitative scoring scale (similar to that used in CAD prognosis studies),

Table 17. Recommendations for Radionuclide Techniques to Assess Myocardial Viability

Indication	Test	Class	Level of Evidence
1. Predicting improvement in regional and global LV function after revascularization	Stress/redistribution/reinjection Tl-201	I	B
	Rest-redistribution imaging	I	B
	Perfusion plus PET FDG imaging	I	B
	Resting sestamibi imaging	I	B
	Gated-SPECT sestamibi imaging	IIa	B
	Late Tl-201 redistribution imaging (after stress)	IIb	B
	Dobutamine RNA	IIb	C
	Postexercise RNA	IIb	C
2. Predicting improvement in heart failure symptoms after revascularization	Perfusion plus PET FDG imaging	IIa	B
	Postnitroglycerin RNA	IIb	C
3. Predicting improvement in natural history after revascularization	Tl-201 imaging (rest-redistribution and stress/redistribution/reinjection)	I	B
	Perfusion plus PET FDG imaging	I	B

FDG indicates flurodeoxyglucose; PET, positron emission tomography; RNA, radionuclide angiography; SPECT, single-photon emission computed tomography; Tl-201, thallium-201.

there is good correlation with quantitatively analyzed images and good correlation with predicting improvement in function (398). Most software packages available on radionuclide imaging cameras and computers do however contain quantitative software for assessing regional tracer uptake. Thus, a combination of semiquantitative visual analysis (accounting for defect severity) and quantitative analysis should provide information to the clinician similar to that developed in the literature.

5. Comparison of Techniques

There is now a substantial body of literature evaluating the ability of the various radionuclide techniques for predicting improvements in regional function, and the literature on this topic has been subject to meta-analysis. Recommendations are summarized in Table 17. Bax *et al.* (395) found that all of the radionuclide techniques (and dobutamine echocardiography) perform in a relatively similar manner regarding positive and negative predictive values for predicting improvements in regional function. Single photon radionuclide techniques (Tl-201 and sestamibi) appeared to be slightly more sensitive, whereas PET and dobutamine echocardiography appeared to be more specific. Overall the PET techniques appeared to have slightly better accuracy. This slight improvement in overall accuracy, however, is accompanied by less accessibility and a higher level of technical complexity and higher cost. A meta-analysis of outcome studies related to myocardial viability has demonstrated no difference between the techniques commonly used to assess viability (PET versus single-photon radionuclide versus dobutamine echocardiography) with regard to reduction of mortality or unfavorable cardiac events after revascularization (377).

MRI has emerged as an alternative noninvasive imaging approach for discrimination of fixed scar versus viable but dysfunctional myocardium. Reports indicate that infarct-avid imaging analogous to that formerly performed with Tc-99m-pyrophosphate can be performed by using MRI and a con-

ventional gadolinium-based contrast agent (399,400). Potential advantages include the improved resolution now available with MRI and an ability to image chronic and acute infarctions. Additional clinical experience will be needed to place this approach in proper context.

Thus, for the clinician faced with a patient with CAD and LV dysfunction, the key decision is whether or not to proceed toward revascularization with an expectation of clinical benefit to the patient. The presence of active angina in the setting of LV dysfunction would itself suggest a clinical benefit from revascularization (401). Otherwise, radionuclide assessment of the extent of myocardial ischemia and viability can contribute importantly to a revascularization decision. If substantial ischemia or viability of dysfunctional territories is found in the setting of stenotic coronary arteries technically amenable to revascularization, the literature would suggest a clinical benefit from revascularization. In the absence of substantial ischemia or viability, such a benefit is significantly less likely.

E. Etiologies of Heart Failure

1. Dilated Cardiomyopathy

a. Diagnosis

Dilated cardiomyopathy is diagnosed when heart failure is associated with the geometric and functional findings of LV chamber dilatation with depressed systolic function (ie, EF less than 40%). RV systolic dysfunction and chamber enlargement may also be present. RNA at rest is a valuable imaging modality to determine if the functional mechanism of heart failure is LV systolic dysfunction. The differentiation of ischemic versus nonischemic dilated cardiomyopathy, and the differentiation of viable versus nonviable myocardium are discussed above. The roles of radionuclide techniques in specific etiologies of dilated cardiomyopathy are discussed later in this section and summarized in Table 18.

b. Risk Stratification and Prognosis

Determination of the functional mechanism of heart failure provides a powerful means for risk stratification, in addition to clinical assessment, sex, and age. The prognosis of heart failure due to LV systolic dysfunction is worse than the prognosis of heart failure with preserved systolic function (and the presumption of diastolic dysfunction) in age- and sex-matched cohorts from large population studies (402). It is not yet established whether serial assessment of the severity of systolic or diastolic dysfunction in individual heart failure patients confers additional information for risk stratification, treatment, and prognosis.

c. Therapy

The accurate determination of the presence and magnitude of LV systolic dysfunction (ie, LVEF less than 40%) directly guides the management of patients with heart failure using current national consensus guidelines (356).

Table 18 summarizes diagnostic recommendations for specific subsets of patients.

2. Dilated Cardiomyopathy due to Doxorubicin/Anthracycline Cardiotoxicity

a. Diagnosis

Chemotherapy with doxorubicin and other anthracyclines such as epirubicin produces a dose-dependent depression of LV function in part mediated by free radical injury. Toxic damage of cardiac myocytes is associated with an abrupt irreversible reduction in myocardial shortening with acute hemodynamic decompensation (403). The initially normal-sized LV remodels into an irreversible dilated cardiomyopathy with profound LV dysfunction, culminating in symptomatic congestive heart failure. Continued use of doxorubicin after there is objective evidence of LV dysfunction results in progressive chamber dilatation and deterioration in systolic function (403). RNA is an ideal noninvasive tool to provide for longitudinal quantitative assessment of LV function in patients treated with doxorubicin (403-405).

b. Risk Stratification and Prognosis

LV dysfunction as measured by reduced EF and serial reduction in EF are important determinants of prognosis both in patients who have received or are receiving doxorubicin. Ejection fraction should be measured by RNA in all patients before receiving doxorubicin, especially in patients with pre-existing heart disease and suspected LV dysfunction because they are at greater risk of congestive heart failure. Radionuclide ventriculography is a sensitive and reproducible method for detecting small serial decrements in LV function. Three combined criteria have been identified as predictive for development of heart failure after initiation of doxorubicin therapy; these include age greater than 50 years, EF less than 60%, and a decrease in EF to 50% or less (406). In addition, recent observations suggest that therapy with trastuzumab, a monoclonal antibody directed against the HER2 receptor, may increase the risk of developing heart failure during cancer chemotherapy with doxorubicin at standard doses (407). Alternative chemotherapeutic strategies can be entertained with prior assessment of LV function or use of concomitant adjuvant therapy that protects against anthracycline cardiotoxicity (408).

c. Assessment of Therapy

Serial assessment of LVEF at rest by RNA is an effective method of monitoring patients during the course of doxorubicin therapy. The initial dose of doxorubicin frequently results in immediate deterioration in LV function that usually reverses over several days. Data from several studies indicate that doxorubicin therapy is safe to continue if resting EF remains within the normal range, even if there is a consistent decline below baseline values. If doxorubicin therapy is discontinued when EF becomes abnormal, LV function usually stabilizes (403,405), but a decrease in EF to less than 50% is strongly predictive for development of heart failure (406). Further continuation of doxorubicin after EF becomes abnormal is associated with serious, life-threatening irreversible heart failure (403). Stress exercise assessment does not appear to add to resting EF in deciding when to discontinue

Table 18. Recommendations for the Use of Radionuclide Imaging to Diagnose Specific Causes of Dilated Cardiomyopathy

Indication	Test	Class	Level of Evidence
1. Baseline and serial monitoring of LV function during therapy with cardiotoxic drugs (eg, doxorubicin)	Rest RNA	I	A
2. RV dysplasia	Rest RNA	IIa	B
3. Assessment of posttransplant obstructive CAD	Exercise perfusion imaging	IIb	B
4. Diagnosis and serial monitoring of Chagas disease	Exercise perfusion imaging	IIb	B
5. Diagnosis of amyloid heart disease	Tc-99m-pyrophosphate imaging	IIb	B
6. Diagnosis and serial monitoring of sarcoid heart disease	Rest perfusion imaging	IIb	B
	Rest gallium-67 imaging	IIb	B
7. Detection of myocarditis	Rest gallium-67 imaging	IIb	B
	Indium-111 antimyosin antibody imaging	IIb	C

CAD indicates coronary artery disease; LV, left ventricular; RNA, radionuclide angiography; RV, right ventricular; Tc-99m, technetium-99m.

doxorubicin therapy (409). Radionuclide evaluation of EF is also of paramount importance in monitoring the cardioprotective effects of agents such as dexrazoxane when doxorubicin is used in high dosages for solid malignant tumors. Because of the possibility of changes in LV function, RNA studies to follow the long-term progression of cardiotoxicity should be timed at least 10 to 14 days after the last dose of doxorubicin (408).

3. Dilated Cardiomyopathy due to Myocarditis

a. Diagnosis

Myocarditis, related to viral infection or secondary autoimmune response, is a potentially (partially) reversible cause of heart failure. Historically, RV endomyocardial biopsy has been the method used for its identification, but its limitations include sampling error due to patchy or focal involvement of the myocardium, morbidity, and cost.

Radioisotope imaging has been reported to identify myocarditis of diverse etiologies with gallium (which detects inflammation), antimyosin antibody (which detects myocardial necrosis and is myosin specific) (410-412), and metaiodobenzylguanidine (MIBG, which assesses adrenergic neuronal function) (411). Antimyosin antibody imaging has the formal potential to identify myocardial necrosis in both myocarditis and AMI. When cardiac myocytes undergo necrosis, their cell membrane integrity is lost, exposing intracellular myosin heavy chains. Antimyosin antibody specifically binds to these exposed myosin molecules when the antibody is injected intravenously into patients. Intraventricular conduction abnormalities in patients with suspected myocarditis were more strongly associated with active and more severe myocardial necrosis as judged by antimyosin imaging than in patients with normal ECGs (413). At minimum, once correlation has been established in an individual patient between biopsy and radioisotope scanning, imaging may be a more useful technique for serial evaluation and estimation of prognosis of the patient (414). Comparison of scintigraphic results with histologic and clinical standards indicates a high sensitivity of antimyosin scans for the detection of myocarditis (91 to 100%), as well as a negative predictive value (93 to 100%). The specificity (31 to 44%) and positive predictive value (28 to 33%), however, are low (415). Used alone, endomyocardial biopsy has a poor sensitivity (35%) but a high specificity of 79% (415).

Radionuclide imaging has been used in small studies to support or confirm the diagnosis of myocarditis, primarily by use of indium-111 antimyosin antibody imaging, in acute rheumatic fever (416), clinically suspected myocarditis of unspecified etiology (410,417,418), acute onset of dilated cardiomyopathy (419), myocarditis masquerading as AMI (419), and the presence of AMI itself (420). RV perfusion tomography with a Tc-99m-labeled tracer is clinically useful for the noninvasive detection of RV myocardial damage in patients with RV tachycardia and for differentiating organic from idiopathic RV tachycardia (421).

b. Risk Stratification, Prognosis, and Assessment of Therapy

As discussed above, RNA and other noninvasive imaging techniques can be used to estimate LV systolic function and to track serial changes in function in patients with heart failure of any etiology, including documented or suspected myocarditis. RNA has the potential to detect and follow acute inflammatory changes in the heart. As addressed in the ACC/AHA Guidelines for the Evaluation and Management of Chronic Heart Failure (356) (http://www.acc.org/clinical/guidelines/failure/pdfs/hf_fulltext.pdf), however, review of evidence-based clinical trials in heart failure patients indicates that the identification of biopsy-documented myocarditis does not confer a differing prognosis in comparison with biopsy-negative dilated cardiomyopathy in most patients with heart failure. Also, randomized clinical trials thus far have not demonstrated clear benefit of immunosuppressant therapy in patients with biopsy-documented myocarditis (356). Therefore, an effective and specific treatment pathway for myocarditis has not yet been identified, and routine use of immunosuppressant drugs cannot be recommended. Although this controversy is under investigation, the identification of myocarditis by radionuclide or other imaging modalities, as well as endomyocardial biopsy, does not yet guide therapy in most patients. Thus, the usefulness of radionuclide imaging to detect myocarditis in heart failure patients is not well established and data describing use of this approach are based on nonrandomized studies.

4. Posttransplant Rejection and Allograft Vasculopathy

Cardiac transplant recipients require serial monitoring of both acute graft rejection, causing myocardial inflammation and necrosis, and the later development of allograft vasculopathy (posttransplantation CAD). Indium-111 antimyosin antibody imaging has been described as a technique to detect rejection after cardiac transplantation in multiple small observational studies since the first report of this application in 1987 (422). In a prospective analysis of antimyosin imaging and endomyocardial biopsy in 70 serial studies in 22 patients after cardiac transplantation, the predictive value of a negative antimyosin imaging study was 98%; however, the false-positive rate was extremely high (6 true-positive and 31 false-positive studies), yielding a very low positive predictive value of an abnormal antimyosin imaging study (423). Thus, because of many false-positive results, endomyocardial biopsy continues to be the technique of choice for serial monitoring and detection of acute cardiac transplantation rejection. Allograft vasculopathy is the major limitation for long-term survival in cardiac transplant recipients, and many centers use yearly invasive surveillance coronary angiography for detection because of the variable sensitivity and specificity of noninvasive approaches including rest and stress radionuclide perfusion imaging and echocardiography (424). A prospective comparison of 255 SPECT and coronary angiography studies in 67 cardiac transplant recipients suggests that yearly scintigraphy is highly sensitive as a screening tool to

detect both focal segmental stenoses and diffuse circumferential narrowing, whereas a SPECT study with no reversible perfusion defects has a negative predictive value of about 98% and virtually excludes coronary lesions appropriate for revascularization (425). Pharmacologic (dobutamine) stress MPI has also been useful in identifying posttransplant CAD, whereas the negative predictive value is approximately 79% (426).

5. Chagas Myocarditis and/or Cardiomyopathy

Chagas myocarditis and/or cardiomyopathy has several features that are distinctive in comparison with dilated cardiomyopathy due to presumed viral myocarditis. Several observational studies that used RNA and perfusion imaging have reported that chronic Chagas cardiomyopathy is frequently associated with LV regional wall motion abnormalities and perfusion defects in the absence of epicardial CAD, and RV dyssynergy is common in asymptomatic patients with no other clinical signs of heart failure (427). In correlative investigations, there is a marked topographic association between regional defects in sympathetic denervation detected by iodine-123-meta-iodobenzylguanidine (123-MIBG) imaging and perfusion defects detected by TI-201 imaging, which develop before echocardiographic segmental wall motion abnormalities in the same segments (428). The magnitude of impaired 123-MIBG uptake and TI-201 uptake appear to be associated with the progression of ventricular dysfunction in patients with Chagas disease.

6. Sarcoid Heart Disease

Myocardial SPECT with Tc-99m-sestamibi has been used to detect myocardial involvement in patients with sarcoidosis. Perfusion defects are more common in the RV than in the LV and correlate with atrioventricular block, heart failure, and ventricular tachycardia of RV origin (429). These defects are frequently reversible which makes it unlikely that they represent deposition of granulomata or fibrosis (430). Gallium-67 was formerly used in sarcoidosis as a marker of the activity and extent of the disease and for predicting the efficacy of corticosteroids, but has been largely superseded by serial chest CT and pulmonary function tests (431).

7. Cardiac Amyloidosis

Cardiac amyloidosis is a form of cardiomyopathy that results in deposition of noncontractile protein in the intercellular space that alters LV diastolic function and, in its most severe form, culminates in restrictive cardiomyopathy. In some patients, LV systolic dysfunction and involvement of the pericardium are also present. Radionuclide angiography enables assessment of diastolic and systolic function including peak filling rates and LV filling volumes during rapid filling and atrial contraction, respectively (432). Iodine-123 MIBG imaging has indicated a high incidence of sympathetically denervated but viable myocardium in cardiac amyloid (433). Echocardiography appears, however, to be a more useful noninvasive method for assessment of possible cardiac amyloidosis because it enables complete characterization of the altered myocardium of the LV and RV myocardium, and the valvular and pericardial involvement.

8. RV Dysplasia

Arrhythmogenic RV dysplasia (ARVD) or complex RV dysplasia (ARVC), also referred to as Uhl's anomaly or parchment RV, is a malformation of the myocardium with altered tissue characteristics (fibrofatty replacement of myocardium) and accounts for approximately 5% of sudden cardiac deaths in people age 35 and younger in the United States (434). ARVD should be distinguished from other RV outflow tract ventricular tachycardias, because ARVD is associated with a more benign course, and can be treated with radiofrequency ablation. The RV in ARVD is characterized by marked dilatation and depressed EFs, which can be readily identified with RV RNA. The RV also has temporal dispersion of electrical and mechanical contractile activation, as evidenced by epsilon waves or localized prolongation (more than 110 ms) of the QRS complex in right precordial leads (V1-V3), late potentials on signal-averaged ECG, and Fourier phase images of the RV (435). These abnormal findings are predictive of sudden arrhythmic cardiac death. ARVD can be reliably distinguished from RV enlargement and dysfunction associated with acute or chronic pulmonary embolism by RV RNA.

Table 19. Recommendations for the Use of Radionuclide Imaging to Evaluate Hypertrophic Heart Disease

Indication	Test	Class	Level of Evidence
1. Diagnosis of CAD in hypertrophic cardiomyopathy	Rest and exercise perfusion imaging	Ib	B
2. Diagnosis and serial monitoring of hypertensive hypertrophic heart disease	Rest RNA	Ib	B
3. Diagnosis and serial monitoring of hypertrophic cardiomyopathy, with and without outflow obstruction	Rest RNA	III	B

CAD indicates coronary artery disease; RNA, radionuclide angiography.

9. Hypertrophic Cardiomyopathy

a. Diagnosis

The diagnosis of hypertrophic cardiomyopathy is suggested by the clinical history, family history, physical examination, and ECG, and confirmed by 2D Doppler echocardiography that is the diagnostic modality of choice in this condition. Radionuclide angiographic studies are not usually indicated in the diagnosis of hypertrophic cardiomyopathy (see Table 19). In patients with poor quality transthoracic echocardiographic images the diagnosis can be made on the basis of a small hyperdynamic LV cavity with asymmetric septal hypertrophy, supranormal EF, and abnormal diastolic filling (436,437). Characteristically, the hypertrophied myocardium demonstrates increased thallium uptake that is especially prevalent in the basal interventricular septum (438).

Chest pain is a frequent symptom in patients with hypertrophic cardiomyopathy resulting from increased myocardial demand, but raises the possibility of coexistent occlusive CAD. Fixed and reversible exercise-induced myocardial perfusion defects on thallium scans that suggest scar or ischemia, respectively, have been reported in patients with hypertrophic cardiomyopathy in the absence of significant epicardial coronary artery stenoses (439,440). Reversible perfusion defects may reflect ischemia related to diminished coronary flow reserve (441-443), which is favorably modified by treatment with calcium channel antagonists (444,445), or decreased sympathoneural function in hypertrophied but not in nonhypertrophied myocardium (446). Reversible myocardial perfusion defects are associated with sudden cardiac arrest and syncope, which suggests that these symptoms are frequently related to ischemia rather than to a primary arrhythmogenic ventricular substrate (447). Fixed myocardial perfusion defects in hypertrophic cardiomyopathy are associated with syncope and decreased exercise capacity (439). Neither reversible nor fixed stress-induced myocardial perfusion defects, however, are predictive of long-term survival. Because reversible and fixed myocardial perfusion defects occur so frequently (approximately 50%) in patients in whom the epicardial coronary arteries are nonobstructive, the detection of coexistent CAD with exercise or pharmacologic stress thallium imaging is ordinarily not possible (see Table 19).

b. Risk Stratification and Prognosis

There are no compelling data to recommend radionuclide imaging techniques for routine risk stratification in patients with hypertrophic cardiomyopathy. Depressed LV systolic function identifies a subgroup of patients with a higher incidence of congestive heart failure and a relatively poor prognosis (448). The presence of reversible defects in young patients is associated with increased risk for syncope, cardiac arrest, and ischemia-induced ventricular arrhythmias (439,447).

c. Assessment of Therapy

Demonstration of normal or increased LV function by RNA in patients with symptomatic congestive heart failure is useful clinically in determining the appropriateness of negatively inotropic therapeutic agents such as beta-adrenergic receptor blockers or calcium channel antagonists. Serial assessment of LV systolic and diastolic function may be useful in selected patients with progressive symptoms despite aggressive medical therapy and in monitoring the time-dependent LV remodeling after surgical or alcohol septal ablation or after initiation of atrioventricular (DDD) pacing. MPI may prove useful in assessing the effects of therapies designed to reduce myocardial ischemia (445), or confirming alcohol septal ablation, although there are limited data to support these approaches.

10. Hypertensive Heart Disease

a. Diagnosis

RNA enables detection of LVH, its distribution (concentric vs. asymmetric), and its impact on LV geometry in hypertensive subjects. With planar imaging, these findings are best determined when imaging is performed in the left anterior oblique projection. On a theoretical basis, blood pool SPECT provides an advantage in this regard. Accurate quantitative assessment of resting LV global systolic function and chamber topography can be obtained. Diastolic function can be evaluated from time-activity curves during diastole (449); as peak rapid filling rate, time to peak filling rate, and the contribution of atrial filling to total LV diastolic filling. RNA allows recognition of abnormal diastolic ventricular function in hypertensive subjects even when resting systolic global and regional functions are normal. This is important because approximately one third of patients presenting with heart failure have isolated diastolic dysfunction (450) and a large proportion of these patients have hypertensive hypertrophic heart disease.

Early radionuclide angiographic studies in hypertensive subjects with chest pain and suspected CAD did not reliably discriminate between those with and those without coronary disease. More than 25% of hypertensive patients with normal coronary anatomy developed abnormal wall motion with exercise (451). Furthermore, EF did not augment with exercise in hypertensive subjects independent of the presence of coronary disease that in normotensive subjects suggests coronary insufficiency. Lower resting EF and failure to increase with exercise in patients with LVH in the absence of obstructive coronary disease may be due to diminished coronary flow reserve (441-443) as a result of elevated resistance of the coronary microvasculature (452) due to coronary endothelial dysfunction (453) and/or to impaired sympathetic innervation (454). Stratification of patients by prevalence of cardiac risk factors suggested a greater likelihood of abnormal radionuclide stress imaging than in normotensive patients (455). These difficulties with radionuclide exercise stress imaging in hypertensive patients are further complicated when the resting ECG has criteria for LVH. Abnormal

response to exercise is most common in hypertensive patients with LVH, whereas most hypertensive patients without hypertrophy exhibit normal augmentation of function with exercise (456).

Hypertension is common in patients presenting with chest pain for stress testing in whom CAD is suspected. In patients without LVH, stress perfusion imaging is useful for detecting both reversible and fixed defects in those with coexistent ischemic heart disease. The diagnostic accuracy of myocardial stress-perfusion imaging appears to be more reliable than is RNA in identifying coexistent CAD in hypertensive patients with LVH, although an increased incidence of false-positive test results has been reported (277,453,455). In several large cohorts of patients with chest pain and LVH by electrocardiography or by 2D echocardiography, however, the assessment by exercise and pharmacologic stress TI-201 SPECT identified the presence and location of coronary insufficiency with high sensitivity and specificity (278,457,458).

b. Risk Stratification

Assessment of LV size and function (EF) by RNA provides prognostic information concerning clinical outcome and thereby can influence decisions regarding levels of activity and work status. Patients with hypertension and LVH have an increased adverse cardiovascular event rate compared with that of normotensive controls. SPECT imaging provides significant incremental predictive information regarding cardiac risk over and above that derived from clinical and historic demographics in hypertensive patients with LVH (278).

c. Evaluation of Therapy

Radionuclide angiographic assessment of ventricular remodeling, global and regional function, and regression of hypertrophy can be useful clinically to determine the long and short-term efficacy of specific antihypertensive therapeutic regimens particularly in hypertensive patients with LV dysfunction. Alternative approaches include 2D echocardiography and MRI.

11. Valvular Heart Disease

a. Diagnosis and Risk Stratification

In daily practice, 2D Doppler echocardiography studies have become the modality of choice for diagnosing valvular heart disease. This imaging modality assesses valve patho-anatomy, ventricular geometry, and ventricular function and also provides a fairly accurate estimate of lesion severity. The

potential usefulness of RNA in assessing valvular heart disease stems from the ability of RNA to quantify LV and RV function. In addition, MPI has been used to examine for the presence of flow-limiting coronary disease, especially in aortic stenosis.

b. Aortic Stenosis

Aortic stenosis usually develops in the fourth through the ninth decades of life, more frequently in men, and shares many of the pathologic characteristics and risk factors with coronary disease (459). Accordingly, approximately 35% of patients with aortic stenosis have concomitant coronary disease (460,461). Although it has been surprisingly difficult to prove that coronary revascularization at the time of aortic valve replacement improves long-term prognosis, many studies suggest concomitant revascularization is beneficial and it is also logical (462-464). Thus, coronary disease should be detected before aortic valve surgery. Although controversial, the presence or absence of angina is thought to be a relatively poor guide to the presence or absence of coronary disease. As many as 25% of patients without angina may have flow limiting coronary disease (465,466), whereas coronary disease is present in 40 to 80% of aortic stenosis patients complaining of angina (460,461).

Because of the lack of specificity and sensitivity that angina has for the concomitant presence of coronary disease in aortic stenosis, there has been much interest in the use of MPI in the preoperative evaluation of aortic stenosis patients for coronary disease. A partial tabulation of these results is shown in Table 20 (467-471). As can be seen, the sensitivity and specificity of stress perfusion in patients with aortic stenosis is relatively good but probably not adequate for patients about to undergo valve surgery in which the failure to detect coronary disease preoperatively could lead to adverse postoperative results. Thus, in practice, perfusion imaging has not supplanted coronary angiography in the preoperative work-up of patients with aortic stenosis.

c. Aortic Regurgitation

Initially, the most promising use of RNA in valvular heart disease appeared to be in the evaluation of patients with aortic regurgitation in whom exercise RNA seemed to provide additional information to resting studies (472). EF normally increases with exercise. The failure of EF to rise during exercise seemed to mark the onset of LV dysfunction and predict a poorer prognosis, or mark that the asymptomatic patient would shortly become symptomatic. The premise of exercise RNA is that myocardial contractility is augmented during

Table 20. Sensitivity and Specificity of Myocardial Perfusion Imaging in Detecting Coronary Disease in Patients With Aortic Stenosis

Author	n	Sensitivity	Specificity
Patsilinkos (467)	50	0.85	0.77
Kupari (468)	44	0.90	0.70
Samuels (469)	35	0.92	0.71
Kettunen (470)	61	0.91	0.73
Rask (471)	57	1.0 men; 0.61 women	0.75 men; 0.64 women

exercise resulting in increased EF. The failure of EF to rise during exercise was taken to indicate the reduction of contractile reserve and thus an early sign of myocardial dysfunction. Ejection fraction, however, is dependent not only on contractility but also on loading that can change dramatically in patients with aortic regurgitation during exercise (473). Increased heart rate reduces regurgitation time and the amount of regurgitation, thereby reducing LV preload, in turn reducing EF. Large increases in blood pressure during exercise increase afterload, also potentially reducing EF. Thus, failure of EF to increase during exercise might not indicate the presumed reduction in contractile reserve. It is probably these factors that led to the finding that exercise angiography does not usually add additional prognostic information to the measurement of resting LVEF and end-systolic dimension in predicting the response to aortic valve replacement worsens. More recently, Borer *et al.* (316) found enhanced prognostic ability of exercise RNA when the calculation of systolic wall stress was added to the interpretation of the test. Blunting of the exercise-induced rise of EF out of proportion to the exercise-mediated increase in wall stress had prognostic value for postsurgical outcome and also was sensitive in detecting a small group of patients who suffered sudden death.

In summary, exercise RNA in aortic regurgitation has largely been abandoned, although some practitioners still find the failure of EF to rise during exercise useful in helping to decide difficult cases. However, routine use of exercise RNA probably adds little to the assessment of resting EF and echocardiographic ventricular dimensions in timing surgery. The addition of the formal calculation of load seems to add prognostic information as logically it should. However, the additional effort required for the wall-stress determination may ultimately limit the usefulness of this index.

On the other hand, RNA accurately measures rest EF, which is clearly a useful tool in timing aortic valve replacement for patients with aortic regurgitation. Once LVEF falls below a value of approximately 55%, prognosis worsens (316,474). In practice, LVEF is usually visually estimated at echocardiography rather than at RNA because Doppler echocardiography studies give additional information about the amount of aortic regurgitation and about ventricular size and geometry which further aids in timing of surgery (475). There have been no prospective studies comparing visual estimates of LVEF by echocardiography versus quantitative RNA computation with regard to prognosis and risk stratification.

d. Mitral Regurgitation

Perhaps the most compelling use of RNA in valvular heart disease is in the preoperative evaluation of patients with mitral regurgitation. Mitral regurgitation not only burdens the LV with volume overload, but also promotes pulmonary hypertension in turn imparting a pressure overload on the RV. Although pulmonary artery pressure can often be estimated by Doppler echocardiography, the echocardiogram does not evaluate RV function well, whereas RV function assessment is a strength of RNA. Hochreiter *et al.* (476) found that patients with mitral regurgitation and combined LV and RV dysfunction fared worse than did patients with isolated LV dysfunction. The additional RV information enhanced the ability to predict outcome compared with that of any LV parameter. Still unknown is whether the addition of Doppler-obtained pulmonary pressure to indices of LV function in patients with mitral regurgitation would be as powerful prognostically as the combination of RNA LVEF and RVEF determinations.

As with aortic regurgitation, resting EF is a useful guide to mitral valve repair or replacement and RNA is suitable to make this assessment. When LVEF falls to less than approximately 60%, prognosis worsens (477-479). As with aortic regurgitation, however, the Doppler echocardiography technique can also make this assessment as a visual estimate while adding other prognostic information (480) as well as crucial anatomic data, helping to decide whether or not the valve can be repaired or must be replaced.

e. Evaluation of Therapy

The definitive therapy for valvular heart disease is valve surgery or, in the case of mitral stenosis, balloon valvuloplasty. RNA is useful postoperatively in gauging changes in LV and RV performance, occurring secondary to the loading alterations produced by valve surgery.

In summary, RNA has potential use in the preoperative assessment of patients with regurgitant valvular heart disease (Table 21). However, its use has largely been supplanted by the 2D Doppler echocardiography study that not only assesses chamber function but also gives important information about chamber dimensions, valve anatomy, and the amount of regurgitation. Standard exercise RNA seems to add little to resting RNA and echocardiography in evaluating patients for the timing of aortic valve replacement in aortic regurgitation. The addition of exercise hemodynamic data to exercise RNA is attractive and possibly useful but should be regarded as an experimental tool until more evidence is obtained. In mitral

Table 21. Recommendations for the Use of Radionuclide Imaging in Valvular Heart Disease

Indication	Test	Class	Level of Evidence
1. Initial and serial assessment of LV and RV function	Rest RNA	I	B
2. Initial and serial assessment of LV function	Exercise RNA	IIb	B
3. Assessment of the copresence of coronary disease	MPI	IIb	B

LV indicates left ventricular; MPI, myocardial perfusion imaging; RNA, radionuclide angiography; RV, right ventricular.

Table 22. Recommendations for the Use of Radionuclide Imaging in Adults With Congenital Heart Disease

Indication	Test	Class	Level of Evidence
1. Initial and serial assessment of LV and RV function	Rest RNA	I	B
2. Shunt detection and quantification	FPRNA	IIa	B

FPRNA indicates first-pass radionuclide angiography; LV, left ventricular; RNA, radionuclide angiography; RV, right ventricular.

regurgitation, addition of RVEF to either LVEF or echocardiographic parameters may have potential and should be studied further.

12. Adults With Congenital Heart Disease

a. Diagnosis

Because Doppler echocardiographic studies can detect intracardiac shunts and also assess the cardiac anatomy responsible for them, 2D Doppler echocardiography imaging is clearly the noninvasive study of choice in assessing congenital heart disease (481).

RNA can be used effectively in congenital heart disease to assess RV and LV systolic performance as it can with any heart disease. In addition, left-to-right shunting causes persistently high levels of activity in the lung or RV during FPRNA because of early recirculation (482). The resultant time-activity curve can be used to calculate pulmonary to systemic flow ratios quite accurately. The early appearance of tracer in the left chambers of the heart can be used to detect right-to-left shunts. A recent study found Tc-99m more sensitive than Doppler studies for determining abnormal lung flow after the Fontan and Glenn procedures (483).

In general, however, radionuclide studies are rarely practiced in assessing congenital heart disease and are unlikely to be accurate if used only occasionally at individual centers. Thus, 2D Doppler echocardiography imaging should usually be the diagnostic modality of choice unless special effort has been made to emphasize nuclear techniques in a given institution (Table 22).

STAFF

American College of Cardiology Foundation

Christine W. McEntee, Chief Executive Officer
Marie T. Hayes, Associate Specialist, Knowledge Development
Paula M. Thompson, MPH, Associate Director, Clinical Knowledge
Dawn R. Phoubandith, MSW, Associate Director, Clinical Policy and Documents

American Heart Association

M. Cass Wheeler, Chief Executive Officer
Rose Marie Robertson, MD, FACC, FAHA, Chief Science Officer
Kathryn A. Taubert, PhD, FAHA, Vice President, Science and Medicine

American Society of Nuclear Cardiology

Steven D. Carter, Executive Director
Dawn M. Edgerton, Associate Executive Director

APPENDIX 1: PROCEDURES AND PRINCIPLES

A. Introduction to Nuclear Cardiology

The first recorded nuclear cardiology study was performed in 1926 by Herman Blumgart and his colleagues who used a diluted solution of Radon to study the circulation (484). Since that time there has been steady progress in the development of imaging hardware, computer techniques, and radiopharmaceuticals, which has propelled nuclear cardiology into a mature field with clinically relevant and accurate imaging of molecular processes. These include measurement of myocardial perfusion, myocardial metabolism, and cardiac function.

This appendix summarizes the principles of nuclear cardiology equipment and techniques underpinning the recommendations on clinical applications included in this document. A more detailed review of the technical aspects of each of these subjects can be found in the *Imaging Guidelines For Nuclear Cardiology Procedures* published by the American Society of Nuclear Cardiology (485-491) and at <http://www.asnc.org/policy/g1003.htm>, <http://www.asnc.org/policy/g53-84imagingguidelines.pdf>.

B. Nuclear Cardiology Instrumentation

Most current nuclear cardiology applications use a gamma camera of either: 1) the single-crystal type or 2) the multicrystal type. The single-crystal gamma camera (Anger camera) is the most widely available system. Most cameras have a scintillation device, such as a thallium-activated sodium-iodide crystal, capable of emitting light in response to absorbed gamma rays. These gamma rays are generally focused by collimators attached to the front of the crystal, which allow localization of the object that is emitting radioactivity. The light emitted by the crystal is transformed into an electrical pulse by a series of light pipes and photomultiplier tubes, proportional to the energy of the gamma rays absorbed. The information about photon energy, position, and time of the event can be transformed into an image with multiple techniques, ranging from analog recording on film or paper in the past, to current digital computer recordings, which can be analyzed subsequently in a quantitative fashion. The optimal photon energy detected with these devices is 100 to 200 keV, but modifications in collimator design and crystal thickness allow a wide range of isotopes energies to be imaged. The multicrystal camera has been used as a low-resolution, high-count sensitive device for rapid dynamic assessment of flow and function, as in FPRNA.

These Anger-type scintillation cameras are used to generate most of the clinically important nuclear cardiology informa-

tion, including planar and SPECT for MPI, FPRNA and gated-equilibrium blood pool RNA, and myocardial infarct-avid imaging. SPECT images are tomographic reconstructions derived from either a single- or multiple-head gamma camera that rotates around the patient. Multiple-headed gamma cameras increase sampling rates, and thus decrease acquisition time for planar or tomographic imaging. With improved hardware, ECG-gated SPECT imaging of myocardial perfusion and blood pool has developed over the past decade, providing detailed comparison of 8 to 16 frames per cardiac cycle for wall motion and EF.

By using similar principles, multiple rings of stationary detectors that encircle the thorax are used for PET scanning. They are designed to detect the high-energy photons (511 keV) that are released from positron-emitting tracers, and to produce a series of multiple tomographic images encompassing the heart. Positron emission tomography devices rely upon coincidence-counting circuitry to detect the simultaneous and oppositely directed 511-keV positron annihilation photons. In this array, radiation detectors are placed facing one another, so that one "count" occurs when each of these two detectors is simultaneously struck by each one of the pair of annihilation photon. The ability to detect these two simultaneously generated photons (by coincidence detection) allows the PET scanner to identify and localize true events and reject single (ie, unpaired) photons as random, scattered photons. Such high-energy photons and coincidence detection allow improved spatial resolution compared with that of SPECT. Thus, PET cameras are electronically "collimated" by ignoring stray single photons and localizing the source of coincidence photons by backprojection. PET tracers simultaneously emit two high-energy photons in opposite directions.

PET tracers have been developed for the evaluation of numerous physiological processes, including regional MBF, metabolic processes, oxygen consumption, receptor activity, and membrane function. Improved quantification of these processes is possible with PET because of exacting methods of attenuation correction. Because PET scanners are more costly and less widely available than are standard Anger cameras, many single-photon cameras have been modified to image positron emitting isotopes. This has been accomplished by using high-energy collimation on SPECT cameras, or by adoption of the coincidence counting mechanism described above for PET, but with a rotating camera mounted on a gantry used for SPECT.

As noted above, coincidence detection with PET provides a means of correcting for tissue photon attenuation. Such attenuation correction results in improved measurement of regional tracer activity compared with SPECT methods and permits true quantification of this activity, which can be translated into quantification of physiologic and metabolic processes. Such quantification is facilitated further by the high temporal resolution capability not available with SPECT.

C. Radiopharmaceuticals

1. Single-Photon MPI

There are currently 5 radiopharmaceuticals approved for radionuclide MPI in the United States. These include the potassium analogs Tl-201 (Tl-201, gamma decay and electron capture, 68-80, 135, and 167 keV) and rubidium-82 (Rb-82, positron decay, 511 keV), and 3 agents labeled with Tc-99m (Tc-99m, isomeric transition, 140 keV).

Tl-201 (like Rb-82) shares the cationic properties of potassium and, therefore, has active membrane transport mechanisms, which are markers of cell membrane integrity and, therefore, myocardial viability. Early after tracer injection, the myocardial concentration of Tl-201 reflects regional MBF. The tracer then undergoes monoexponential washout. The washout rate decreases when initial tracer delivery and/or MBF are diminished. The rapid washout of tracer from myocardial segments with normal activity, and the slower washout from segments with reduced tracer activity, leads to normalization of myocardial perfusion defects over time; this is termed the redistribution phenomenon.

The currently approved Tc-99m-labeled agents include two cationic lipid soluble compounds with predominantly hepatobiliary excretion, Tc-99m-sestamibi and Tc-99m-tetrofosmin, and one neutral lipophilic compound with an affinity for the myocellular membrane, Tc-99m-teboroxime. The clinical use and marketing of the latter agent has been limited because of rapid washout from the myocardium, requiring nontraditional imaging modes for its use. By contrast, there is clinically negligible washout of Tc-99m-tetrofosmin and Tc-99m-sestamibi from the myocardium after injection. This, combined with the superior imaging characteristics of Tc-99m, have spurred the widespread use of these agents, using same-day or two-day, rest-stress or stress-rest, or dual-isotope (Tl-201 rest and Tc-99m stress) imaging protocols (489). For same-day protocols, a low dose of the Tc-99m tracer (eg, 8 to 10 mCi) is used first followed by either tripling the dose (24 to 30 mCi) or using a smaller increment after a 2- to 3-hour delay to allow decay of the initial injection. For 2-day protocols, full doses (24 to 30 mCi) are administered each day.

2. Positron Emission Tomography

A number of tracers have been developed for clinical PET studies. These include oxygen-15 (O-15, half-life, 2 minutes), nitrogen-13 (N-13, half-life, 10 minutes), C-11 (half-life, 20 minutes), and fluorine-18 (F-18, half-life, 110 minutes), which may be coupled to a number of physiologically active molecules. These tracers require a local or on-site cyclotron for production, except for F-18, which can be shipped for same-day use. Rubidium-82 (half-life 75 seconds) does not require a cyclotron and may be delivered directly to the patient from an on-site generator. The most frequently used agents to assess myocardial perfusion with PET are rubidium-82, N-13-ammonia, and O-15 water. C-11-labeled fatty acids and F-18 FDG are common metabolic

tracers, and C-11 acetate is used as an agent to assess oxidative metabolism and oxygen consumption. These tracers have also been imaged by using high-energy collimators and SPECT equipment.

PET perfusion imaging has been performed in research laboratories with several other agents, including copper-62-pyruvaldehyde bis (N-methyl-thiosemicarbazone) (PTSM), Tc-94m-sestamibi or -tetrofosmin, and gallium-68, but these are not widely available or utilized at this time.

3. First-Pass RNA

FPRNA assessment of ventricular function can be performed with essentially any intravenous tracer that can be injected with enough radioactivity to provide adequate counting statistics (ie, more than 8 mCi), and does *not* have a high degree of first-pass extraction or capillary trapping in the lung after injection, as do Tc-99m-teboroxime and Tc-99m-macroaggregated albumin, respectively. This feature of FPRNA allows both RV and LV functional assessment to be combined with other nuclear techniques, such as bone scintigraphy, gated blood pool equilibrium RNA, and myocardial perfusion SPECT.

4. Gated-Equilibrium RNA

Radiopharmaceuticals for planar, SPECT, and PET gated equilibrium blood pool RNA (also called MUGA for multi-gated acquisition, or RNV for radionuclide ventriculography) include Tc-(99m or 94)-human serum albumin, Tc-(99m or 94)-labeled red blood cells, and O-15-labeled carbon monoxide. Red cell labeling can be performed by combining sodium pertechnetate with stannous pyrophosphate either *in vivo* (injecting tracer after stannous pyrophosphate), or *in vitro* (removing 50 ml of blood, adding stannous pyrophosphate followed by sodium pertechnetate, and then reinjecting the labeled red cells). Although *in vitro* labeling gives slightly superior red-cell tagging, *in vivo* labeling allows bolus of sodium-pertechnetate for FPRNA, a superior method for determination of RVEF and detection of shunts. For this reason, many laboratories that wish to perform FPRNA combined with gated-equilibrium blood pool RNA will use a hybrid of the *in vivo* and *in vitro* techniques (often referred to as “*in vitro*” labeling), in which 30 to 50 ml of blood is mixed with the stannous pyrophosphate briefly in a large syringe, followed by a bolus of sodium pertechnetate for FPRNA acquisition.

D. Image Acquisition, Analysis, and Display

1. SPECT MPI

SPECT MPI is most often performed with poststress ECG gating, although ungated SPECT imaging is often performed at rest or in patients with cardiac arrhythmias. The projection images for SPECT reconstruction images are usually acquired by using high-resolution collimation, although some systems use high quality general-purpose cast (rather than foil) collimators. A total of 180° of projection images

are usually obtained, scanning from right anterior oblique 45° to left posterior oblique 45°. A total of 60 projections of 15 to 30 seconds duration at 3° steps will give adequate count density, for a usual total of 15- to 25-minute acquisition time. Acquisition time is reduced by the use of multiple-headed gamma cameras. For ECG gating, at each projection either 8 or 16 frames per cardiac cycle should be acquired.

SPECT myocardial perfusion images are generally obtained 10 minutes after injection at rest or stress with Tl-201. Tc-99m-tetrofosmin and sestamibi have a large fraction of hepatobiliary excretion, which can interfere with myocardial image reconstruction. An additional 15 to 60 minutes after rest is helpful to allow liver clearance of these tracers. Exercise, which lowers splanchnic blood flow, results in higher myocardial to hepatic tracer ratios, and therefore allows earlier imaging, generally at 15 to 20 minutes after exercise. Pharmacologic stress testing, however, increases splanchnic blood flow, necessitating a longer waiting period before to poststress imaging, unless the pharmacologic stress is combined with low-level walking on a treadmill or slowly walking in place. The addition of some form of exercise to pharmacologic stress testing decreases splanchnic blood flow and improves perfusion SPECT image quality (492).

For SPECT image processing, a wide range of reconstruction filters and settings have been used, depending upon the tracer characteristics, the amount of myocardial tracer activity, the system and collimator characteristics, and the software used for analysis. After collimator sensitivity and center of rotation correction, low-pass prefiltered projections are reconstructed into transaxial slices for each of the 8 or 16 frames of the cardiac cycle for gated SPECT, or the single ungated or summed-gated projection set. Transaxial slices are usually reconstructed by using a Butterworth back projection filter. The transaxial slice sets are then reoriented in cardiac planes (ie, short axis, horizontal long axis, and vertical long axis) for each of the eight frames of the cardiac cycle. Short-axis images of perfusion SPECT are often combined into a polar map or “bull’s-eye” plot display, with the apical segments in the center and basal segments on the outer rim.

Midventricular horizontal, vertical long-axis, and short-axis slices, as well as 3D reconstructions, can be analyzed for regional wall motion or EF (see gated SPECT section below). If 8 frames are acquired, these 8 slices can be expanded to 16 frames by weighted frame interpolation and temporal filtering for a smoother cinematic display.

2. Planar MPI

This technique is rarely performed, primarily when tomographic imaging is not feasible (eg, an obese patient who exceeds the weight limit of the SPECT imaging table). Tomographic imaging, by displaying data in the format of slices with discrete thickness, provides better contrasts, allows better separation of myocardial and other nonmyocardial structures and individual coronary artery beds, and is inherently quantitative. A guide to the planar technique can

be found at http://www.asnc.org/policy/#MYOCARDIAL_PERFUSION_PLANAR_PROTOCOLS.

3. PET Perfusion Imaging

PET differs from SPECT in that tracer kinetic modeling and accurate measurements of attenuation coefficients are used to reconstruct myocardial perfusion maps, which can be quantified for determination of MBF in milliliters of blood-per-gram of tissue-per-minute. These attenuation maps are typically acquired using a Ga-67 ring source over 360°. In addition to perfusion imaging, myocardial metabolism can be measured by using tracers such as F-18-2-deoxyglucose (glucose metabolism), C-11-acetate (oxidative metabolism), and C-11-palmitate (fatty acid metabolism). Metabolic imaging can complement perfusion imaging to determine the viability of myocardial segments with poor perfusion and function.

4. First-Pass RNA

FPRNA can be performed with a single crystal high-count rate gamma camera fitted with a high-sensitivity parallel-hole collimator or with a multicrystal camera. If gated-equilibrium blood pool RNA is also to be performed, after placement of a large bore (14- or 16-gauge) antecubital intravenous line, 1.5 mg of stannous pyrophosphate is mixed with 30 ml of the patient's blood for approximately 60 seconds and is then infused. Resting FPRNA is performed after a 10-minute delay to allow further red blood cell uptake of stannous ion. Tc-99m-pertechnetate (25 to 30 mCi) in a volume of less than 1 ml, is given by rapid flushing with at least 30 ml of normal saline through the indwelling catheter. Tc-99m-diethylenetriamine pentaacetic acid (DTPA) is often used if no gated images are required. Perfusion agents such as Tc-99m-sestamibi or tetrofosmin may be used if perfusion images are desired. Images are acquired in the right anterior oblique or anterior projection using 25 (plus or minus 4) frames per cardiac cycle.

FPRNA data are analyzed by using the frame method for LVEF, which creates a representative LV volume curve by summing frames of several (usually 5 to 10) cardiac cycles, aligned by matching their end-diastoles (histogram peaks) and end-systoles (histogram valleys) during the operator defined levophase of tracer transit. The pulmonary frame background-corrected representative cycle is then interrogated with a fixed ROI in order to obtain the final first-pass LV time-activity curve. This ROI is usually drawn over the LV as defined by a first harmonic Fourier transformation phase image, which clearly distinguishes the LV from aortic counts. End-diastole is taken as the first frame of the representative cycle, and end-systole is defined as the frame with the minimum counts in the histogram. Historically, the LVEF was taken as the end-diastolic counts minus the end-systolic counts, divided by the background subtracted end-diastolic counts.

5. ECG-Gated Planar Equilibrium Blood Pool RNA

Similar to SPECT blood pool imaging, planar-gated blood pool images are also best when acquired by using high-resolution collimation after red cell labeling described above. Images for LVEF calculation are obtained in the best-septal (shallow) left-anterior oblique view. This angle, usually 25° to 60°, must be carefully set by use of a persistence mode before acquisition. For regional wall motion assessment, the best-septal view plus and minus 45° should be obtained (anterior and lateral views). Each planar-gated image is acquired for 6- to 10-minute duration.

For LVEF, automated variable regions of interest are generated on the planar-gated equilibrium blood pool RNA blood pool data throughout the cardiac cycle. These methods require either a manual or an automatically identified LV master ROI. Fourier phase imaging, requiring no operator intervention, can identify the LV, followed by the automated or semi-automated edge detection technique described above for gated blood pool. An automatically generated periventricular background ROI must routinely be adjusted to avoid inclusion of high-count structures (eg, spleen, descending aorta), which could artifactually increase the LVEF.

For analysis of diastolic function with any gated technique, it is important to obtain high temporal resolution, such that small changes in LV volume can be measured over small intervals of time, preferably more than 20 frames during diastole. The first derivative of the LV volume curve can then be used to obtain filling rates and emptying rates, time to peak filling, and the fraction of early versus late diastolic filling.

See Figure 1 for examples of first-pass and blood pool imaging.

6. ECG-Gated Tomographic Equilibrium Blood Pool Imaging

Acquisition of projections for gated SPECT reconstruction of blood pool images is usually obtained by using high-resolution collimation in a fashion similar to gated SPECT MPI, after red blood cell labeling as described above.

Reconstruction and display parameters also parallel those used for SPECT MPI. Once the transaxial slices are reoriented into cardiac planes (ie, short axis, horizontal long axis, and vertical long axis) for each of the 8 or 16 frames of the cardiac cycle, EF information can be obtained with either 3D and volume-rendering techniques or by analysis of biplane horizontal and vertical long-axis slices using the center of mass, combination first and second derivative automated edge detection algorithm commonly used for planar-gated blood pool analysis. This technique will require manual placement of a ROI at end-diastole for both horizontal and vertical long axes, which can serve as an edge search limiting master region, because automated valve plane definition is limited by the lack of count density changes at the mitral or tricuspid valves. Because of the uniformly high contrast and lack of overlap between cardiac blood pool and extra-

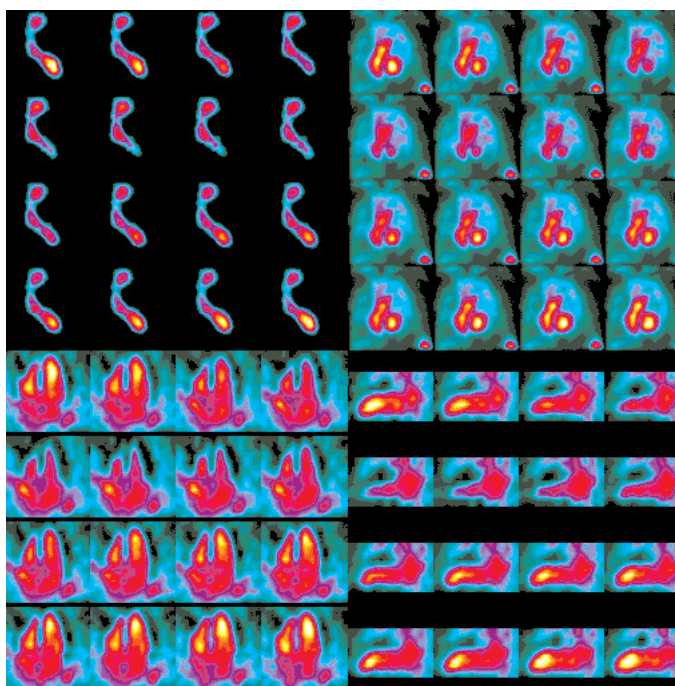


Figure 1. First-pass and blood pool imaging. Examples of anterior projection FPRNA background corrected representative cycle (top left), left anterior oblique planar gated equilibrium blood pool radionuclide angiography (top right), and gated SPECT horizontal (bottom left) and vertical (bottom right) long axis images are shown on a normal subject, with 16 frames of the cardiac cycle for each technique. These images were acquired sequentially by bolus of Tc-99m-pertechnetate after injection of stannous pyrophosphate (in vitro labeling), which allows red blood cell tagging for planar and SPECT blood pool images. Source: Dr. Kim A. Williams, University of Chicago, Chicago, Illinois.

cardiac structures, no background subtraction algorithm should be used for this analysis. LVEF and RVEF can be calculated for each long axis as the end-diastolic counts minus the end-systolic counts, divided by the end-diastolic counts, combining them for a biplane EF.

E. Quality Assurance, Artifact Detection, and Correction

1. Quality Control

For quality control, each detector in a planar, SPECT, or PET system should be examined for detector alignment and flood field uniformity on a daily basis. Periodic examination of the center of rotation should be performed for SPECT systems. Quality assurance of each patient's myocardial perfusion image data set includes examination of raw projection images for overlying tissue attenuation, motion artifacts, and noncardiac tracer uptake patterns (eg, malignancies in lung or breast tissue). Reconstructed images should be inspected for proper angles of reconstruction and for activity near the myocardium that could result in subtraction artifacts (ie, negative lobe or ramp artifacts) or artificially increased counts due to scattered photons.

Differential soft-tissue attenuation is well recognized as a source of reduced diagnostic specificity, and possibly sensitivity, of SPECT perfusion studies. A variety of indirect, and in general, only partial solutions, such as use of ECG gating, breast binders, and prone imaging have been proposed. ECG gating can be helpful in distinguishing CAD from artifact

when an apparent defect is unchanged (ie, a fixed defect) between the stress and rest images, and regional wall motion is either normal (artifact) or abnormal (CAD). However, this approach fails in the common circumstance of soft-tissue attenuation that “shifts” between the stress and rest images. In such cases, a defect that is reversible or partially reversible may be created; the finding of normal wall motion is consistent with either CAD or artifact. Prone imaging, in the absence of either a low attenuation or chest cut-out imaging table, requires additional camera time for performance of both supine and prone acquisitions, as opposed to one view only being required. This improves only diaphragmatic attenuation artifacts. Also, many patients are unable to lie prone, and, in others, attenuating soft tissue remains a problem even in this position.

An advantage of Tc-99m-sestamibi or tetrofosmin over Tl-201 imaging is that images can be repeated when patient motion, soft-tissue attenuation, or other artifacts are considered to be responsible for producing an alteration in image characteristics, because with these tracers the radiopharmaceutical distribution does not change over time. Thus, when images in the supine position show questionable perfusion defects, images can be repeated in the prone position which is associated with less patient motion, less inferior wall attenuation, and a shift in other soft-tissue artifacts (136,493,494). The combination of supine and prone imaging also is helpful in identifying breast attenuation and attenuation due to excessive lateral wall fat, because of the shift in position of

the attenuating structures that occurs in the prone position. Because the prone position frequently causes an anteroseptal defect secondary to increased sternal and imaging table attenuation in this position, however, imaging in this position is considered by most to be an adjunct to, not a replacement for, supine imaging.

2. Attenuation Correction

To further address these problems, over the past few years, direct corrections for attenuation-based artifacts have become widely available. There are significant differences in approaches taken for attenuation correction, dependent upon the equipment configuration (eg, the number of detectors), whether correction for photon scatter and depth-dependent resolution is also offered, and the type of radionuclide used to generate the transmission scan.

Attenuation-correction algorithms can ameliorate the effects of tissue attenuation (eg, from diaphragmatic, chest wall, or breast shadowing). With the appropriate hardware, a transmission source is used to acquire an estimate of attenuation coefficients. This transmission tomogram provides anatomically specific density maps of the thorax that can be used to correct SPECT image data for photon attenuation (152-156). The transmission images can be obtained with either a fixed source or a scanning line source, and can be performed sequentially or simultaneously.

Attenuation-correction SPECT techniques represent a significant advance in MPI and hold great promise for improved assessment of cardiac patients. Substantial technical advances have been made in the past several years, including the recognition of the importance of effective quality control and the continued development of scatter correction and resolution compensation. Advanced SPECT perfusion imaging systems, including features such as attenuation correction, must undergo complete system characterization, development of normal activity distribution profiles, and definition of differences among various manufacturers' solutions. Finally, quantitative analysis programs adapted for each camera system and radiopharmaceutical are limited but are under active development. Ideally, reference databases from normal subjects should be sex-independent after total correction for attenuation.

Clinical validation has been performed for several commercially available systems, although "complete" correction still does not occur in all patients. The true value of these methods, compared with other techniques to improve diagnostic accuracy has yet to be fully defined. Attenuation-correction methods offer the potential for improved diagnostic accuracy, but require a modified approach to image interpretation accounting for the effects of these methods on the resultant images. Technologist and physician education in the details of these advanced imaging techniques, along with effective quantitative tools and improved processing algorithms, will continue to advance the value and acceptance of attenuation-corrected SPECT imaging.

Based on available clinical evidence and the rapid development of attenuation-correction technology, it is recommended that providers (institutions and practitioners) consider the addition of hardware and software that have undergone clinical validation and include appropriate quality control tools to perform nonuniform attenuation correction. At the present time, it is suggested that both noncorrected and corrected image sets be reviewed and integrated into the final report. But as the reader gains the appropriate experience and confidence in the correction methodology, only the corrected images may be necessary, as is the standard in PET. Based on current information and the rate of technology improvement, the Society of Nuclear Medicine and the American Society of Nuclear Cardiology believe that attenuation correction should be regarded as a rapidly evolving standard for SPECT MPI, for which the weight of evidence/opinion is in favor of its usefulness (164).

3. Motion Correction and Depth-Dependent Blurring

There are also software packages that will correct for patient motion artifacts, which occur when the patient fails to hold one position during the 15- to 30-minute acquisition interval. These algorithms may use automated or manual realignment of frame positions to avoid artifacts during reconstruction due to misplacement of cardiac counts. However, this "correction" may worsen reconstruction artifacts, especially in cases in which there is little motion artifact in the original acquisition.

Another concerning feature of SPECT acquisition with parallel-hole collimation is "depth-dependent blurring," which increases as the imaged tissue plane is further away from the collimator surface. Algorithms for simultaneous automated attenuation, scatter, depth-dependent blurring, and motion correction have been proposed (157), and will likely have further development in the near future.

F. Clinical Procedures

1. Myocardial Perfusion Imaging

Planar and SPECT MPI are established and widely performed methods of assessing relative regional MBF. The advantages of these techniques include a diagnostically and prognostically important assessment of the presence, extent, and severity of CAD; detection of myocardial viability; and, more recently, myocardial wall mass, regional thickening, wall motion, and global ventricular function by using gated perfusion imaging. As described above, the major limitations to the accuracy of these techniques have been tissue attenuation artifacts, photon scatter, motion artifacts, and limited spatial resolution.

Each of the aforementioned technical details of acquisition and processing should be considered when interpreting perfusion images. Detection and correction of artifacts, when feasible, has resulted in marked improvements in specificity of these highly sensitive techniques. When artifacts cannot

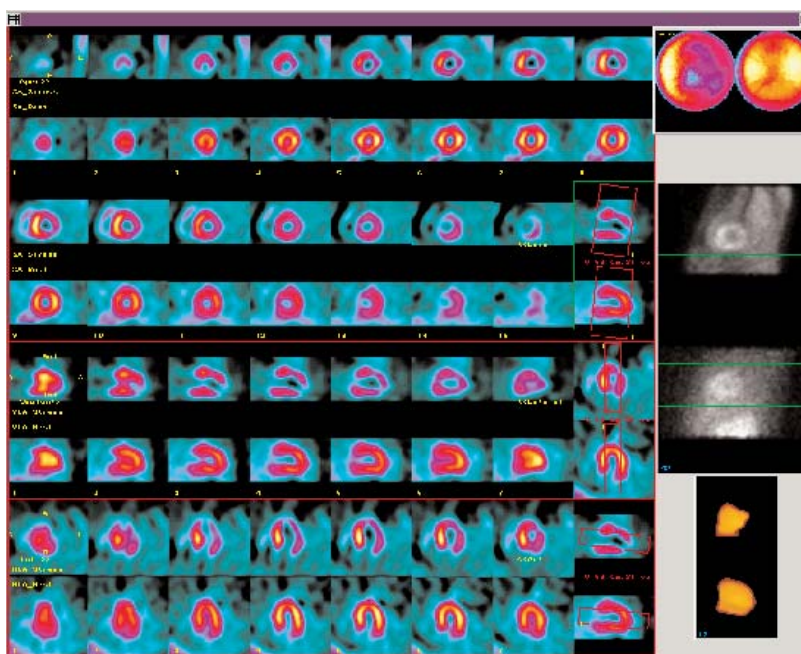


Figure 2. Abnormal SPECT perfusion display. Example of an abnormal SPECT perfusion display showing corresponding rest TI-201 (even rows) and stress Tc-99m-tetrofosmin (odd rows) slices. This is an example of multivessel CAD and reversible ischemia, with transient dilatation of the ventricle and increased RV uptake of Tc-99m-tetrofosmin. Fifteen short axis slices comprise the first four rows. The vertical long axis images are shown on rows 5 and 6. The horizontal long axis images are shown on rows 7 and 8. The polar maps (“bull’s-eye” images) are shown in the upper right aspect of the display. Below these images are the raw data projections, which are shown to the interpreter in cine format with horizontal reference lines to aid detection of patient motion that can create artifacts and noncardiac foci of abnormal tracer uptake, and volume rendered images of the myocardium are shown below the raw projections. Source: Dr. Kim A. Williams, University of Chicago, Chicago, Illinois.

be corrected successfully, image acquisition should be repeated.

Myocardial perfusion images can be interpreted visually, as well as with the aid of computer quantification. This technique allows the clinically important description of the perfusion defect extent (in terms of the amount of myocardium or number of segments involved), defect severity (in terms of the intensity of the perfusion defect), and defect reversibility (comparing images to determine if stress perfusion defects are less intense or absent on rest or redistribution images). Each of these indices has proven diagnostic and prognostic value. These images should also be analyzed for the presence of increased LV cavity size at rest or induced by stress (transient ischemic dilatation) reflective of severe and extensive CAD, RV dilatation, hypertrophy, or prominence after exercise stress (consistent with severe LV ischemia). When available, detailed comparison with previous images should be performed; this provides additional insight into changes in perfusion over time, and may help to distinguish myocardial hypoperfusion from attenuation artifacts.

See Figures 2 through 4 for examples of SPECT perfusion images and myocardial segmentation and nomenclature standards.

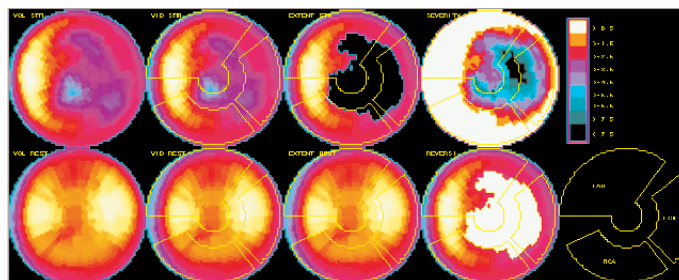


Figure 3. Polar maps. An example of polar maps used for analysis of myocardial perfusion SPECT is shown (from the same patient as in Figure 2). Polar maps plot the tracer activity in each short axis slice with the apex in the center and basal slices on the out rings. Stress images are on top, rest on the bottom. The left column represents the volume-weighted polar maps, which accentuates the apical segments. Maps constructed in the classic “bull’s-eye” fashion of representing each short axis slice width equally in the map are shown in the second column. The third column contains a “blackout” polar map, indicating the extent of perfusion defects by blackening the area of myocardium that is less than 2.5 SD below the sex-specific normal data base comparison. The spatial distribution of the SDs is shown in the upper panel of column four, with the translation table in column five. On the lower panel, column four shows the reversible fraction of the blackout map. On the lower right, the area corresponding to the usual territory perfused by each coronary artery is shown. Source: Dr. Kim A. Williams, University of Chicago, Chicago, Illinois.

Coronary Artery Territories

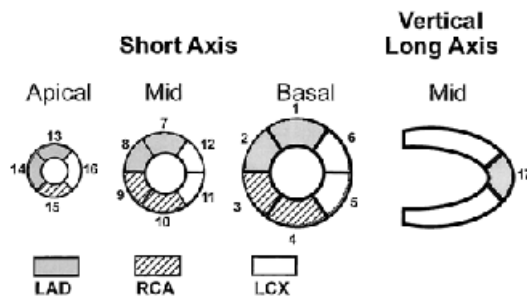


Figure 4. Assignment of the 17 myocardial segments to the territories of the left anterior descending (LAD), right coronary artery (RCA), and the left circumflex coronary artery (LCX). Reprinted with permission from Cerqueira MD et al. Standardized myocardial segmentation and nomenclature for tomographic imaging of the heart: a statement for healthcare professionals from the Cardiac Imaging Committee of the Council on Clinical Cardiology of the American Heart Association. *Circulation*. 2002;105:539-42.

a. Exercise and Pharmacologic Modalities Used in Stress Imaging

A variety of methods can be used to induce stress: (1) exercise (treadmill or upright or supine bicycle) and (2) pharmacologic techniques (either vasodilators or dobutamine), with perfusion agents administered through an indwelling intravenous line at peak exercise. The patient then exercises for an additional 30 seconds to 2 minutes after injection.

When the patient can exercise to develop an appropriate level of cardiovascular stress (eg, more than 85% MPHR), exercise stress testing (generally with a treadmill) is preferable to pharmacologic stress testing because of the additional information obtained with regard to physical capacity and exercise-induced arrhythmias. The purpose of the stress is to increase the myocardial oxygen demand, and therefore increase MBF by autoregulation, in order to answer the clinical question of regional perfusion disparities, indicative of coronary artery stenoses. An exercise test that increases the heart rate to more than 85% MPHR for age and/or a peak systolic pressure/heart rate product ("double product") of more than 25 000 is considered adequate for diagnostic perfusion imaging.

When the patient cannot exercise to the necessary level or in other specified circumstances (eg, LBBB, paced rhythm), however, pharmacologic stress testing may be preferable, because this results in fewer conduction-related septal perfusion defects. Nonetheless, in patients who exercise only to a submaximal level because of the effect of drugs, perfusion imaging still affords higher sensitivity than does the exercise ECG alone (495). Three drugs are commonly used as substitutes for exercise stress testing: dipyridamole, adenosine, and dobutamine. Dipyridamole and adenosine are vasodilators that are most commonly used in conjunction with myocardial perfusion scintigraphy, whereas dobutamine is a positive inotropic (and chronotropic) agent used principally when patients have a contraindication to the use of adenosine or

dipyridamole. It is generally recommended that if the patient who can exercise achieves less than 85% MPHR and does not develop ischemic symptoms, the myocardial perfusion radiopharmaceutical is not injected during exercise, but the test is converted to a pharmacologic stress imaging procedure. Of note, pharmacologic stress testing now comprises more than 30% of the myocardial perfusion studies performed in the United States.

DIPYRIDAMOLE AND ADENOSINE. Dipyridamole was the first agent approved for inducing myocardial hyperemia in patients unable to exercise. The mechanism of action is inhibition of cellular uptake of adenosine; adenosine then accumulates after either oral (slowly) or intravenous (quickly) dipyridamole administration. Because of its slow and relatively unpredictable gastrointestinal absorption rate, oral dipyridamole is rarely used and is no longer recommended.

Intravenous dipyridamole is given as a slow or intermittent infusion of $0.14 \text{ mg} \cdot \text{kg}^{-1} \cdot \text{min}^{-1}$ over 4 minutes (a total of 0.56 mg/kg), followed by tracer injection 4 minutes later. Similarly, adenosine is infused typically at $0.14 \text{ mg} \cdot \text{kg}^{-1} \cdot \text{min}^{-1}$ for 6 minutes, with tracer injection at 3 minutes. Imaging is typically performed 20 to 60 minutes after injection with either agent, depending upon the rate of clearance from the liver.

The flow increase with adenosine or dipyridamole is of a lesser magnitude through stenotic arteries, creating heterogeneous myocardial perfusion, which can be depicted with perfusion tracers. Although this mechanism can exist independently of myocardial ischemia, in some patients, true myocardial ischemia can occur with either dipyridamole or adenosine because of a coronary steal phenomenon, especially in collateral flow dependent arteries.

Both dipyridamole and adenosine are safe and well tolerated despite frequent mild side effects, which occur in 50% (116) and 80% (117) of patients, respectively. With dipyridamole infusion, the most common side effect is chest pain (18 to 42%), with arrhythmia occurring in less than 2%. Noncardiac side effects have included headache (5 to 23%), dizziness (5 to 21%), nausea (8 to 12%), and flushing (3%) (116). With adenosine infusion, chest pain has been reported in 57%, headache in 35%, flushing in 25%, shortness of breath in 15%, and first-degree atrioventricular block in 18%. The side effects of adenosine or dipyridamole are less frequent when vasodilator stress is combined with low-level exercise. Severe side effects are rare, but both dipyridamole and adenosine may cause severe bronchospasm in patients with asthma or reactive airway disease; therefore, they are contraindicated in these patients. Dipyridamole and adenosine side effects are antagonized by theophylline; however, this drug is ordinarily not needed after adenosine because of the latter's ultrashort half-life (less than 10 seconds). The ability of these drugs to cause coronary vasodilation can be blocked by caffeine and other methylxanthines. Thus, patients are instructed to avoid these agents for 24 hours before testing.

DOBUTAMINE. Dobutamine in high doses (20 to 40 mcg · kg⁻¹ · min⁻¹) increases the three main determinants of myocardial oxygen demand (ie, heart rate, systolic blood pressure, and myocardial contractility), thereby eliciting a secondary increase in MBF and potentially provoking myocardial ischemia. The flow increase (2- to 3-fold baseline values) is less than that elicited by adenosine or dipyridamole but is sufficient to demonstrate heterogeneous perfusion by radionuclide imaging. Although side effects are frequent during dobutamine infusion, the test appears to be relatively safe, even in the elderly (106,118,119,496-498). The most frequently reported noncardiac side effects (total 26%) in a study of 1118 patients included nausea (8%), anxiety (6%), headache (4%), and tremor (4%) (497). Common arrhythmias included premature ventricular beats (15%), premature atrial beats (8%), supraventricular tachycardia, and nonsustained ventricular tachycardia (3 to 4%). Atypical chest pain was reported in 8% and angina pectoris in approximately 20%.

b. Concomitant Use of Drugs

Medications that decrease myocardial oxygen demand, such as beta-adrenergic or calcium channel blocking agents, may limit the development of ischemia during the exercise test. Beta-blockers tend to attenuate the exercise-induced increase in heart rate and blood pressure. Consequently, the sensitivity of the exercise perfusion study for the diagnosis of CAD appears to be lower in patients taking such agents (96,499-502).

Several studies have shown that nitrates may also decrease the extent of perfusion defects or even convert abnormal exercise scan results to normal results (230,232,503,504). Therefore, when feasible, long-acting nitrates should be discontinued at least 12 hours before the test, although sublingual nitroglycerin may be given as needed up to 2 hours before the test. It is also generally recommended that patients not take caffeine-containing medicines, foods, or beverages for 24 hours before exercise stress testing. By preparing patients in this manner, if the patients fail to achieve 85% of MPHR during exercise, then pharmacologic testing with adenosine or dipyridamole can be immediately substituted before this stress injection of radiopharmaceutical. This process can avoid the potential uncertainty that might arise in an exercise myocardial perfusion study in which 85% MPHR was not achieved. It has been shown that the extent and sensitivity of myocardial perfusion defects on SPECT is lower in patients failing to achieve 85% of MPHR than in those achieving greater than 85% MPHR (96). Pharmacologic perfusion imaging using dipyridamole or adenosine appears to be less affected by antianginal drugs and thus provides an appropriate alternative to exercise (230) in patients who are not taken off cardiac medications before testing. When patients are unable to exercise adequately and they are under the effects of caffeine, dobutamine stress is a reasonable substitute form of stress. Dobutamine stress, however, would be

expected to have a blunted and possibly nondiagnostic response in patients on beta blockers.

Although it is generally recommended that the initial risk stratification study be performed with the patients off of cardiac active medications, it is recognized that potentially useful clinical information can be derived from exercise myocardial perfusion SPECT study performed on cardiac medications.

c. Procedural Aspects of MPI

As noted above, there are currently four perfusion tracers approved for single-photon perfusion imaging: 1) Tl-201, 2) Tc-99m-sestamibi, 3) Tc-99m-teboroxime, and 4) Tc-99m-tetrofosmin. Another tracer, Tc-99m-NOET (Tc-99m-labeled (bis(N-ethoxy, N-ethyl dithiocarbamate) nitroind technetium[V])) (Tc-NOET), is currently undergoing evaluation (505). Currently utilized clinical imaging protocols are listed in <http://www.asnc.org/policy/gl003.htm> - MYOCARDIAL PERFUSION SPECT PROTOCOLS and <http://www.asnc.org/policy/gl003.htm> - Acquisition Protocols-SPECT.

THALLIUM-201. Images of the heart shortly after Tl-201 administration show deficits in regions in which blood flow is relatively reduced (eg, myocardial ischemia), and in zones of nonviable myocardium (eg, previous MI). After Tl-201 injection during exercise, images are generally acquired immediately and again 3 to 4 hours after administration to examine "redistribution." Over time, redistribution of isotope generally occurs in previously ischemic zones (ie, defects related to ischemic myocardium normalize or "fill in"). Defects related to infarcted or scarred myocardium typically do not redistribute over time and remain fixed. However, imaging at 24 hours or after reinjection of Tl-201 may show viable but hypoperfused segments not otherwise identified by a standard redistribution study performed at 3 to 4 hours after isotope injection. Assessment of lung Tl-201 activity on an anterior planar image, acquired immediately after exercise, provides a means to assess exercise-induced increases in pulmonary venous pressures. Finally, in patients with UA or AMI, a perfusion study can be performed at rest. As with exercise, serial imaging can be performed after pharmacologic or rest thallium administration and demonstrate redistribution in regions of rest ischemia or underperfused but viable myocardium

TC-99M-BASED AGENTS The shorter half-life of Tc-99m (6 hours) compared with Tl-201 (73 hours) allows administration of a larger dose, with resulting improved count statistics. The more favorable imaging characteristics of Tc-99m (higher emission energy, less scattered radiation, and less tissue attenuation) are additional benefits of using these agents. There is a good correlation between Tl-201, sestamibi, or tetrofosmin uptake and MBF when the latter is normal, decreased, or moderately increased (up to two times the baseline values). Despite good correlation between the clinical results, myocardial uptake of sestamibi and tetrofosmin

underestimate blood flow more significantly than does Tl-201 when flow is increased more than 2.0 to 2.5 times the baseline values. Because sestamibi and tetrofosmin only undergo a small amount of washout after initial myocardial uptake, the distinction between transient, stress-induced perfusion defects and fixed-perfusion defects requires administration of two separate injections, one during stress and one at rest. Images are obtained after resting or stress injection at appropriate intervals (15 to 90 minutes) to allow clearance of hepatic activity, which may interfere with the assessment of myocardial tracer activity. Pharmacologic stress images require a longer interval between tracer injection and imaging because of the increase in hepatic blood flow, whereas splanchnic blood flow decreases with high levels of exercise.

Tc-99m-TEBOROXIME. Tc-99m-teboroxime is another myocardial perfusion agent approved for use, although not currently marketed, in the United States. Because it undergoes rapid washout after initial accumulation in the myocardium, imaging with teboroxime is technically more difficult and must be completed within 2 to 8 minutes from the time of injection. This requirement is especially difficult to meet with single-head SPECT systems. Imaging may be optimized by the use of multiheaded detectors. Fast, dynamic acquisition by planar imaging has also been used to minimize the problem of rapid washout, but has not been widely used or validated. Teboroxime undergoes prominent liver uptake, which may render interpretation of the inferior wall of the heart difficult. Imaging with the patient sitting upright has been proposed to overcome the liver activity by displacing it inferiorly.

Tc-99m-NOET. Tc-99m-NOET is currently undergoing multicenter trials. This tracer initially tracks MBF, and is less influenced by myocardial viability, making it a potential agent for detection of successful reperfusion therapy in acute ischemic syndromes (505). In addition, there is significant redistribution (ie, flow-mediated differential washout) of the tracer, giving thallium-like physiologic characteristics in a Tc-99m labeled agent.

d. Dual-Isotope MPI

Dual isotope SPECT imaging takes advantage of the myocardial viability properties of Tl-201 and the higher energy quality imaging characteristics of Tc-99m (84). This is usually performed with sequential imaging of a resting injection Tl-201 followed by a stress injection of Tc-99m-sestamibi or Tc-99m-tetrofosmin. If “fixed” defects are present (ie, an unchanged defect from rest to stress), images can be repeated at 24 hours or later, reflecting the delayed redistribution of Tl-201, for better detection of defect reversibility. Because of the differences between Tl-201 and Tc-99m in terms of tracer energy, scatter, and attenuation, this technique requires somewhat greater experience for recognition of details, such as ischemic dilatation of the LV or the RV perfusion pattern.

e. Gated-Planar MPI

ECG gating has enhanced both planar and tomographic MPI by the addition of complementary information on regional wall motion, regional thickening, myocardial mass, and global ventricular performance. For planar imaging, three or more projections are obtained and used for evaluation of regional wall motion. The best septal planar projection, however, can also be used for determination of LVEF (506). This technique is not commonly performed in the United States.

f. Gated-SPECT MPI

Acquisition of SPECT data synchronized with the electrocardiographic R-wave is generally performed using 8 or 16 gating intervals and allows evaluation of both global (EF) and regional (myocardial wall motion and wall thickening) cardiac function. These 8 sets of projection images are routinely summed to obtain a single planar projection set (“ungated”) for perfusion evaluation and comparison with nongated images.

Gated SPECT has been used extensively for determination of EF and wall motion, adding incremental diagnostic and prognostic information. The addition of wall motion has improved the specificity of myocardial perfusion SPECT by distinguishing myocardial scarring from attenuation artifacts, both of which may result in “fixed” defects.

Estimates indicate that more than 80% of all SPECT studies in the United States are currently performed by using the gated acquisition technique, an increase from only about 3% in 1993 (124), and this technique is now recommended for perfusion acquisitions whenever possible. Although it was initially held that gated-perfusion SPECT acquisitions were only possible in conjunction with Tc-99m-sestamibi or other Tc-99m-based agents, published experience from multiple sites indicates that gated Tl-201 SPECT imaging is eminently feasible, especially if a multidetector camera is used (504).

The exponential increase in the use of gated SPECT has been fueled by the increased availability of automatic and semiautomatic algorithms for the quantification of functional cardiac parameters. Several methods have been developed for quantitative measurements of myocardial function from gated SPECT. DePuey *et al.* (507) and Boonyaprapa *et al.* (508) have described methods based on the detection of endocardial borders. Williams *et al.* (509) developed a method based on inverting the counts and analyzing the change in counts occurring in the ventricular chamber using methods similar to conventional RNA. Germano *et al.* (510) developed a method of fitting geometric shapes to the endocardial borders to obtain systolic and diastolic volumes and EF. This method can function without operator intervention. Smith *et al.* (511) have used the partial volume effect to estimate regional thickening fractions and LVEF. This method requires no edge detection or edge delineation. Each of these techniques has been well correlated with standard methods of performing EF.

See Figures 5 and 6 for examples of gated-SPECT display.

2. Analysis of Ventricular Function

a. Radionuclide Angiography

FPRNA (REST, STRESS). FPRNA uses rapidly acquired image frames to observe a bolus of Tc-99m or another suitable radionuclide as it moves through the venous system into the right atrium, RV, pulmonary artery, lungs, left atrium, LV, and aorta. Because the sampling rate is short relative to the RR interval, it is possible to sample continuously several cardiac cycles as the bolus passes through the RV and then the LV. By determining the change in radioactivity over time (ie, by generating time-activity curves), it is possible to derive EF measurements from both the RV and LV. It is also possible to measure ventricular and pulmonary blood volumes and to assess regional ventricular wall motion. The first-pass approach is uniquely well-suited for shunt detection and quantification and evaluation of RV function because the RV and LV can be temporally isolated. Left-to-right shunts can be quantified by application of a mathematical approach to a ROI placed over the lung. The first-pass approach can be applied to patients both at rest and during exercise stress.

PLANAR AND SPECT-GATED EQUILIBRIUM BLOOD POOL RNA (REST, STRESS). Planar-gated equilibrium blood pool RNA generates reliable LVEF values and a means for assessing regional wall motion. It can be applied both at rest and during exercise stress or pharmacologic stress. In addition, it can be used to measure ventricular volumes, changes in pulmonary blood volumes with stress, and valvular regurgitant fractions. However, assessment of RV function is technically limited by overlap of right atrium and LV chambers. Despite these limitations, multiple studies have documented the diagnostic and prognostic value of LVEF and RVEF values, as well as a fall in LVEF with exercise.

As with MPI, SPECT blood pool images can be displayed for detailed analysis in long- and short-axis slices or projected into volume-rendered 3D images. The resultant images are used for analysis of myocardial topography (eg, after MI), regional wall motion, and EF. The major advantage of SPECT reconstruction is the ability to analyze ventricular function without overlapping of myocardial segments. However, the experience with determination of LVEF and RVEF with this technique is limited.

b. Comparison of Scintigraphic Techniques for Determination of EF and Volumes

Evaluation of ventricular size and systolic function has become one of the most common applications of nuclear imaging, using FPRNA, planar-gated equilibrium blood pool RNA, and, more recently, gated-tomographic perfusion and equilibrium blood pool imaging. Each technique has been compared with contrast ventriculography, and cross-compared with the other scintigraphic methods, showing good correlation, adequate substitutability, and excellent inter- and intraobserver variability. Each technique has its clinical limitations and advantages (141,509,512-515).

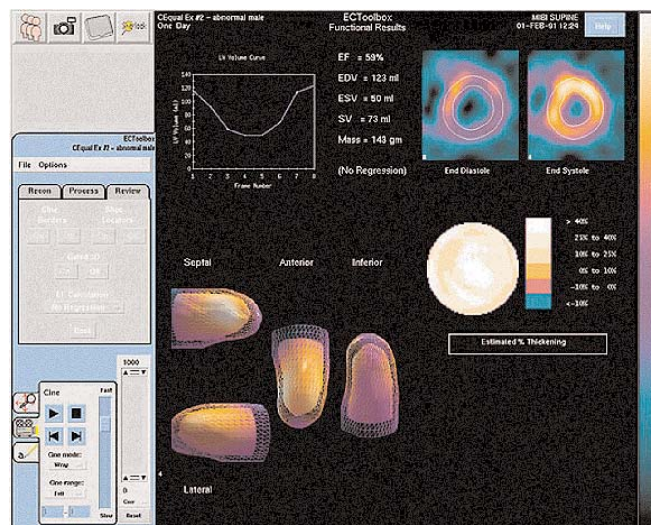


Figure 5. Gated-SPECT myocardial perfusion LVEF determination. An example of gated-SPECT myocardial perfusion LVEF determination, with a ventricular volume curve, thickening fraction, regional wall motion maps, and images at end-diastole and end-systole are shown. Source: Dr. Ernest V. Garcia, Emory University School of Medicine, Atlanta, Georgia.

FIRST-PASS RNA. FPRNA has some distinct advantages, including (1) the most rapid acquisition of data (in less than 30 seconds); (2) assessment of RV function with less overlap of tracer activity in other chambers (as seen on gated-equilibrium blood pool RNA); (3) the use of many radiopharmaceuticals, including bone, renal, and myocardial scintigraphic agents, allowing multipurpose imaging from a single tracer injection; (4) the ability to obtain high quality studies even in morbidly obese individuals; (5) a proven robust measurement of stress ventricular function at true peak exercise; and (6) the presence of a wealth of prognostic information avail-

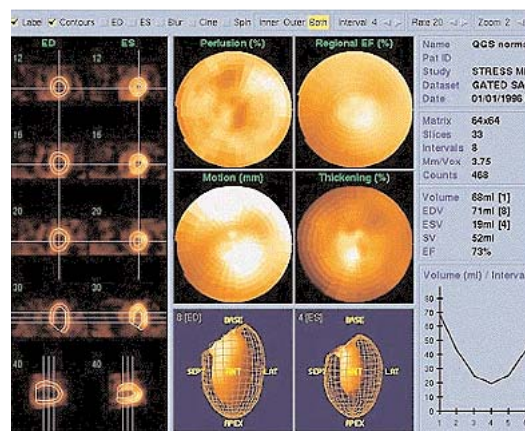


Figure 6. Gated-SPECT myocardial perfusion using gaussian edge detection fit. Another example of gated-SPECT myocardial perfusion is shown, with LVEF determination using a gaussian edge detection fit on horizontal long axis, vertical long axis, and three levels of short axis images, with perfusion, regional EF, thickening and motion polar maps, and a ventricular volume curve. Source: Dr. Guido Germano, Cedars-Sinai Medical Center, Los Angeles, California.

able for the management of patients with ischemic heart disease based on stratification by exercise FPRNA LVEF.

Relative to FPRNA, echocardiography is less easily quantified. The 3D techniques, CT and magnetic resonance, are both more time consuming. No other technique can isolate the actual peak of exercise, as obtained with a 10- to 15-second acquisition by use of first-pass. Because of the demands for meticulous bolus injection technique for tracer administration and an especially high count-rate capable gamma camera, however, first-pass is one of the least commonly performed scintigraphic techniques for ventricular function in the United States.

FPRNA is highly reproducible in terms of repeated measures on the same data set (509). The clinically important issue of how reproducible the technique is when performed serially on the same patient over a period of time has not been studied using modern (ie, dual ROI) approaches to analysis. The reproducibility of the first-pass approach has been shown to depend upon the counting statistics and the resultant EF, with greater degrees of accuracy occurring in poorer ventricular function (ie, large chamber volumes resulting in high count acquisition), in which the EF carries more clinical and prognostic importance. A variability of 10 EF units with an EF of 75% is far less important clinically than with an EF of 25%.

RVEF is normally slightly lower than is the LVEF because of a slightly greater end-diastolic volume but an equivalent stroke volume. It is readily quantified with background subtraction from the right atrium (514). The first-pass technique is also useful for shunt quantification and detection, but has largely been supplanted by echocardiographic techniques in this regard (512).

LV volumes are typically obtained by using geometric (Sandler and Dodge) equations, but ventricular volumes can also be calculated with a count-proportional method requiring measurement of the total counts in the LV, the counts in the hottest pixel in the LV, and the area of a pixel (515).

GATED-EQUILIBRIUM BLOOD POOL RNA. Gated-equilibrium blood pool RNA has been used for three decades to evaluate LVEF and RVEF and volumes. Equilibrium studies can be acquired by either planar or SPECT approaches, as discussed above. Advantages of this noninvasive approach are that the quantitative calculation of EF does not depend on mathematical assumptions of ventricular geometry. Automated computer-based edge detection allows determination of the change in counts in a variable ROI throughout the cardiac cycle, and largely eliminates subjective operator bias in defining the chamber borders. A potential source of error is selection of a proper region for calculation and subtraction of background activity.

It is not yet established whether 3D-gated SPECT blood pool data are more accurate than are planar data for calculation of EF in normal hearts or in hearts with depressed EF and abnormal geometry. In clinical research settings, gated simultaneous measurements of LV volume and pressure can be recorded throughout the cardiac cycle to obtain LV pressure/volume loops applicable to calculation of indices of

myocardial contractility, which are relatively independent of ventricular loading, such as end-systolic pressure/volume relations. Absolute ventricular volumes can be measured by using a count-based technique, which estimates attenuation and calibrates counts per unit of volume using a 5 ml sample of the patient's blood, or from the same count-proportionality method used for first-pass (516).

Gated-equilibrium blood pool RNA has been used in multiple contemporary clinical trials to track serial changes in quantitative measurements of LVEF and LV volumes in patients with chronic heart failure and can accurately discriminate quantitative changes in LV systolic function in individual patients over time. For this reason, quantitative measurements of LVEF measured by RNA are often required for entry into many current randomized clinical trials of heart failure; when visual estimates of EF by using 2D echocardiography are permitted, an additional objective quantitative measurement of LV dimension acquired by M-mode imaging is often required.

GATED-SPECT PERFUSION IMAGING. Gated tomographic perfusion imaging is rapidly evolving as a gold standard for scintigraphic EF, because it is performed more frequently than the other techniques in nuclear cardiology everyday practice. Automated techniques have been developed that can be totally operator independent or can allow operator intervention when deemed necessary (124,141,508-511,513,517-521). Gated-SPECT perfusion imaging has been compared with FPRNA, gated-equilibrium blood pool RNA, contrast ventriculography, and MR for validation of both LVEF and volumes. The limits of agreement with other techniques are typically within 2 to 5%, with correlation coefficients of approximately 0.9 for EF. Ventricular volume measurements have been less widely validated and may vary with the tracer used (Tc-99m vs. Tl-201), and reconstruction methods (eg, the backprojection filter critical frequency) (513,518-521).

The expected sources of error in gated SPECT EF include automated selection of noncardiac structures in juxtaposition to the myocardium, higher EF in small hearts having end-systolic dimensions that challenge the limited reconstructed spatial resolution of the SPECT systems, delineation of myocardial edges when perfusion to a given segment of myocardium is severely diminished or absent, and the lowering of EF by reversible stress induced myocardial perfusion defects (214). This is a common problem, because the majority of the EF calculations are performed poststress in patients undergoing evaluation for known or suspected CAD, and can be eliminated by gating the resting acquisition instead of the stress, if a rest-stress images sequence is performed.

3. Myocardial Infarct-Avid Imaging

Another unique aspect of radionuclide imaging involves the administration of Tc-99m (stannous) pyrophosphate or indium-111-labeled antibody to cardiac myosin for imaging MI. These agents are localized in zones of infarcted myocardium. The most intense visualization of infarcted regions usually occurs 48 to 72 hours after infarction for Tc-99m-pyrophos-

phate. However, with the advent of improved enzymatic methods of detecting myocardial necrosis, the use of these techniques has declined dramatically.

4. Myocardial Ischemia Imaging

Tc-99m-annexin-V and Tc-99m-glucuronic acid have been introduced for imaging apoptotic and acutely ischemic myocardium, respectively, and are being investigated. Neither of these agents has received FDA approval at the time of writing.

5. Positron Emission Tomography

There are two specific clinical applications of cardiac PET that have been proposed for the evaluation of patients with CAD. The first is the noninvasive detection of CAD and estimation of the severity of the disease. This is performed by using a PET perfusion agent at rest and during pharmacologic vasodilation (Figure 7). The short half-lives of these agents permit rapid sequential examinations, such as rest dipyridamole studies, within a short time frame (1 to 2 hours). A unique application of PET is the noninvasive calculation of absolute regional MBF or absolute MBF reserve in humans by using O-15 water or N-13-ammonia. However, most centers rely on the qualitative or semiquantitative interpretation of rubidium-82 or N-13-ammonia images for both the diagnosis of CAD and the estimation of its severity. The second

clinical application of PET is the assessment of myocardial viability in patients with CAD and LV dysfunction. The most common approach is to determine whether metabolic activity is preserved in regions with reduced perfusion, by using F-18 FDG as a marker of glucose utilization and thus tissue viability.

Because of its declining hardware costs, PET is becoming more frequently used and may become cost-competitive with SPECT perfusion imaging in laboratories with high patient volumes.

A number of studies, involving a total of several hundred patients, indicate that perfusion imaging with PET using dipyridamole and either rubidium-82 or N-13-ammonia demonstrates abnormal coronary perfusion patterns in a very high proportion of patients with CAD.

At the present time, rubidium-82 is the only PET perfusion tracer approved by the FDA for clinical use; N-13-ammonia is also used for assessment of myocardial perfusion, yet is still considered investigational by the FDA. The advantage of rubidium-82 is that it is obtained from a generator, obviating the need for a cyclotron; the disadvantage is the high cost of the generator. Overall, because of the higher resolution of PET and the routine application of attenuation correction, it is considered likely that the sensitivity and specificity of PET is slightly higher than SPECT.

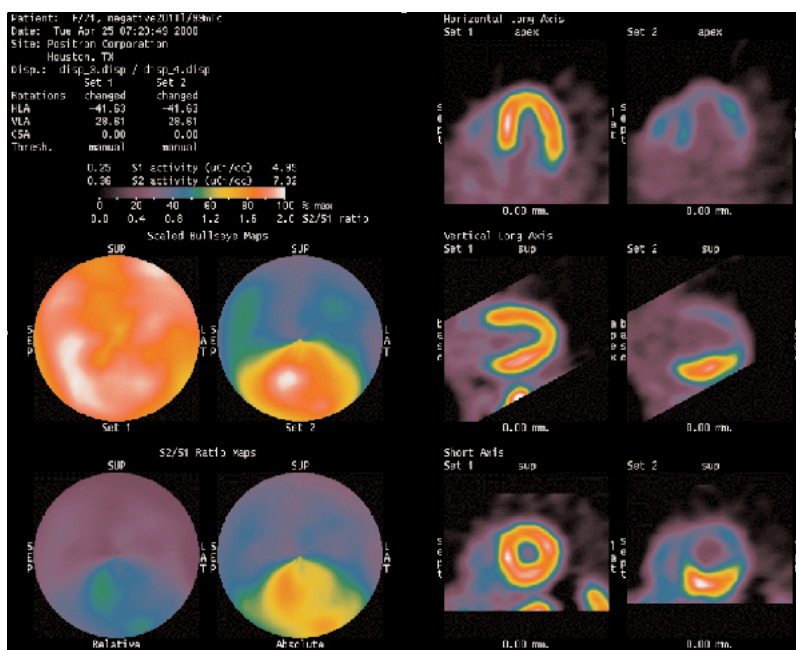


Figure 7. PET perfusion display. An example of a PET perfusion display in a patient with a left main CAD pattern with severe anterior, septal, apical, and lateral reversible ischemia, demonstrated by the comparison of rest (left) and vasodilator stress (right). Polar maps or "bull's-eye" images comprised of short axis tracer activity from apex (center of plot) to base of the heart (outer rim of plot) are shown at rest, stress, and the ratio of the two. Source: Positron Corporation, Houston, Texas.

APPENDIX 2: ABBREVIATIONS

123-MIBG	=	iodine-123-meta-iodobenzylguanidine
ACS	=	acute coronary syndrome
AMI	=	acute myocardial infarction
ARVC	=	complex right ventricular dysplasia
ARVD	=	arrhythmogenic right ventricular dysplasia
C-11	=	carbon 11
CABG	=	coronary artery bypass graft surgery
CAD	=	coronary artery disease
CCS	=	coronary calcium score
CT	=	computed tomography
cTnI	=	cardiac troponin I
EBCT	=	electron-beam computed tomography
ECG	=	electrocardiogram
EF	=	ejection fraction
F-18	=	fluorine 18
FDG	=	flurodeoxyglucose
FPRNA	=	first pass radionuclide angiography
Gated SPECT	=	ECG-gated myocardial perfusion SPECT
LBBB	=	left bundle-branch block
LV	=	left ventricular or left ventricle
LVEF	=	left ventricular ejection fraction
LVH	=	left ventricular hypertrophy
MBF	=	myocardial blood flow
MI	=	myocardial infarction
MPHR	=	maximal-predicted heart rate
MPI	=	myocardial perfusion imaging
MRI	=	magnetic resonance imaging
N-13	=	nitrogen-13
NSTEMI	=	non-ST-segment elevation myocardial infarction
O-15	=	oxygen-15
PCI	=	percutaneous coronary intervention
PET	=	positron emission tomography
PTSM	=	copper-62-pyruvaldehyde bis (N-methyl-hiosemicarbazone)
QA	=	quantitative analysis
RA	=	right atrium
RNA	=	
ROI	=	region of interest
RR	=	relative risk
RV	=	right ventricular or right ventricle
RVEF	=	right ventricular ejection fraction
SDS	=	summed difference score
SPECT	=	single-photon emission computed tomography
SQVA	=	semiquantitative visual analysis
SRS	=	summed rest score
SSS	=	summed stress score
STEMI	=	ST-segment elevation myocardial

		infarction
Tc-99m	=	technetium-99m
Tc-99m-NOET	=	technetium-99m-labeled (bis(N-ethoxy, N-ethyl dithiocarbamato) nitrido technetium[V])
Tl-201	=	thallium-201
UA	=	unstable angina

REFERENCES

- Heller GV, Stowers SA, Hendel RC, et al. Clinical value of acute rest technetium-99m tetrofosmin tomographic myocardial perfusion imaging in patients with acute chest pain and nondiagnostic electrocardiograms. *J Am Coll Cardiol.* 1998;31:1011-7.
- Tatum JL, Jesse RL, Kontos MC, et al. Comprehensive strategy for the evaluation and triage of the chest pain patient. *Ann Emerg Med.* 1997;29:116-25.
- Braunwald E, Antman E, Beasley J, et al. ACC/AHA 2002 guideline update for the management of patients with unstable angina and non-ST-segment elevation myocardial infarction: a report of the American College of Cardiology/American Heart Association Task Force on Practice Guidelines (Committee to Update Guidelines on the Management of Patients with Unstable Angina). 2002; American College of Cardiology Web site. Available at: http://www.acc.org/clinical/guidelines/unstable/incorporated/UA_incorporated.pdf. Accessed June 12, 2002.
- van der Wieken LR, Kan G, Belfer AJ, et al. Thallium-201 scanning to decide CCU admission in patients with non-diagnostic electrocardiograms. *Int J Cardiol.* 1983;4:285-99.
- Wackers FJ, Lie KI, Liem KL, et al. Potential value of thallium-201 scintigraphy as a means of selecting patients for the coronary care unit. *Br Heart J.* 1979;41:111-7.
- Bilodeau L, Theroux P, Gregoire J, et al. Technetium-99m sestamibi tomography in patients with spontaneous chest pain: correlations with clinical, electrocardiographic and angiographic findings. *J Am Coll Cardiol.* 1991;18:1684-91.
- Varetto T, Cantalupi D, Altieri A, et al. Emergency room technetium-99m sestamibi imaging to rule out acute myocardial ischemic events in patients with nondiagnostic electrocardiograms. *J Am Coll Cardiol.* 1993;22:1804-8.
- Duca MD, Giri S, Wu AH, et al. Comparison of acute rest myocardial perfusion imaging and serum markers of myocardial injury in patients with chest pain syndromes. *J Nucl Cardiol.* 1999;6:570-6.
- Kontos MC, Jesse RL, Anderson FP, et al. Comparison of myocardial perfusion imaging and cardiac troponin I in patients admitted to the emergency department with chest pain. *Circulation.* 1999;99:2073-8.
- Hilton TC, Thompson RC, Williams HJ, et al. Technetium-99m sestamibi myocardial perfusion imaging in the emergency room evaluation of chest pain. *J Am Coll Cardiol.* 1994;23:1016-22.
- Hilton TC, Fulmer H, Abuan T, et al. Ninety-day follow-up of patients in the emergency department with chest pain who undergo initial single-photon emission computed tomographic perfusion scintigraphy with technetium 99m-labeled sestamibi. *J Nucl Cardiol.* 1996;3:308-11.
- Stowers SA, Eisenstein EL, Th Wackers FJ, et al. An economic analysis of an aggressive diagnostic strategy with single photon emission computed tomography myocardial perfusion imaging and early exercise stress testing in emergency department patients

- who present with chest pain but nondiagnostic electrocardiograms: results from a randomized trial. *Ann Emerg Med.* 2000;35:17-25.
13. Udelson JE, Beshansky JR, Ballin DS, et al. Myocardial perfusion imaging for evaluation and triage of patients with suspected acute cardiac ischemia: a randomized controlled trial. *JAMA.* 2002;288:2693-2700.
 14. Ryan TJ, Antman EL, Brooks NH, et al. ACC/AHA guidelines for the management of patients with acute myocardial infarction: 1999 update: a report of the American College of Cardiology/American Heart Association Task Force on Practice Guidelines (Committee on Management of Acute Myocardial Infarction). 1999; American College of Cardiology Web site. Available at: <http://www.acc.org/clinical/guidelines/nov96/1999/amipdf99.pdf>. Accessed July 30, 2002.
 15. Verani MS, Jeroudi MO, Mahmarian JJ, et al. Quantification of myocardial infarction during coronary occlusion and myocardial salvage after reperfusion using cardiac imaging with technetium-99m hexakis 2-methoxyisobutyl isonitrile. *J Am Coll Cardiol.* 1988;12:1573-81.
 16. Christian TF, Clements IP, Gibbons RJ. Noninvasive identification of myocardium at risk in patients with acute myocardial infarction and nondiagnostic electrocardiograms with technetium-99m-Sestamibi. *Circulation.* 1991;83:1615-20.
 17. Gibbons RJ, Verani MS, Behrenbeck T, et al. Feasibility of tomographic 99mTc-hexakis-2-methoxy-2-methylpropyl-isonitrile imaging for the assessment of myocardial area at risk and the effect of treatment in acute myocardial infarction. *Circulation.* 1989;80:1277-86.
 18. Miller TD, Christian TF, Hopfenspirger MR, et al. Infarct size after acute myocardial infarction measured by quantitative tomographic 99mTc sestamibi imaging predicts subsequent mortality. *Circulation.* 1995;92:334-41.
 19. Cerqueira MD, Maynard C, Ritchie JL, et al. Long-term survival in 618 patients from the Western Washington Streptokinase in Myocardial Infarction trials. *J Am Coll Cardiol.* 1992;20:1452-9.
 20. Brown KA, O'Meara J, Chambers CE, et al. Ability of dipyridamole-thallium-201 imaging one to four days after acute myocardial infarction to predict in-hospital and late recurrent myocardial ischemic events. *Am J Cardiol.* 1990;65:160-7.
 21. Brown KA. Prognostic value of thallium-201 myocardial perfusion imaging: a diagnostic tool comes of age. *Circulation.* 1991;83:363-81.
 22. Dakik HA, Mahmarian JJ, Kimball KT, et al. Prognostic value of exercise 201Tl tomography in patients treated with thrombolytic therapy during acute myocardial infarction. *Circulation.* 1996;94:2735-42.
 23. Gibson RS, Watson DD, Craddock GB, et al. Prediction of cardiac events after uncomplicated myocardial infarction: a prospective study comparing predischARGE exercise thallium-201 scintigraphy and coronary angiography. *Circulation.* 1983;68:321-36.
 24. Leppo JA, O'Brien J, Rothendler JA, et al. Dipyridamole-thallium-201 scintigraphy in the prediction of future cardiac events after acute myocardial infarction. *N Engl J Med.* 1984;310:1014-18.
 25. Shaw LJ, Eagle KA, Gersh BJ, et al. Meta-analysis of intravenous dipyridamole-thallium-201 imaging (1985 to 1994) and dobutamine echocardiography (1991 to 1994) for risk stratification before vascular surgery. *J Am Coll Cardiol.* 1996;27:787-98.
 26. Verani MS. Risk stratifying patients who survive an acute myocardial infarction. *J Nucl Cardiol.* 1998;5:96-108.
 27. Basu S, Senior R, Dore C, et al. Value of thallium-201 imaging in detecting adverse cardiac events after myocardial infarction and thrombolysis: a follow up of 100 consecutive patients. *BMJ.* 1996;313:844-8.
 28. Mahmarian JJ, Mahmarian AC, Marks GF, et al. Role of adenosine thallium-201 tomography for defining long-term risk in patients after acute myocardial infarction. *J Am Coll Cardiol.* 1995;25:1333-40.
 29. Mahmarian JJ, Pratt CM, Nishimura S, et al. Quantitative adenosine 201Tl single-photon emission computed tomography for the early assessment of patients surviving acute myocardial infarction. *Circulation.* 1993;87:1197-1210.
 30. Brown KA, Heller GV, Landin RS, et al. Early dipyridamole (99m)Tc-sestamibi single photon emission computed tomographic imaging 2 to 4 days after acute myocardial infarction predicts in-hospital and postdischarge cardiac events: comparison with submaximal exercise imaging. *Circulation.* 1999;100:2060-6.
 31. Dakik HA, Kleiman NS, Farmer JA, et al. Intensive medical therapy versus coronary angioplasty for suppression of myocardial ischemia in survivors of acute myocardial infarction: a prospective, randomized pilot study. *Circulation.* 1998;98:2017-23.
 32. Braunwald E. Unstable angina: an etiologic approach to management. *Circulation.* 1998;98:2219-22.
 33. Theroux P, Fuster V. Acute coronary syndromes: unstable angina and non-Q-wave myocardial infarction. *Circulation.* 1998;97:1195-1206.
 34. Pozen MW, D'Agostino RB, Selker HP, et al. A predictive instrument to improve coronary-care-unit admission practices in acute ischemic heart disease: a prospective multicenter clinical trial. *N Engl J Med.* 1984;310:1273-8.
 35. Selker HP, Griffith JL, D'Agostino RB. A tool for judging coronary care unit admission appropriateness, valid for both real-time and retrospective use: a time-insensitive predictive instrument (TIPI) for acute cardiac ischemia: a multicenter study. *Med Care.* 1991;29:610-27.
 36. Brieger DB, Mak KH, White HD, et al. Benefit of early sustained reperfusion in patients with prior myocardial infarction (the GUSTO-I trial): Global Utilization of Streptokinase and TPA for occluded arteries. *Am J Cardiol.* 1998;81:282-7.
 37. Brown KA. Prognostic value of thallium-201 myocardial perfusion imaging in patients with unstable angina who respond to medical treatment. *J Am Coll Cardiol.* 1991;17:1053-7.
 38. Amanullah AM, Lindvall K. Prevalence and significance of transient-predominantly asymptomatic-myocardial ischemia on Holter monitoring in unstable angina pectoris, and correlation with exercise test and thallium-201 myocardial perfusion imaging. *Am J Cardiol.* 1993;72:144-8.
 39. Stratmann HG, Younis LT, Wittry MD, et al. Exercise technetium-99m myocardial tomography for the risk stratification of men with medically treated unstable angina pectoris. *Am J Cardiol.* 1995;76:236-40.
 40. Madsen JK, Stubgaard M, Utne HE, et al. Prognosis and thallium-201 scintigraphy in patients admitted with chest pain without confirmed acute myocardial infarction. *Br Heart J.* 1988;59:184-9.
 41. Kroll D, Farah W, McKendall GR, et al. Prognostic value of stress-gated Tc-99m sestamibi SPECT after acute myocardial infarction. *Am J Cardiol.* 2001;87:381-6.
 42. Bodenheimer MM, Wackers FJ, Schwartz RG, et al. Prognostic significance of a fixed thallium defect one to six months after onset of acute myocardial infarction or unstable angina: Multicenter Myocardial Ischemia Research Group. *Am J Cardiol.* 1994;74:1196-1200.
 43. Miller DD, Stratmann HG, Shaw L, et al. Dipyridamole tech-

- netium 99m sestamibi myocardial tomography as an independent predictor of cardiac event-free survival after acute ischemic events. *J Nucl Cardiol.* 1994;1:72-82.
44. Stratmann HG, Tamesis BR, Younis LT, et al. Prognostic value of predischARGE dipyridamole technetium 99m sestamibi myocardial tomography in medically treated patients with unstable angina. *Am Heart J.* 1995;130:734-40.
 45. Freeman MR, Chisholm RJ, Armstrong PW. Usefulness of exercise electrocardiography and thallium scintigraphy in unstable angina pectoris in predicting the extent and severity of coronary artery disease. *Am J Cardiol.* 1988;62:1164-70.
 46. Berger BC, Watson DD, Burwell LR, et al. Redistribution of thallium at rest in patients with stable and unstable angina and the effect of coronary artery bypass surgery. *Circulation.* 1979;60:1114-25.
 47. Grundy SM, Pasternak R, Greenland P, et al. Assessment of cardiovascular risk by use of multiple-risk-factor assessment equations: a statement for healthcare professionals from the American Heart Association and the American College of Cardiology. *Circulation.* 1999;100:1481-92.
 48. Pryor DB, Harrell FE Jr, Lee KL, et al. Estimating the likelihood of significant coronary artery disease. *Am J Med.* 1983;75:771-80.
 49. Pryor DB, Shaw L, Harrell FE Jr, et al. Estimating the likelihood of severe coronary artery disease. *Am J Med.* 1991;90:553-62.
 50. Pryor DB, Shaw L, McCants CB, et al. Value of the history and physical in identifying patients at increased risk for coronary artery disease. *Ann Intern Med.* 1993;118:81-90.
 51. Diamond GA, Staniloff HM, Forrester JS, et al. Computer-assisted diagnosis in the noninvasive evaluation of patients with suspected coronary artery disease. *J Am Coll Cardiol.* 1983;1:444-55.
 52. Gibbons RJ, Chatterjee K, Daley J, et al. ACC/AHA 2002 guideline update for the management of patients with chronic stable angina: a report of the American College of Cardiology/American Heart Association Task Force on Practice Guidelines (Committee to Update the 1999 Chronic Stable Angina Guidelines). 2002; American College of Cardiology Web site. Available at: http://www.acc.org/clinical/guidelines/stable/stable_clean.pdf. Accessed August 20, 2002.
 53. Kiat H, Berman DS, Maddahi J. Comparison of planar and tomographic exercise thallium-201 imaging methods for the evaluation of coronary artery disease. *J Am Coll Cardiol.* 1989;13:613-6.
 54. Iskandrian AS, Heo J, Kong B, et al. Use of technetium-99m isonitrile (RP-30A) in assessing left ventricular perfusion and function at rest and during exercise in coronary artery disease, and comparison with coronary arteriography and exercise thallium-201 SPECT imaging. *Am J Cardiol.* 1989;64:270-5.
 55. Taillefer R, Laflamme L, Dupras G, et al. Myocardial perfusion imaging with 99mTc-methoxy-isobutyl-isonitrile (MIBI): comparison of short and long time intervals between rest and stress injections: preliminary results. *Eur J Nucl Med.* 1988;13:515-22.
 56. Maddahi J, Kiat H, Van Train KF, et al. Myocardial perfusion imaging with technetium-99m sestamibi SPECT in the evaluation of coronary artery disease. *Am J Cardiol.* 1990;66:55E-62E.
 57. Kahn JK, McGhie I, Akers MS, et al. Quantitative rotational tomography with 201Tl and 99mTc 2-methoxy-isobutyl-isonitrile: a direct comparison in normal individuals and patients with coronary artery disease. *Circulation.* 1989;79:1282-93.
 58. Wackers FJ, Berman DS, Maddahi J, et al. Technetium-99m hexakis 2-methoxyisobutyl isonitrile: human biodistribution, dosimetry, safety, and preliminary comparison to thallium-201 for myocardial perfusion imaging. *J Nucl Med.* 1989;30:301-11.
 59. Maisey MN, Mistry R, Sowton E. Planar imaging techniques used with technetium-99m sestamibi to evaluate chronic myocardial ischemia. *Am J Cardiol.* 1990;66:47E-54E.
 60. Maddahi J, Kiat H, Friedman JD, et al. Technetium-99m-sestamibi myocardial perfusion imaging for evaluation of coronary artery disease. In: Zaret BL, Beller GA, eds. *Nuclear Cardiology: State of the Art and Future Directions.* St Louis, Mo: Mosby; 1993:191-200.
 61. Verani MS. Thallium-201 and technetium-99m perfusion agents: where we are in 1992. In: Zaret BL, Beller GA, eds. *Nuclear Cardiology: State of the Art and Future Directions.* St Louis, Mo: Mosby; 1993: 216-24.
 62. Sridhara BS, Braat S, Rigo P, et al. Comparison of myocardial perfusion imaging with technetium-99m tetrofosmin versus thallium-201 in coronary artery disease. *Am J Cardiol.* 1993;72:1015-9.
 63. Zaret BL, Rigo P, Wackers FJ, et al. Myocardial perfusion imaging with 99mTc tetrofosmin: comparison to 201Tl imaging and coronary angiography in a phase III multicenter trial. Tetrofosmin International Trial Study Group. *Circulation.* 1995;91:313-9.
 64. Fleischmann KE, Hunink MG, Kuntz KM, et al. Exercise echocardiography or exercise SPECT imaging? A meta-analysis of diagnostic test performance. *JAMA.* 1998;280:913-20.
 65. Elhendy A, van Domburg RT, Sozzi FB, et al. Impact of hypertension on the accuracy of exercise stress myocardial perfusion imaging for the diagnosis of coronary artery disease. *Heart.* 2001;85:655-61.
 66. Azzarelli S, Galassi AR, Foti R, et al. Accuracy of 99mTc-tetrofosmin myocardial tomography in the evaluation of coronary artery disease. *J Nucl Cardiol.* 1999;6:183-9.
 67. San Roman JA, Vilacosta I, Castillo JA, et al. Selection of the optimal stress test for the diagnosis of coronary artery disease. *Heart.* 1998;80:370-6.
 68. Budoff MJ, Gillespie R, Georgiou D, et al. Comparison of exercise electron beam computed tomography and sestamibi in the evaluation of coronary artery disease. *Am J Cardiol.* 1998;81:682-7.
 69. Santana-Boado C, Candell-Riera J, Castell-Conesa J, et al. Diagnostic accuracy of technetium-99m-MIBI myocardial SPECT in women and men. *J Nucl Med.* 1998;39:751-5.
 70. Acampa W, Cuocolo A, Sullo P, et al. Direct comparison of technetium 99m-sestamibi and technetium 99m-tetrofosmin cardiac single photon emission computed tomography in patients with coronary artery disease. *J Nucl Cardiol.* 1998;5:265-74.
 71. Ho Y, Wu C, Huang P, et al. Assessment of coronary artery disease in women by dobutamine stress echocardiography: comparison with stress thallium-201 single-photon emission computed tomography and exercise electrocardiography. *Am Heart J.* 1998;135:655-62.
 72. Iskandrian AE, Heo J, Nallamotheu N. Detection of coronary artery disease in women with use of stress single-photon emission computed tomography myocardial perfusion imaging. *J Nucl Cardiol.* 1997;4:329-35.
 73. Candell-Riera J, Santana-Boado C, Castell-Conesa J, et al. Simultaneous dipyridamole/maximal subjective exercise with 99mTc-MIBI SPECT: improved diagnostic yield in coronary artery disease. *J Am Coll Cardiol.* 1997;29:531-6.
 74. Yao Z, Liu XJ, Shi R, et al. A comparison of 99m Tc-MIBI myocardial SPECT with electron beam computed tomography in the assessment of coronary artery disease. *Eur J Nucl Med.* 1997;24:1115-20.

75. Heiba SI, Hayat NJ, Salman HS, et al. Technetium-99m-MIBI myocardial SPECT: supine versus right lateral imaging and comparison with coronary arteriography. *J Nucl Med.* 1997;38:1510-4.
76. Ho YL, Wu CC, Huang PJ, et al. Dobutamine stress echocardiography compared with exercise thallium-201 single-photon emission computed tomography in detecting coronary artery disease—effect of exercise level on accuracy. *Cardiology.* 1997;88:379-85.
77. Taillefer R, DePuey EG, Udelson JE, et al. Comparative diagnostic accuracy of Tl-201 and Tc-99m sestamibi SPECT imaging (perfusion and ECG-gated SPECT) in detecting coronary artery disease in women. *J Am Coll Cardiol.* 1997;29:69-77.
78. Van Eck-Smit BLF, Poots S, Zwinderman AH, et al. Myocardial SPECT imaging with 99Tc m-tetrofosmin in clinical practice: comparison of a 1 day and a 2 day imaging protocol. *Nucl Med Commun.* 1997;18:24-30.
79. Hambye AS, Vervaeke A, Lieber S, et al. Diagnostic value and incremental contribution of bicycle exercise, first-pass radionuclide angiography, and 99mTc-labeled sestamibi single-photon emission computed tomography in the identification of coronary artery disease in patients without infarction. *J Nucl Cardiol.* 1996;3:464-74.
80. Palmas W, Friedman JD, Diamond GA, et al. Incremental value of simultaneous assessment of myocardial function and perfusion with technetium-99m sestamibi for prediction of extent of coronary artery disease. *J Am Coll Cardiol.* 1995;25:1024-31.
81. Rubello D, Zanco P, Candelpergher G, et al. Usefulness of 99mTc-MIBI stress myocardial SPECT bull's-eye quantification in coronary artery disease. *Q J Nucl Med.* 1995;39:111-5.
82. Sylven C, Hagerman I, Ylen M, et al. Variance ECG detection of coronary artery disease: a comparison with exercise stress test and myocardial scintigraphy. *Clin Cardiol.* 1994;17:132-40.
83. Van Train KF, Garcia EV, Maddahi J, et al. Multicenter trial validation for quantitative analysis of same-day rest-stress technetium-99m-sestamibi myocardial tomograms. *J Nucl Med.* 1994;35:609-18.
84. Berman DS, Kiat H, Friedman JD, et al. Separate acquisition rest thallium-201/stress technetium-99m sestamibi dual-isotope myocardial perfusion single-photon emission computed tomography: a clinical validation study. *J Am Coll Cardiol.* 1993;22:1455-64.
85. Forster T, McNeill AJ, Salustri A, et al. Simultaneous dobutamine stress echocardiography and technetium-99m isonitrile single-photon emission computed tomography in patients with suspected coronary artery disease. *J Am Coll Cardiol.* 1993;21:1591-6.
86. Chae SC, Heo J, Iskandrian AS, et al. Identification of extensive coronary artery disease in women by exercise single-photon emission computed tomographic (SPECT) thallium imaging. *J Am Coll Cardiol.* 1993;21:1305-11.
87. Minoves M, Garcia A, Magrina J, et al. Evaluation of myocardial perfusion defects by means of "bull's eye" images. *Clin Cardiol.* 1993;16:16-22.
88. Van Train KF, Areeada J, Garcia EV, et al. Quantitative same-day rest-stress technetium-99m-sestamibi SPECT: definition and validation of stress normal limits and criteria for abnormality. *J Nucl Med.* 1993;34:1494-502.
89. Quinones MA, Verani MS, Haichin RM, et al. Exercise echocardiography versus 201Tl single-photon emission computed tomography in evaluation of coronary artery disease: analysis of 292 patients. *Circulation.* 1992;85:1026-31.
90. Coyne E, Belvedere D, Vande Streek PR, et al. Thallium-201 scintigraphy after intravenous infusion of adenosine compared with exercise thallium testing in the diagnosis of coronary artery disease. *J Am Coll Cardiol.* 1991;17:1289-94.
91. Pozzoli MM, Fioretti PM, Salustri A, et al. Exercise echocardiography and technetium-99m MIBI single-photon emission computed tomography in the detection of coronary artery disease. *Am J Cardiol.* 1991;67:350-5.
92. Kiat H, Van Train KF, Maddahi J, et al. Development and prospective application of quantitative 2-day stress-rest Tc-99m methoxy isobutyl isonitrile SPECT for the diagnosis of coronary artery disease. *Am Heart J.* 1990;120:1255-66.
93. Mahmarian JJ, Boyce TM, Goldberg RK, et al. Quantitative exercise thallium-201 single photon emission computed tomography for the enhanced diagnosis of ischemic heart disease. *J Am Coll Cardiol.* 1990;15:318-29.
94. Nguyen T, Heo J, Ogilby JD, et al. Single photon emission computed tomography with thallium-201 during adenosine-induced coronary hyperemia: correlation with coronary arteriography, exercise thallium imaging and two-dimensional echocardiography. *J Am Coll Cardiol.* 1990;16:1375-83.
95. Van Train KF, Maddahi J, Berman DS, et al. Quantitative analysis of tomographic stress thallium-201 myocardial scintigrams: a multicenter trial. *J Nucl Med.* 1990;31:1168-79.
96. Iskandrian AS, Heo J, Kong B, et al. Effect of exercise level on the ability of thallium-201 tomographic imaging in detecting coronary artery disease: analysis of 461 patients. *J Am Coll Cardiol.* 1989;14:1477-86.
97. Smart SC, Bhatia A, Hellman R, et al. Dobutamine-atropine stress echocardiography and dipyridamole sestamibi scintigraphy for the detection of coronary artery disease: limitations and concordance. *J Am Coll Cardiol.* 2000;36:1265-73.
98. Takeishi Y, Takahashi N, Fujiwara S, et al. Myocardial tomography with technetium-99m-tetrofosmin during intravenous infusion of adenosine triphosphate. *J Nucl Med.* 1998;39:582-6.
99. Watanabe K, Sekiya M, Ikeda S, et al. Comparison of adenosine triphosphate and dipyridamole in diagnosis by thallium-201 myocardial scintigraphy. *J Nucl Med.* 1997;38:577-81.
100. He ZX, Iskandrian AS, Gupta NC, et al. Assessing coronary artery disease with dipyridamole technetium-99m-tetrofosmin SPECT: a multicenter trial. *J Nucl Med.* 1997;38:44-8.
101. Cuocolo A, Sullo P, Pace L, et al. Adenosine coronary vasodilation in coronary artery disease: technetium-99m tetrofosmin myocardial tomography versus echocardiography. *J Nucl Med.* 1997;38:1089-94.
102. Amanullah AM, Berman DS, Kiat H, et al. Usefulness of hemodynamic changes during adenosine infusion in predicting the diagnostic accuracy of adenosine technetium-99m sestamibi single-photon emission computed tomography (SPECT). *Am J Cardiol.* 1997;79:1319-22.
103. Miller DD, Younis LT, Chaitman BR, et al. Diagnostic accuracy of dipyridamole technetium 99m-labeled sestamibi myocardial tomography for detection of coronary artery disease. *J Nucl Cardiol.* 1997;4:18-24.
104. Aksut SV, Pancholy S, Cassel D, et al. Results of adenosine single photon emission computed tomography thallium-201 imaging in hemodynamic nonresponders. *Am Heart J.* 1995;130:67-70.
105. Miyagawa M, Kumano S, Sekiya M, et al. Thallium-201 myocardial tomography with intravenous infusion of adenosine triphosphate in diagnosis of coronary artery disease. *J Am Coll Cardiol.* 1995;26:1196-1201.
106. Marwick T, Willemart B, D'Hondt AM, et al. Selection of the optimal nonexercise stress for the evaluation of ischemic regional myocardial dysfunction and malperfusion: comparison of dobuta-

- mine and adenosine using echocardiography and 99mTc-MIBI single photon emission computed tomography. *Circulation*. 1993;87:345-54.
107. Nishimura S, Mahmarian JJ, Boyce TM, et al. Quantitative thallium-201 single-photon emission computed tomography during maximal pharmacologic coronary vasodilation with adenosine for assessing coronary artery disease. *J Am Coll Cardiol*. 1991;18:736-45.
108. Verani MS, Mahmarian JJ, Hixson JB, et al. Diagnosis of coronary artery disease by controlled coronary vasodilation with adenosine and thallium-201 scintigraphy in patients unable to exercise. *Circulation*. 1990;82:80-7.
- 108a. Miller TD, Hodge DO, Christian TF, et al. Effects of adjustment for referral bias on the sensitivity and specificity of single photon emission computed tomography for the diagnosis of coronary artery disease. *Am J Med*. 2002;112:322-4.
- 108b. Cecil MP, Kosinski AS, Jones MT, et al. The importance of workup (verification) bias correction in assessing the accuracy of SPECT thallium-201 testing for the diagnosis of coronary artery disease. *J Clin Epidemiol*. 1996;49:735-42.
- 108c. Diamond GA. Reverend Bayes' silent majority: an alternative factor affecting sensitivity and specificity of exercise electrocardiography. *Am J Cardiol*. 1986;57:1175-80.
109. White CW, Wright CB, Doty DB, et al. Does visual interpretation of the coronary arteriogram predict the physiologic importance of a coronary stenosis? *N Engl J Med*. 1984;310:819-24.
110. Rozanski A, Diamond GA, Berman D, et al. The declining specificity of exercise radionuclide ventriculography. *N Engl J Med*. 1983;309:518-22.
111. Berman D, Kiat H, Germano G, et al. Tc-sestamibi SPECT. In: DePuey EG, Berman DS, Garcia EV, eds. *Cardiac SPECT Imaging*. New York, NY: Raven Press; 1995:121-46.
112. Zeiher AM, Krause T, Schachinger V, et al. Impaired endothelium-dependent vasodilation of coronary resistance vessels is associated with exercise-induced myocardial ischemia. *Circulation*. 1995;91:2345-52.
113. Gould KL. Noninvasive assessment of coronary stenoses by myocardial perfusion imaging during pharmacologic coronary vasodilatation, I: physiologic basis and experimental validation. *Am J Cardiol*. 1978;41:267-78.
114. Gould KL, Westcott RJ, Albro PC, et al. Noninvasive assessment of coronary stenoses by myocardial imaging during pharmacologic coronary vasodilatation, II: clinical methodology and feasibility. *Am J Cardiol*. 1978;41:279-87.
115. Albro PC, Gould KL, Westcott RJ, et al. Noninvasive assessment of coronary stenoses by myocardial imaging during pharmacologic coronary vasodilatation, III: clinical trial. *Am J Cardiol*. 1978;42:751-60.
116. Leppo JA. Dipyridamole-thallium imaging: the lazy man's stress test. *J Nucl Med*. 1989;30:281-7.
117. Abreu A, Mahmarian JJ, Nishimura S, et al. Tolerance and safety of pharmacologic coronary vasodilation with adenosine in association with thallium-201 scintigraphy in patients with suspected coronary artery disease. *J Am Coll Cardiol*. 1991;18:730-5.
118. Mason JR, Palac RT, Freeman ML, et al. Thallium scintigraphy during dobutamine infusion: nonexercise-dependent screening test for coronary disease. *Am Heart J*. 1984;107:481-5.
119. Hays JT, Mahmarian JJ, Cochran AJ, et al. Dobutamine thallium-201 tomography for evaluating patients with suspected coronary artery disease unable to undergo exercise or vasodilator pharmacologic stress testing. *J Am Coll Cardiol*. 1993;21:1583-90.
120. Gupta NC, Esterbrooks DJ, Hilleman DE, et al. Comparison of adenosine and exercise thallium-201 single-photon emission computed tomography (SPECT) myocardial perfusion imaging. The GE SPECT Multicenter Adenosine Study Group. *J Am Coll Cardiol*. 1992;19:248-57.
121. Ogilby JD, Iskandrian AS, Untereker WJ, et al. Effect of intravenous adenosine infusion on myocardial perfusion and function: hemodynamic/angiographic and scintigraphic study. *Circulation*. 1992;86:887-95.
122. Nishimura S, Mahmarian JJ, Boyce TM, et al. Equivalence between adenosine and exercise thallium-201 myocardial tomography: a multicenter, prospective, crossover trial. *J Am Coll Cardiol*. 1992;20:265-75.
123. Verani MS. Pharmacologic stress myocardial perfusion imaging. *Curr Probl Cardiol*. 1993;18:481-525.
124. Wintergreen summary: panel on instrumentation and quantification. *J Nucl Cardiol*. 1999;6:94-103.
125. Borges-Neto S, Mahmarian JJ, Jain A, et al. Quantitative thallium-201 single photon emission computed tomography after oral dipyridamole for assessing the presence, anatomic location and severity of coronary artery disease. *J Am Coll Cardiol*. 1988;11:962-9.
126. Parodi O, Marcassa C, Casucci R, et al. Accuracy and safety of technetium-99m hexakis 2-methoxy-2-isobutyl isonitrile (Sestamibi) myocardial scintigraphy with high dose dipyridamole test in patients with effort angina pectoris: a multicenter study. Italian Group of Nuclear Cardiology. *J Am Coll Cardiol*. 1991;18:1439-44.
127. Soman P, Taillefer R, DePuey EG, et al. Enhanced detection of reversible perfusion defects by Tc-99m sestamibi compared to Tc-99m tetrofosmin during vasodilator stress SPECT imaging in mild-to-moderate coronary artery disease. *J Am Coll Cardiol*. 2001;37:458-62.
128. Iftikhar I, Koutelou M, Mahmarian JJ, et al. Simultaneous perfusion tomography and radionuclide angiography during dobutamine stress. *J Nucl Med*. 1996;37:1306-10.
129. Wu JC, Yun JJ, Heller EN, et al. Limitations of dobutamine for enhancing flow heterogeneity in the presence of single coronary stenosis: implications for technetium-99m-sestamibi imaging. *J Nucl Med*. 1998;39:417-25.
130. Calnon DA, Glover DK, Beller GA, et al. Effects of dobutamine stress on myocardial blood flow, 99mTc sestamibi uptake, and systolic wall thickening in the presence of coronary artery stenoses: implications for dobutamine stress testing. *Circulation*. 1997;96:2353-60.
131. Maddahi J, Garcia EV, Berman DS, et al. Improved noninvasive assessment of coronary artery disease by quantitative analysis of regional stress myocardial distribution and washout of thallium-201. *Circulation*. 1981;64:924-35.
132. Van Train KF, Berman DS, Garcia EV, et al. Quantitative analysis of stress thallium-201 myocardial scintigrams: a multicenter trial. *J Nucl Med*. 1986;27:17-25.
133. Heo J, Powers J, Iskandrian AE. Exercise-rest same-day SPECT sestamibi imaging to detect coronary artery disease. *J Nucl Med*. 1997;38:200-3.
134. Nicolai E, Cuocolo A, Pace L, et al. Adenosine coronary vasodilation quantitative technetium 99m methoxy isobutyl isonitrile myocardial tomography in the identification and localization of coronary artery disease. *J Nucl Cardiol*. 1996;3:9-17.
135. Heo J, Wolmer I, Kegel J, et al. Sequential dual-isotope SPECT imaging with thallium-201 and technetium-99m-sestamibi. *J Nucl Med*. 1994;35:549-53.
136. Kiat H, Van Train KF, Friedman JD, et al. Quantitative stress-

- redistribution thallium-201 SPECT using prone imaging: methodologic development and validation. *J Nucl Med.* 1992;33:1509-15.
137. Fintel DJ, Links JM, Brinker JA, et al. Improved diagnostic performance of exercise thallium-201 single photon emission computed tomography over planar imaging in the diagnosis of coronary artery disease: a receiver operating characteristic analysis. *J Am Coll Cardiol.* 1989;13:600-12.
 138. Kirac S, Wackers FJ, Liu YH. Validation of the Yale circumferential quantification method using ²⁰¹Tl and ^{99m}Tc: a phantom study. *J Nucl Med.* 2000;41:1436-41.
 139. Faber TL, Cooke CD, Folks RD, et al. Left ventricular function and perfusion from gated SPECT perfusion images: an integrated method. *J Nucl Med.* 1999;40:650-9.
 140. Liu YH, Sinusas AJ, Deman P, et al. Quantification of SPECT myocardial perfusion images: methodology and validation of the Yale-CQ method. *J Nucl Cardiol.* 1999;6:190-204.
 141. Germano G, Kiat H, Kavanagh PB, et al. Automatic quantification of ejection fraction from gated myocardial perfusion SPECT. *J Nucl Med.* 1995;36:2138-47.
 142. DePasquale EE, Nody AC, DePuey EG, et al. Quantitative rotational thallium-201 tomography for identifying and localizing coronary artery disease. *Circulation.* 1988;77:316-27.
 143. Maddahi J, Van Train K, Prigent F, et al. Quantitative single photon emission computed thallium-201 tomography for detection and localization of coronary artery disease: optimization and prospective validation of a new technique. *J Am Coll Cardiol.* 1989;14:1689-99.
 144. Caldwell JH, Williams DL, Harp GD, et al. Quantitation of size of relative myocardial perfusion defect by single-photon emission computed tomography. *Circulation.* 1984;70:1048-56.
 145. Garcia EV, Van Train K, Maddahi J, et al. Quantification of rotational thallium-201 myocardial tomography. *J Nucl Med.* 1985;26:17-26.
 146. Germano G, Kavanagh PB, Waechter P, et al. A new algorithm for the quantitation of myocardial perfusion SPECT. I: technical principles and reproducibility. *J Nucl Med.* 2000;41:712-9.
 147. Sharir T, Germano G, Waechter PB, et al. A new algorithm for the quantitation of myocardial perfusion SPECT. II: validation and diagnostic yield. *J Nucl Med.* 2000;41:720-7.
 148. Berman DS, Kang X, Van Train KF, et al. Comparative prognostic value of automatic quantitative analysis versus semiquantitative visual analysis of exercise myocardial perfusion single-photon emission computed tomography. *J Am Coll Cardiol.* 1998;32:1987-95.
 149. DePuey EG, Rozanski A. Using gated technetium-99m-sestamibi SPECT to characterize fixed myocardial defects as infarct or artifact. *J Nucl Med.* 1995;36:952-5.
 150. Choi JY, Lee KH, Kim SJ, et al. Gating provides improved accuracy for differentiating artifacts from true lesions in equivocal fixed defects on technetium 99m tetrofosmin perfusion SPECT. *J Nucl Cardiol.* 1998;5:395-401.
 151. Smanio PE, Watson DD, Segalla DL, et al. Value of gating of technetium-99m sestamibi single-photon emission computed tomographic imaging. *J Am Coll Cardiol.* 1997;30:1687-92.
 152. Ficaro EP, Fessler JA, Shreve PD, et al. Simultaneous transmission/emission myocardial perfusion tomography: diagnostic accuracy of attenuation-corrected ^{99m}Tc-sestamibi single-photon emission computed tomography. *Circulation.* 1996;93:463-73.
 153. Ficaro EP, Fessler JA, Ackermann RJ, et al. Simultaneous transmission-emission thallium-201 cardiac SPECT: effect of attenuation correction on myocardial tracer distribution. *J Nucl Med.* 1995;36:921-31.
 154. Kluge R, Sattler B, Seese A, et al. Attenuation correction by simultaneous emission-transmission myocardial single-photon emission tomography using a technetium-99m-labelled radiotracer: impact on diagnostic accuracy. *Eur J Nucl Med.* 1997;24:1107-14.
 155. Gallowitsch HJ, Sykora J, Mikosch P, et al. Attenuation-corrected thallium-201 single-photon emission tomography using a gadolinium-153 moving line source: clinical value and the impact of attenuation correction on the extent and severity of perfusion abnormalities. *Eur J Nucl Med.* 1998;25:220-8.
 156. Hendel RC, Berman DS, Cullom SJ, et al. Multicenter clinical trial to evaluate the efficacy of correction for photon attenuation and scatter in SPECT myocardial perfusion imaging. *Circulation.* 1999;99:2742-9.
 157. Links JM, Becker LC, Rigo P, et al. Combined corrections for attenuation, depth-dependent blur, and motion in cardiac SPECT: a multicenter trial. *J Nucl Cardiol.* 2000;7:414-25.
 158. Duvernoy CS, Ficaro EP, Karabajakian MZ, et al. Improved detection of left main coronary artery disease with attenuation-corrected SPECT. *J Nucl Cardiol.* 2000;7:639-48.
 159. Bateman TM, et al. Diagnostic accuracy of stress-only attenuation corrected SPECT myocardial perfusion scintigraphy: results of a multicenter interpretation. *Circulation.* 2001;104:II-611. Abstract.
 160. Heller GV, et al. Value of attenuation correction in interpretation of stress-only exercise Tc-99m sestamibi SPECT imaging: results of a multicenter trial. *J Am Coll Cardiol.* 2002;39:343A. Abstract.
 161. Gibson PB, Demus D, Noto R, et al. Low event rate for stress-only perfusion imaging in patients evaluated for chest pain. *J Am Coll Cardiol.* 2002;39:999-1004.
 162. Lee DS, So Y, Cheon GJ, et al. Limited incremental diagnostic values of attenuation-noncorrected gating and ungated attenuation correction to rest/stress myocardial perfusion SPECT in patients with an intermediate likelihood of coronary artery disease. *J Nucl Med.* 2000;41:852-9.
 163. Links JM, DePuey EG, Taillefer R, et al. Attenuation correction and gating synergistically improve the diagnostic accuracy of myocardial perfusion SPECT. *J Nucl Cardiol.* 2002;9:183-7.
 164. Hendel RC, Corbett JR, Cullom SJ, et al. The value and practice of attenuation correction for myocardial perfusion SPECT imaging: a joint position statement from the American Society of Nuclear Cardiology and the Society of Nuclear Medicine. *J Nucl Cardiol.* 2002;9:135-43.
 165. Stewart RE, Schwaiger M, Molina E, et al. Comparison of rubidium-82 positron emission tomography and thallium-201 SPECT imaging for detection of coronary artery disease. *Am J Cardiol.* 1991;67:1303-10.
 166. Schelbert HR, Wisenberg G, Phelps ME, et al. Noninvasive assessment of coronary stenoses by myocardial imaging during pharmacologic coronary vasodilation, VI: detection of coronary artery disease in human beings with intravenous N-13 ammonia and positron computed tomography. *Am J Cardiol.* 1982;49:1197-207.
 167. Gould KL, Goldstein RA, Mullani NA, et al. Noninvasive assessment of coronary stenoses by myocardial perfusion imaging during pharmacologic coronary vasodilation, VIII: clinical feasibility of positron cardiac imaging without a cyclotron using generator-produced rubidium-82. *J Am Coll Cardiol.* 1986;7:775-89.
 168. Goldstein RA, Kirkeeide RL, Smalling RW, et al. Changes in myocardial perfusion reserve after PTCA: noninvasive assessment with positron tomography. *J Nucl Med.* 1987;28:1262-7.
 169. Tamaki N, Yonekura Y, Senda M, et al. Value and limitation of

- stress thallium-201 single photon emission computed tomography: comparison with nitrogen-13 ammonia positron tomography. *J Nucl Med.* 1988;29:1181-8.
170. Demer LL, Gould KL, Goldstein RA, et al. Noninvasive assessment of coronary collaterals in man by PET perfusion imaging. *J Nucl Med.* 1990;31:259-70.
171. Demer LL, Gould KL, Goldstein RA, et al. Assessment of coronary artery disease severity by positron emission tomography: comparison with quantitative arteriography in 193 patients. *Circulation.* 1989;79:825-35.
172. Go RT, Marwick TH, MacIntyre WJ, et al. A prospective comparison of rubidium-82 PET and thallium-201 SPECT myocardial perfusion imaging utilizing a single dipyridamole stress in the diagnosis of coronary artery disease. *J Nucl Med.* 1990;31:1899-905.
173. Grover-McKay M, Ratib O, Schwaiger M, et al. Detection of coronary artery disease with positron emission tomography and rubidium 82. *Am Heart J.* 1992;123:646-52.
174. Marwick TH, Nemecek JJ, Stewart WJ, et al. Diagnosis of coronary artery disease using exercise echocardiography and positron emission tomography: comparison and analysis of discrepant results. *J Am Soc Echocardiogr.* 1992;5:231-8.
175. Yusuf S, Zucker D, Peduzzi P, et al. Effect of coronary artery bypass graft surgery on survival: overview of 10-year results from randomised trials by the Coronary Artery Bypass Graft Surgery Trialists Collaboration. *Lancet.* 1994;344:563-70.
176. Comparison of coronary bypass surgery with angioplasty in patients with multivessel disease. The Bypass Angioplasty Revascularization Investigation (BARI) Investigators. *N Engl J Med.* 1996;335:217-25.
177. Little WC, Constantinescu M, Applegate RJ, et al. Can coronary angiography predict the site of a subsequent myocardial infarction in patients with mild-to-moderate coronary artery disease? *Circulation.* 1988;78:1157-66.
178. Ambrose JA, Tannenbaum MA, Alexopoulos D, et al. Angiographic progression of coronary artery disease and the development of myocardial infarction. *J Am Coll Cardiol.* 1988; 12:56-62.
179. Hasdai D, Gibbons RJ, Holmes DR Jr, et al. Coronary endothelial dysfunction in humans is associated with myocardial perfusion defects. *Circulation.* 1997;96:3390-5.
180. Kinsella JP, Torielli F, Ziegler JW, et al. Dipyridamole augmentation of response to nitric oxide. *Lancet.* 1995;346:647-8.
181. Sharir T, Germano G, Kang X, et al. Prediction of myocardial infarction versus cardiac death by gated myocardial perfusion SPECT: risk stratification by the amount of stress-induced ischemia and the poststress ejection fraction. *J Nucl Med.* 2001;42:831-7.
182. Gibbons RJ, Hodge DO, Berman DS, et al. Long-term outcome of patients with intermediate-risk exercise electrocardiograms who do not have myocardial perfusion defects on radionuclide imaging. *Circulation.* 1999;100:2140-5.
183. Hachamovitch R, Berman DS, Shaw LJ, et al. Incremental prognostic value of myocardial perfusion single photon emission computed tomography for the prediction of cardiac death: differential stratification for risk of cardiac death and myocardial infarction [published erratum appears in *Circulation* 1998;98:190]. *Circulation.* 1998;97:535-43.
184. Berman DS, Hachamovitch R, Kiat H, et al. Incremental value of prognostic testing in patients with known or suspected ischemic heart disease: a basis for optimal utilization of exercise technetium-99m sestamibi myocardial perfusion single-photon emission computed tomography. *J Am Coll Cardiol.* 1995;26:639-47.
185. Berman DS, Kang X, Hayes SW, et al. Adenosine myocardial perfusion single-photon emission computed tomography in women compared with men: impact of diabetes mellitus on incremental prognostic value and effect on patient management. *J Am Coll Cardiol.* 2003;41:1125-33.
186. Galassi AR, Azzarelli S, Tomaselli A, et al. Incremental prognostic value of technetium-99m-tetrofosmin exercise myocardial perfusion imaging for predicting outcomes in patients with suspected or known coronary artery disease. *Am J Cardiol.* 2001;88:101-6.
187. Vanzetto G, Ormezzano O, Fagret D, et al. Long-term additive prognostic value of thallium-201 myocardial perfusion imaging over clinical and exercise stress test in low to intermediate risk patients: study in 1137 patients with 6-year follow-up. *Circulation.* 1999;100:1521-7.
188. Olmos LI, Dakik H, Gordon R, et al. Long-term prognostic value of exercise echocardiography compared with exercise 201Tl, ECG, and clinical variables in patients evaluated for coronary artery disease. *Circulation.* 1998;98:2679-86.
189. Alkeylani A, Miller DD, Shaw LJ, et al. Influence of race on the prediction of cardiac events with stress technetium-99m sestamibi tomographic imaging in patients with stable angina pectoris. *Am J Cardiol.* 1998;81:293-7.
190. Snader CE, Marwick TH, Pashkow FJ, et al. Importance of estimated functional capacity as a predictor of all-cause mortality among patients referred for exercise thallium single-photon emission computed tomography: report of 3,400 patients from a single center. *J Am Coll Cardiol.* 1997;30:641-8.
191. Boyne TS, Koplman BA, Parsons WJ, et al. Predicting adverse outcome with exercise SPECT technetium-99m sestamibi imaging in patients with suspected or known coronary artery disease. *Am J Cardiol.* 1997;79:270-4.
192. Geleijnse ML, Elhendy A, van Domburg RT, et al. Cardiac imaging for risk stratification with dobutamine-atropine stress testing in patients with chest pain: echocardiography, perfusion scintigraphy, or both? *Circulation.* 1997;96:137-47.
193. Heller GV, Herman SD, Travin MI, et al. Independent prognostic value of intravenous dipyridamole with technetium-99m sestamibi tomographic imaging in predicting cardiac events and cardiac-related hospital admissions. *J Am Coll Cardiol.* 1995;26: 1202-8.
194. Machecourt J, Longere P, Fagret D, et al. Prognostic value of thallium-201 single-photon emission computed tomographic myocardial perfusion imaging according to extent of myocardial defect: study in 1,926 patients with follow-up at 33 months. *J Am Coll Cardiol.* 1994;23:1096-106.
195. Kamal AM, Fattah AA, Pancholy S, et al. Prognostic value of adenosine single-photon emission computed tomographic thallium imaging in medically treated patients with angiographic evidence of coronary artery disease. *J Nucl Cardiol.* 1994;1:254-61.
196. Stratmann HG, Tamesis BR, Younis LT, et al. Prognostic value of dipyridamole technetium-99m sestamibi myocardial tomography in patients with stable chest pain who are unable to exercise. *Am J Cardiol.* 1994;73:647-52.
197. Stratmann HG, Williams GA, Wittry MD, et al. Exercise technetium-99m sestamibi tomography for cardiac risk stratification of patients with stable chest pain. *Circulation.* 1994;89:615-22.
198. Hachamovitch R, Hayes S, Friedman JD, et al. Determinants of risk and its temporal variation in patients with normal stress myocardial perfusion scans: what is the warranty period of a normal scan? *J Am Coll Cardiol.* 2003;41:1329-40.

199. Groutars RG, Verzijlbergen JF, Muller AJ, et al. Prognostic value and quality of life in patients with normal rest thallium-201/stress technetium 99m-tetrofosmin dual-isotope myocardial SPECT. *J Nucl Cardiol.* 2000;7:333-41.
200. Soman P, Parsons A, Lahiri N, et al. The prognostic value of a normal Tc-99m sestamibi SPECT study in suspected coronary artery disease. *J Nucl Cardiol.* 1999;6:252-6.
201. Iskandrian AS, Chae SC, Heo J, et al. Independent and incremental prognostic value of exercise single-photon emission computed tomographic (SPECT) thallium imaging in coronary artery disease. *J Am Coll Cardiol.* 1993;22:665-70.
202. Nishimura S, Mahmarian JJ, Verani MS. Significance of increased lung thallium uptake during adenosine thallium-201 scintigraphy. *J Nucl Med.* 1992;33:1600-7.
203. Beller GA. Radionuclide perfusion imaging techniques for evaluation of patients with known or suspected coronary artery disease. *Adv Intern Med.* 1997;42:139-201.
204. Cox JL, Wright LM, Burns RJ. Prognostic significance of increased thallium-201 lung uptake during dipyridamole myocardial scintigraphy: comparison with exercise scintigraphy. *Can J Cardiol.* 1995;11:689-94.
205. Bacher-Stier C, Sharir T, Kavanagh PB, et al. Postexercise lung uptake of 99mTc-sestamibi determined by a new automatic technique: validation and application in detection of severe and extensive coronary artery disease and reduced left ventricular function. *J Nucl Med.* 2000;41:1190-7.
206. Boucher CA, Zir LM, Beller GA, et al. Increased lung uptake of thallium-201 during exercise myocardial imaging: clinical, hemodynamic and angiographic implications in patients with coronary artery disease. *Am J Cardiol.* 1980;46:189-96.
207. Gill JB, Ruddy TD, Newell JB, et al. Prognostic importance of thallium uptake by the lungs during exercise in coronary artery disease. *N Engl J Med.* 1987;317:1486-9.
208. Weiss AT, Berman DS, Lew AS, et al. Transient ischemic dilation of the left ventricle on stress thallium-201 scintigraphy: a marker of severe and extensive coronary artery disease. *J Am Coll Cardiol.* 1987;9:752-9.
209. Krawczynska EG, Weintraub WS, Garcia EV, et al. Left ventricular dilatation and multivessel coronary artery disease on thallium-201 SPECT are important prognostic indicators in patients with large defects in the left anterior descending distribution. *Am J Cardiol.* 1994;74:1233-9.
210. Veilleux M, Lette J, Mansur A, et al. Prognostic implications of transient left ventricular cavity dilation during exercise and dipyridamole-thallium imaging. *Can J Cardiol.* 1994;10:259-62.
211. McClellan JR, Travin MI, Herman SD, et al. Prognostic importance of scintigraphic left ventricular cavity dilation during intravenous dipyridamole technetium-99m sestamibi myocardial tomographic imaging in predicting coronary events. *Am J Cardiol.* 1997;79:600-5.
212. Mazzanti M, Germano G, Kiat H, et al. Identification of severe and extensive coronary artery disease by automatic measurement of transient ischemic dilation of the left ventricle in dual-isotope myocardial perfusion SPECT. *J Am Coll Cardiol.* 1996;27:1612-20.
213. Sharir T, Germano G, Kavanagh PB, et al. Incremental prognostic value of post-stress left ventricular ejection fraction and volume by gated myocardial perfusion single photon emission computed tomography. *Circulation.* 1999;100:1035-42.
214. Johnson LL, Verdesca SA, Aude WY, et al. Postischemic stunning can affect left ventricular ejection fraction and regional wall motion on post-stress gated sestamibi tomograms. *J Am Coll Cardiol.* 1997;30:1641-8.
215. Harris PJ, Harrell FE Jr, Lee KL, et al. Survival in medically treated coronary artery disease. *Circulation.* 1979;60:1259-69.
216. Mock MB, Ringqvist I, Fisher LD, et al. Survival of medically treated patients in the coronary artery surgery study (CASS) registry. *Circulation.* 1982;66:562-8.
217. Pryor DB, Harrell FE Jr, Lee KL, et al. Prognostic indicators from radionuclide angiography in medically treated patients with coronary artery disease. *Am J Cardiol.* 1984;53:18-22.
218. Lee KL, Pryor DB, Pieper KS, et al. Prognostic value of radionuclide angiography in medically treated patients with coronary artery disease: a comparison with clinical and catheterization variables. *Circulation.* 1990;82:1705-17.
219. Johnson SH, Bigelow C, Lee KL, et al. Prediction of death and myocardial infarction by radionuclide angiography in patients with suspected coronary artery disease. *Am J Cardiol.* 1991;67:919-26.
220. Upton MT, Palmeri ST, Jones RH, et al. Assessment of left ventricular function by resting and exercise radionuclide angiography following acute myocardial infarction. *Am Heart J.* 1982;104:1232-43.
221. Jones RH, Johnson SH, Bigelow C, et al. Exercise radionuclide angiography predicts cardiac death in patients with coronary artery disease. *Circulation.* 1991;84:152-158.
222. Morris KG, Palmeri ST, Califf RM, et al. Value of radionuclide angiography for predicting specific cardiac events after acute myocardial infarction. *Am J Cardiol.* 1985;55:318-24.
223. Jones RH, Floyd RD, Austin EH, et al. The role of radionuclide angiography in the preoperative prediction of pain relief and prolonged survival following coronary artery bypass grafting. *Ann Surg.* 1983;197:743-54.
224. Mazzotta G, Bonow RO, Pace L, et al. Relation between exertional ischemia and prognosis in mildly symptomatic patients with single or double vessel coronary artery disease and left ventricular dysfunction at rest. *J Am Coll Cardiol.* 1989;13:567-73.
225. Miller TD, Taliercio CP, Zinsmeister AR, et al. Risk stratification of single or double vessel coronary artery disease and impaired left ventricular function using exercise radionuclide angiography. *Am J Cardiol.* 1990;65:1317-21.
226. Bonow RO, Kent KM, Rosing DR, et al. Exercise-induced ischemia in mildly symptomatic patients with coronary-artery disease and preserved left ventricular function. Identification of subgroups at risk of death during medical therapy. *N Engl J Med.* 1984;311:1339-45.
227. Taliercio CP, Clements IP, Zinsmeister AR, et al. Prognostic value and limitations of exercise radionuclide angiography in medically treated coronary artery disease. *Mayo Clin Proc.* 1988;63:573-82.
228. O'Keefe JH Jr, Bateman TM, Ligon RW, et al. Outcome of medical versus invasive treatment strategies for non-high-risk ischemic heart disease. *J Nucl Cardiol.* 1998;5:28-33.
229. Shaw LJ, Hachamovitch R, Berman DS, et al. The economic consequences of available diagnostic and prognostic strategies for the evaluation of stable angina patients: an observational assessment of the value of precatheterization ischemia. Economics of Noninvasive Diagnosis (END) Multicenter Study Group. *J Am Coll Cardiol.* 1999;33:661-9.
230. Mahmarian JJ, Fenimore NL, Marks GF, et al. Transdermal nitroglycerin patch therapy reduces the extent of exercise-induced myocardial ischemia: results of a double-blind, placebo-controlled trial using quantitative thallium-201 tomography. *J Am Coll Cardiol.* 1994;24:25-32.
231. Eichstadt HW, Eskotter H, Hoffman I, et al. Improvement of

- myocardial perfusion by short-term fluvastatin therapy in coronary artery disease. *Am J Cardiol.* 1995;76:122A-125A.
232. Lewin HC, Hachamovitch R, Harris AG, et al. Sustained reduction of exercise perfusion defect extent and severity with isosorbide mononitrate (Imdur) as demonstrated by means of technetium 99m sestamibi. *J Nucl Cardiol.* 2000;7:342-53.
233. Akinboboye O, Idris O, Berekashvili K, et al. Incidence of major cardiovascular events in black patients with normal myocardial stress perfusion studies. *J Nucl Cardiol.* 2001;8:541-7.
234. Williams KA, Lang RM, Reba RC, et al. Comparison of technetium-99m sestamibi-gated tomographic perfusion imaging with echocardiography and electrocardiography for determination of left ventricular mass. *Am J Cardiol.* 1996;77:750-5.
235. Liao Y, Cooper RS, McGee D, et al. The relative effects of left ventricular hypertrophy, coronary artery disease, and ventricular dysfunction on survival among black adults. *JAMA.* 1995; 273:1592-7.
236. Kannel WB. Prevalence, incidence, and hazards of hypertension in the elderly. *Am Heart J.* 1986;112:1362-63.
237. Gibbons RJ, Balady GJ, Bricker JT, et al. ACC/AHA 2002 guideline update for exercise testing: a report of the American College of Cardiology/American Heart Association Task force on Practice Guidelines (Committee on Exercise Testing). 2003; American College of Cardiology Web site. Available at: http://www.acc.org/clinical/guidelines/exercise/exercise_clean.pdf. Accessed February 26, 2003.
238. Detrano R, Janosi A, Lyons KP, et al. Factors affecting sensitivity and specificity of a diagnostic test: the exercise thallium scintigram. *Am J Med.* 1988;84:699-710.
239. Hachamovitch R, Berman DS, Kiat H, et al. Effective risk stratification using exercise myocardial perfusion SPECT in women: gender-related differences in prognostic nuclear testing. *J Am Coll Cardiol.* 1996;28:34-44.
240. Elhendy A, van Domburg RT, Bax JJ, et al. Noninvasive diagnosis of coronary artery stenosis in women with limited exercise capacity: comparison of dobutamine stress echocardiography and 99mTc sestamibi single-photon emission CT. *Chest.* 1998;114: 1097-1104.
241. Amanullah AM, Kiat H, Friedman JD, et al. Adenosine technetium-99m sestamibi myocardial perfusion SPECT in women: diagnostic efficacy in detection of coronary artery disease. *J Am Coll Cardiol.* 1996;27:803-9.
242. Amanullah AM, Berman DS, Hachamovitch R, et al. Identification of severe or extensive coronary artery disease in women by adenosine technetium-99m sestamibi SPECT. *Am J Cardiol.* 1997;80:132-7.
243. Shaw LJ, Miller DD, Romeis JC, et al. Gender differences in the noninvasive evaluation and management of patients with suspected coronary artery disease. *Ann Intern Med.* 1994;120:559-66.
244. Hachamovitch R, Berman DS, Kiat H, et al. Gender-related differences in clinical management after exercise nuclear testing. *J Am Coll Cardiol.* 1995;26:1457-64.
245. Mark DB, Shaw LK, DeLong ER, et al. Absence of sex bias in the referral of patients for cardiac catheterization. *N Engl J Med.* 1994;330:1101-6.
246. Marwick TH, Shaw LJ, Lauer MS, et al. The noninvasive prediction of cardiac mortality in men and women with known or suspected coronary artery disease. Economics of Noninvasive Diagnosis (END) Study Group. *Am J Med.* 1999;106:172-8.
247. Elveback LR, Connolly DC, Melton LJ III. Coronary heart disease in residents of Rochester, Minnesota. VII: Incidence, 1950 through 1982. *Mayo Clin Proc.* 1986;61:896-900.
248. O'Keefe JH Jr, Zinsmeister AR, Gibbons RJ. Value of normal electrocardiographic findings in predicting resting left ventricular function in patients with chest pain and suspected coronary artery disease. *Am J Med.* 1989;86:658-62.
249. Christian TF, Miller TD, Chareonthaitawee P, et al. Prevalence of normal resting left ventricular function with normal rest electrocardiograms. *Am J Cardiol.* 1997;79:1295-8.
250. Rihal CS, Davis KB, Kennedy JW, et al. The utility of clinical, electrocardiographic, and roentgenographic variables in the prediction of left ventricular function. *Am J Cardiol.* 1995;75:220-3.
251. Nallamothu N, Ghods M, Heo J, et al. Comparison of thallium-201 single-photon emission computed tomography and electrocardiographic response during exercise in patients with normal rest electrocardiographic results. *J Am Coll Cardiol.* 1995;25:830-6.
252. Hachamovitch R, Berman DS, Kiat H, et al. Value of stress myocardial perfusion single photon emission computed tomography in patients with normal resting electrocardiograms: an evaluation of incremental prognostic value and cost-effectiveness. *Circulation.* 2002;105:823-9.
253. Ladenheim ML, Kotler TS, Pollock BH, et al. Incremental prognostic power of clinical history, exercise electrocardiography and myocardial perfusion scintigraphy in suspected coronary artery disease. *Am J Cardiol.* 1987;59:270-7.
254. Christian TF, Miller TD, Bailey KR, et al. Exercise tomographic thallium-201 imaging in patients with severe coronary artery disease and normal electrocardiograms. *Ann Intern Med.* 1994;121: 825-32.
255. Mattera JA, Arain SA, Sinusas AJ, et al. Exercise testing with myocardial perfusion imaging in patients with normal baseline electrocardiograms: cost savings with a stepwise diagnostic strategy. *J Nucl Cardiol.* 1998;5:498-506.
256. Gibbons RJ, Zinsmeister AR, Miller TD, et al. Supine exercise electrocardiography compared with exercise radionuclide angiography in noninvasive identification of severe coronary artery disease. *Ann Intern Med.* 1990;112:743-9.
257. Melin JA, Wijns W, Vanbutsele RJ, et al. Alternative diagnostic strategies for coronary artery disease in women: demonstration of the usefulness and efficiency of probability analysis. *Circulation.* 1985;71:535-42.
258. Mark DB, Shaw L, Harrell FE Jr, et al. Prognostic value of a treadmill exercise score in outpatients with suspected coronary artery disease. *N Engl J Med.* 1991;325:849-53.
259. Mark DB, Hlatky MA, Harrell FE Jr, et al. Exercise treadmill score for predicting prognosis in coronary artery disease. *Ann Intern Med.* 1987;106:793-800.
260. Bruce RA, DeRouen TA, Hossack KF. Pilot study examining the motivational effects of maximal exercise testing to modify risk factors and health habits. *Cardiology.* 1980;66:111-19.
261. Hachamovitch R, Berman DS, Kiat H, et al. Exercise myocardial perfusion SPECT in patients without known coronary artery disease: incremental prognostic value and use in risk stratification. *Circulation.* 1996;93:905-14.
262. Morrow K, Morris CK, Froelicher VF, et al. Prediction of cardiovascular death in men undergoing noninvasive evaluation for coronary artery disease. *Ann Intern Med.* 1993;118:689-95.
263. Shaw LJ, Hachamovitch R, Peterson ED, et al. Using an outcomes-based approach to identify candidates for risk stratification after exercise treadmill testing. *J Gen Intern Med.* 1999;14:1-9.
264. Hlatky MA, Pryor DB, Harrell FE Jr, et al. Factors affecting sensitivity and specificity of exercise electrocardiography: multivariable analysis. *Am J Med.* 1984;77:64-71.

265. Braat SH, Brugada P, Bar FW, et al. Thallium-201 exercise scintigraphy and left bundle-branch block. *Am J Cardiol.* 1985; 55:224-6.
266. Hirzel HO, Senn M, Nuesch K, et al. Thallium-201 scintigraphy in complete left bundle-branch block. *Am J Cardiol.* 1984;53:764-9.
267. DePuey EG, Guertler-Krawczynska E, Robbins WL. Thallium-201 SPECT in coronary artery disease patients with left bundle-branch block. *J Nucl Med.* 1988;29:1479-85.
268. Burns RJ, Galligan L, Wright LM, et al. Improved specificity of myocardial thallium-201 single-photon emission computed tomography in patients with left bundle-branch block by dipyridamole. *Am J Cardiol.* 1991;68:504-8.
269. Rockett JF, Wood WC, Moinuddin M, et al. Intravenous dipyridamole thallium-201 SPECT imaging in patients with left bundle-branch block. *Clin Nucl Med.* 1990;15:401-7.
270. O'Keefe JH Jr, Bateman TM, Silvestri R, et al. Safety and diagnostic accuracy of adenosine thallium-201 scintigraphy in patients unable to exercise and those with left bundle-branch block. *Am Heart J.* 1992;124:614-21.
271. Wagdy HM, Hodge D, Christian TF, et al. Prognostic value of vasodilator myocardial perfusion imaging in patients with left bundle-branch block. *Circulation.* 1998;97:1563-70.
272. Nallamothu N, Bagheri B, Acio ER, et al. Prognostic value of stress myocardial perfusion single photon emission computed tomography imaging in patients with left ventricular bundle branch block. *J Nucl Cardiol.* 1997;4:487-93.
273. Nigam A, Humen DP. Prognostic value of myocardial perfusion imaging with exercise and/or dipyridamole hyperemia in patients with preexisting left bundle-branch block. *J Nucl Med.* 1998; 39:579-81.
274. Gil VM, Almeida M, Ventosa A, et al. Prognosis in patients with left bundle-branch block and normal dipyridamole thallium-201 scintigraphy. *J Nucl Cardiol.* 1998;5:414-7.
275. Vaduganathan P, He ZX, Raghavan C, et al. Detection of left anterior descending coronary artery stenosis in patients with left bundle-branch block: exercise, adenosine or dobutamine imaging? *J Am Coll Cardiol.* 1996;28:543-50.
276. Gioia G, Bagheri B, Gottlieb CD, et al. Prediction of outcome of patients with life-threatening ventricular arrhythmias treated with automatic implantable cardioverter-defibrillators using SPECT perfusion imaging. *Circulation.* 1997;95:390-4.
277. Bartram P, Toft J, Hanel B, et al. False-positive defects in technetium-99m sestamibi myocardial single-photon emission tomography in healthy athletes with left ventricular hypertrophy. *Eur J Nucl Med.* 1998;25:1308-12.
278. Amanullah AM, Berman DS, Kang X, et al. Enhanced prognostic stratification of patients with left ventricular hypertrophy with the use of single-photon emission computed tomography. *Am Heart J.* 2000;140:456-62.
279. Hilton TC, Shaw LJ, Chaitman BR, et al. Prognostic significance of exercise thallium-201 testing in patients aged greater than or equal to 70 years with known or suspected coronary artery disease. *Am J Cardiol.* 1992;69:45-50.
280. Hayes SW, Schisterman EF, Lewin HC, et al. Incremental prognostic value of gated myocardial perfusion SPECT in elderly patients. *J Am Coll Cardiol.* 2001;37:425a. Abstract.
281. Blumenthal RS, Becker DM, Moy TF, et al. Exercise thallium tomography predicts future clinically manifest coronary heart disease in a high-risk asymptomatic population. *Circulation.* 1996;93:915-23.
282. Schwartz RS, Jackson WG, Celio PV, et al. Accuracy of exercise 201Tl myocardial scintigraphy in asymptomatic young men. *Circulation.* 1993;87:165-172.
283. Fleg JL, Gerstenblith G, Zonderman AB, et al. Prevalence and prognostic significance of exercise-induced silent myocardial ischemia detected by thallium scintigraphy and electrocardiography in asymptomatic volunteers. *Circulation.* 1990;81:428-36.
284. Diabetes mellitus: a major risk factor for cardiovascular disease. A joint editorial statement by the American Diabetes Association; The National Heart, Lung, and Blood Institute; The Juvenile Diabetes Foundation International; The National Institute of Diabetes and Digestive and Kidney Diseases; and The American Heart Association. *Circulation.* 1999;100:1132-3.
285. Wackers FJ, Zaret BL. Detection of myocardial ischemia in patients with diabetes mellitus. *Circulation.* 2002;105:5-7.
286. Kang X, Berman DS, Lewin HC, et al. Incremental prognostic value of myocardial perfusion single photon emission computed tomography in patients with diabetes mellitus. *Am Heart J.* 1999;138:1025-32.
287. Giri S, Shaw LJ, Murthy DR, et al. Impact of diabetes on the risk stratification using stress single-photon emission computed tomography myocardial perfusion imaging in patients with symptoms suggestive of coronary artery disease. *Circulation.* 2002; 105:32-40.
288. Hayes SW, Schisterman EF, Lewin HC, et al. Gated myocardial perfusion SPECT has incremental value for predicting cardiac death in diabetic patients. *J Am Coll Cardiol.* 2001;37:381. Abstract.
289. He ZX, Hedrick TD, Pratt CM, et al. Severity of coronary artery calcification by electron beam computed tomography predicts silent myocardial ischemia. *Circulation.* 2000;101:244-51.
290. Legrand V, Mancini GB, Bates ER, et al. Comparative study of coronary flow reserve, coronary anatomy and results of radionuclide exercise tests in patients with coronary artery disease. *J Am Coll Cardiol.* 1986;8:1022-32.
291. Miller DD, Donohue TJ, Younis LT, et al. Correlation of pharmacological 99mTc-sestamibi myocardial perfusion imaging with poststenotic coronary flow reserve in patients with angiographically intermediate coronary artery stenoses. *Circulation.* 1994; 89:2150-60.
292. Abdel Fattah A, Kamal AM, Pancholy S, et al. Prognostic implications of normal exercise tomographic thallium images in patients with angiographic evidence of significant coronary artery disease. *Am J Cardiol.* 1994;74:769-71.
293. Brown KA, Rowen M. Prognostic value of a normal exercise myocardial perfusion imaging study in patients with angiographically significant coronary artery disease. *Am J Cardiol.* 1993; 71:865-7.
294. Hecht HS, Shaw RE, Chin HL, et al. Silent ischemia after coronary angioplasty: evaluation of restenosis and extent of ischemia in asymptomatic patients by tomographic thallium-201 exercise imaging and comparison with symptomatic patients. *J Am Coll Cardiol.* 1991;17:670-7.
295. Marie PY, Danchin N, Karcher G, et al. Usefulness of exercise SPECT-thallium to detect asymptomatic restenosis in patients who had angina before coronary angioplasty. *Am Heart J.* 1993; 126:571-7.
296. Bengtson JR, Mark DB, Honan MB, et al. Detection of restenosis after elective percutaneous transluminal coronary angioplasty using the exercise treadmill test. *Am J Cardiol.* 1990;65:28-34.
297. Wagner HJ, Nowacki J, Klose KJ. Propofol versus midazolam for sedation during percutaneous transluminal angioplasty. *J Vasc Interv Radiol.* 1996;7:673-80.

298. Georgoulas P, Demakopoulos N, Kontos A, et al. Tc-99m tetrofosmin myocardial perfusion imaging before and six months after percutaneous transluminal coronary angioplasty. *Clin Nucl Med.* 1998;23:678-82.
299. Garzon PP, Eisenberg MJ. Functional testing for the detection of restenosis after percutaneous transluminal coronary angioplasty: a meta-analysis. *Can J Cardiol.* 2001;17:41-48.
300. Hecht HS, Shaw RE, Bruce TR, et al. Usefulness of tomographic thallium-201 imaging for detection of restenosis after percutaneous transluminal coronary angioplasty. *Am J Cardiol.* 1990;66:1314-18.
301. Amanullah AM. Noninvasive testing in the diagnosis and management of unstable angina. *Int J Cardiol.* 1994;47:95-103.
302. McPherson JA, Robinson PS, Powers ER, et al. Angiographic findings in patients undergoing catheterization for recurrent symptoms within 30 days of successful coronary intervention. *Am J Cardiol.* 1999;84:589-92.A8.
303. Pepine CJ, Cohn PF, Deedwania PC, et al. Effects of treatment on outcome in mildly symptomatic patients with ischemia during daily life. The Atenolol Silent Ischemia Study (ASIST). *Circulation.* 1994;90:762-8.
304. Ho KT, Miller TD, Holmes DR, et al. Long-term prognostic value of Duke treadmill score and exercise thallium-201 imaging performed one to three years after percutaneous transluminal coronary angioplasty. *Am J Cardiol.* 1999;84:1323-7.
305. Ritchie JL, Bateman TM, Bonow RO, et al. ACC/AHA guidelines for clinical use of cardiac radionuclide imaging. a report of the American College of Cardiology/American Heart Association Task Force on Assessment of Diagnostic and Therapeutic Cardiovascular Procedures (Committee on Radionuclide Imaging), developed in collaboration with the American Society of Nuclear Cardiology. *J Am Coll Cardiol.* 1995;25:521-47.
306. Miller TD, Christian TF, Hodge DO, et al. Prognostic value of exercise thallium-201 imaging performed within 2 years of coronary artery bypass graft surgery. *J Am Coll Cardiol.* 1998;31:848-54.
307. Palmas W, Bingham S, Diamond GA, et al. Incremental prognostic value of exercise thallium-201 myocardial single-photon emission computed tomography late after coronary artery bypass surgery. *J Am Coll Cardiol.* 1995;25:403-9.
308. Nallamothu N, Johnson JH, Bagheri B, et al. Utility of stress single-photon emission computed tomography (SPECT) perfusion imaging in predicting outcome after coronary artery bypass grafting. *Am J Cardiol.* 1997;80:1517-21.
309. Lauer MS, Lytle B, Pashkow F, et al. Prediction of death and myocardial infarction by screening with exercise-thallium testing after coronary-artery-bypass grafting. *Lancet.* 1998;351:615-22.
310. Zellweger MJ, Lewin HC, Lai S, et al. When to stress patients after coronary artery bypass surgery? Risk stratification in patients early and late post-CABG using stress myocardial perfusion SPECT: implications of appropriate clinical strategies. *J Am Coll Cardiol.* 2001;37:144-52.
311. Desideri A, Candelpergher G, Zanco P, et al. Exercise technetium 99m sestamibi single-photon emission computed tomography late after coronary artery bypass surgery: long-term follow-up. *Clin Cardiol.* 1997;20:779-84.
312. Smith SC Jr, Dove JT, Jacobs AK, et al. ACC/AHA guidelines for percutaneous coronary intervention (revision of the 1993 PTCA guidelines)-executive summary: a report of the American College of Cardiology/American Heart Association task force on practice guidelines (Committee to revise the 1993 guidelines for percutaneous transluminal coronary angioplasty). *Circulation.* 2001;103:3019-41.
313. Eagle KA, Berger PB, Calkins H, et al. ACC/AHA guideline update for perioperative cardiovascular evaluation for noncardiac surgery: a report of the American College of Cardiology/American Heart Association Task Force on Practice Guidelines (Committee to Update the 1996 Guidelines on Perioperative Cardiovascular Evaluation for Noncardiac Surgery). 2002; American College of Cardiology Web site. Available at: <http://www.acc.org/clinical/guidelines/perioclean/pdf/perioclean.pdf>. Accessed June 11, 2002.
314. Lee TH, Marcantonio ER, Mangione CM, et al. Derivation and prospective validation of a simple index for prediction of cardiac risk of major noncardiac surgery. *Circulation.* 1999;100:1043-9.
315. Lewis MS, Wilson RA, Walker KW, et al. Validation of an algorithm for predicting cardiac events in renal transplant candidates. *Am J Cardiol.* 2002;89:847-50.
316. Borer JS, Hochreiter C, Herrold EM, et al. Prediction of indications for valve replacement among asymptomatic or minimally symptomatic patients with chronic aortic regurgitation and normal left ventricular performance. *Circulation.* 1998;97:525-34.
317. Poldermans D, Boersma E, Bax JJ, et al. The effect of bisoprolol on perioperative mortality and myocardial infarction in high-risk patients undergoing vascular surgery. Dutch Echocardiographic Cardiac Risk Evaluation Applying Stress Echocardiography Study Group. *N Engl J Med.* 1999;341:1789-94.
318. Boucher CA, Brewster DC, Darling C, et al. Determination of cardiac risk by dipyridamole-thallium imaging before peripheral vascular surgery. *N Engl J Med.* 1985;312:389-94.
319. Cutler BS, Leppo JA. Dipyridamole thallium 201 scintigraphy to detect coronary artery disease before abdominal aortic surgery. *J Vasc Surg.* 1987;5:91-100.
320. Fletcher JP, Antico VF, Gruenewald S, et al. Dipyridamole-thallium scan for screening of coronary artery disease prior to vascular surgery. *J Cardiovasc Surg (Torino).* 1988;29:666-9.
321. Sachs RN, Tellier P, Larmignat P, et al. Assessment by dipyridamole-thallium-201 myocardial scintigraphy of coronary risk before peripheral vascular surgery. *Surgery.* 1988;103:584-7.
322. Eagle KA, Coley CM, Newell JB, et al. Combining clinical and thallium data optimizes preoperative assessment of cardiac risk before major vascular surgery. *Ann Intern Med.* 1989;110:859-66.
323. McEnroe CS, O'Donnell TF Jr, Yeager A, et al. Comparison of ejection fraction and Goldman risk factor analysis of dipyridamole-thallium-201 studies in the evaluation of cardiac morbidity after aortic aneurysm surgery. *J Vasc Surg.* 1990;11:497-504.
324. Younis LT, Aguirre F, Byers S, et al. Perioperative and long-term prognostic value of intravenous dipyridamole thallium scintigraphy in patients with peripheral vascular disease. *Am Heart J.* 1990;119:1287-92.
325. Mangano DT, London MJ, Tubau JF, et al. Dipyridamole thallium-201 scintigraphy as a preoperative screening test: a reexamination of its predictive potential. Study of Perioperative Ischemia Research Group. *Circulation.* 1991;84:493-502.
326. Strawn DJ, Guernsey JM. Dipyridamole thallium scanning in the evaluation of coronary artery disease in elective abdominal aortic surgery. *Arch Surg.* 1991;126:880-4.
327. Watters TA, Botvinick EH, Dae MW, et al. Comparison of the findings on preoperative dipyridamole perfusion scintigraphy and intraoperative transesophageal echocardiography: implications regarding the identification of myocardium at ischemic risk. *J Am Coll Cardiol.* 1991;18:93-100.
328. Hendel RC, Whitfield SS, Villegas BJ, et al. Prediction of late cardiac events by dipyridamole thallium imaging in patients

- undergoing elective vascular surgery. *Am J Cardiol.* 1992;70:1243-9.
329. Lette J, Waters D, Cerino M, et al. Preoperative coronary artery disease risk stratification based on dipyridamole imaging and a simple three-step, three-segment model for patients undergoing noncardiac vascular surgery or major general surgery. *Am J Cardiol.* 1992;69:1553-8.
 330. Madsen PV, Vissing M, Munck O, et al. A comparison of dipyridamole thallium 201 scintigraphy and clinical examination in the determination of cardiac risk before arterial reconstruction. *Angiology.* 1992;43:306-11.
 331. Brown KA, Rowen M. Extent of jeopardized viable myocardium determined by myocardial perfusion imaging best predicts perioperative cardiac events in patients undergoing noncardiac surgery. *J Am Coll Cardiol.* 1993;21:325-30.
 332. Kresowik TF, Bower TR, Garner SA, et al. Dipyridamole thallium imaging in patients being considered for vascular procedures. *Arch Surg.* 1993;128:299-302.
 333. Baron JF, Mundler O, Bertrand M, et al. Dipyridamole-thallium scintigraphy and gated radionuclide angiography to assess cardiac risk before abdominal aortic surgery. *N Engl J Med.* 1994;330:663-9.
 334. Bry JD, Belkin M, O'Donnell TF Jr, et al. An assessment of the positive predictive value and cost-effectiveness of dipyridamole myocardial scintigraphy in patients undergoing vascular surgery. *J Vasc Surg.* 1994;19:112-21.
 335. Koutelou MG, Asimacopoulos PJ, Mahmarian JJ, et al. Preoperative risk stratification by adenosine thallium 201 single-photon emission computed tomography in patients undergoing vascular surgery. *J Nucl Cardiol.* 1995;2:389-94.
 336. Marshall ES, Raichlen JS, Forman S, et al. Adenosine radionuclide perfusion imaging in the preoperative evaluation of patients undergoing peripheral vascular surgery. *Am J Cardiol.* 1995;76:817-21.
 337. Van Damme H, Pierard L, Gillain D, et al. Cardiac risk assessment before vascular surgery: a prospective study comparing clinical evaluation, dobutamine stress echocardiography, and dobutamine Tc-99m sestamibi tomoscintigraphy. *Cardiovasc Surg.* 1997;5:54-64.
 338. Camp AD, Garvin PJ, Hoff J, et al. Prognostic value of intravenous dipyridamole thallium imaging in patients with diabetes mellitus considered for renal transplantation. *Am J Cardiol.* 1990;65:1459-63.
 339. Iqbal A, Gibbons RJ, McGoon MD, et al. Noninvasive assessment of cardiac risk in insulin-dependent diabetic patient being evaluated for pancreatic transplantation using thallium-201 myocardial perfusion scintigraphy. *Transplant Proc.* 1991;23:1690-1.
 340. Coley CM, Field TS, Abraham SA, et al. Usefulness of dipyridamole-thallium scanning for preoperative evaluation of cardiac risk for nonvascular surgery. *Am J Cardiol.* 1992;69:1280-5.
 341. Shaw L, Miller DD, Kong BA, et al. Determination of perioperative cardiac risk by adenosine thallium-201 myocardial imaging. *Am Heart J.* 1992;124:861-9.
 342. Takase B, Younis LT, Byers SL, et al. Comparative prognostic value of clinical risk indexes, resting two-dimensional echocardiography, and dipyridamole stress thallium-201 myocardial imaging for perioperative cardiac events in major nonvascular surgery patients. *Am Heart J.* 1993;126:1099-1106.
 343. Younis L, Stratmann H, Takase B, et al. Preoperative clinical assessment and dipyridamole thallium-201 scintigraphy for prediction and prevention of cardiac events in patients having major noncardiovascular surgery and known or suspected coronary artery disease. *Am J Cardiol.* 1994;74:311-17.
 344. Stratmann HG, Younis LT, Wittry MD, et al. Dipyridamole technetium-99m sestamibi myocardial tomography in patients evaluated for elective vascular surgery: prognostic value for perioperative and late cardiac events. *Am Heart J.* 1996;131:923-9.
 345. Bartels C, Bechtel JF, Hossmann V, et al. Cardiac risk stratification for high-risk vascular surgery. *Circulation.* 1997;95:2473-5.
 346. Vanzetto G, Machecourt J, Blendea D, et al. Additive value of thallium single-photon emission computed tomography myocardial imaging for prediction of perioperative events in clinically selected high cardiac risk patients having abdominal aortic surgery. *Am J Cardiol.* 1996;77:143-8.
 347. Mantha S, Roizen MF, Barnard J, et al. Relative effectiveness of four preoperative tests for predicting adverse cardiac outcomes after vascular surgery: a meta-analysis. *Anesth Analg.* 1994;79:422-33.
 348. Fiser WP, Thompson BW, Thompson AR, et al. Nuclear cardiac ejection fraction and cardiac index in abdominal aortic surgery. *Surgery.* 1993;94:736-9.
 349. Fletcher JP, Antico VF, Gruenewald S, et al. Risk of aortic aneurysm surgery as assessed by preoperative gated heart pool scan. *Br J Surg.* 1989;76:26-8.
 350. Kazmers A, Cerqueira MD, Zierler RE. The role of preoperative radionuclide ejection fraction in direct abdominal aortic aneurysm repair. *J Vasc Surg.* 1988;8:128-36.
 351. Lazor L, Russell JC, DaSilva J, et al. Use of the multiple uptake gated acquisition scan for the preoperative assessment of cardiac risk. *Surg Gynecol Obstet.* 1988;167:234-8.
 352. Mosley JG, Clarke JM, Ell PJ, et al. Assessment of myocardial function before aortic surgery by radionuclide angiography. *Br J Surg.* 1985;72:886-7.
 353. Pasternack PF, Imparato AM, Bear G, et al. The value of radionuclide angiography as a predictor of perioperative myocardial infarction in patients undergoing abdominal aortic aneurysm resection. *J Vasc Surg.* 1984;1:320-5.
 354. Pasternack PF, Imparato AM, Riles TS, et al. The value of the radionuclide angiogram in the prediction of perioperative myocardial infarction in patients undergoing lower extremity revascularization procedures. *Circulation.* 1985;72:III13-III17.
 355. Pedersen T, Kelbaek H, Munck O. Cardiopulmonary complications in high-risk surgical patients: the value of preoperative radionuclide cardiography. *Acta Anaesthesiol Scand.* 1990;34:183-9.
 356. Hunt SA, Baker DW, Chin MH, et al. ACC/AHA guidelines for the evaluation and management of chronic heart failure in the adult: a report of the American College of Cardiology/American Heart Association Task Force on Practice Guidelines (Committee to Revise the 1995 Guidelines for the Evaluation and Management of Heart Failure). 2001; American College of Cardiology Web site. Available at: http://www.acc.org/clinical/guidelines/failure/pdfs/hf_fulltext.pdf. Accessed August 20, 2002.
 357. Packer M, Cohn JN. Consensus recommendations for the management of chronic heart failure. *Am J Cardiol.* 1999;83:1A-38A.
 358. Heart Failure Society of America (HFSA) practice guidelines. HFSFA for management of patients with heart failure caused by left ventricular systolic dysfunction—pharmacologic approaches. *J Card Fail.* 1999;5:357-82.
 359. Gibbons RJ, Miller TD. Equilibrium radionuclide angiography. In: Skorton DJ, ed. *A Companion to Braunwald's Heart Disease.* 2 ed. Philadelphia, Pa: W.B. Saunders Co; 1996:942-6.
 360. Muntinga HJ, van den Berg F, Knol HR, et al. Normal values and reproducibility of left ventricular filling parameters by radionu-

- clide angiography. *Int J Card Imaging.* 1997;13:165-71.
361. Schirmer H, Lunde P, Rasmussen K. Mitral flow derived Doppler indices of left ventricular diastolic function in a general population; the Tromso study. *Eur Heart J.* 2000;21:1376-86.
362. Uretsky BF, Thygesen K, Armstrong PW, et al. Acute coronary findings at autopsy in heart failure patients with sudden death: results from the assessment of treatment with lisinopril and survival (ATLAS) trial. *Circulation.* 2000;102:611-16.
363. Tauberg SG, Orié JE, Bartlett BE, et al. Usefulness of thallium-201 for distinction of ischemic from idiopathic dilated cardiomyopathy. *Am J Cardiol.* 1993;71:674-80.
364. Bureau JF, Gaillard JF, Granier R, et al. Diagnostic and prognostic criteria of chronic left ventricular failure obtained during exercise-201TI imaging. *Eur J Nucl Med.* 1987;12:613-6.
365. Bulkley BH, Hutchins GM, Bailey I, et al. Thallium 201 imaging and gated cardiac blood pool scans in patients with ischemic and idiopathic congestive cardiomyopathy: a clinical and pathologic study. *Circulation.* 1977;55:753-60.
366. Saltissi S, Hockings B, Croft DN, et al. Thallium-201 myocardial imaging in patients with dilated and ischaemic cardiomyopathy. *Br Heart J.* 1981;46:290-5.
367. Dianas PG, Ahlberg AW, Clark BA III, et al. Combined assessment of myocardial perfusion and left ventricular function with exercise technetium-99m sestamibi gated single-photon emission computed tomography can differentiate between ischemic and nonischemic dilated cardiomyopathy. *Am J Cardiol.* 1998;82:1253-8.
368. Glamann DB, Lange RA, Corbett JR, et al. Utility of various radionuclide techniques for distinguishing ischemic from nonischemic dilated cardiomyopathy. *Arch Intern Med.* 1992;152:769-72.
369. Hudson RED. Pathology of cardiomyopathy. *Cardiovasc Clin.* 1972;4:3-59.
370. Pasternac A, Noble J, Streulens Y, et al. Pathophysiology of chest pain in patients with cardiomyopathies and normal coronary arteries. *Circulation.* 1982;65:778-89.
371. Cannon RO III, Cunnion RE, Parrillo JE, et al. Dynamic limitation of coronary vasodilator reserve in patients with dilated cardiomyopathy and chest pain. *J Am Coll Cardiol.* 1987;10:1190-1200.
372. Doi YL, Chikamori T, Tukata J, et al. Prognostic value of thallium-201 perfusion defects in idiopathic dilated cardiomyopathy. *Am J Cardiol.* 1991;67:188-93.
373. Bonow RO. Identification of viable myocardium. *Circulation.* 1996;94:2674-80.
374. Udelson JE. Steps forward in the assessment of myocardial viability in left ventricular dysfunction. *Circulation.* 1998;97:833-8.
375. Samady H, Elefteriades JA, Abbott BG, et al. Failure to improve left ventricular function after coronary revascularization for ischemic cardiomyopathy is not associated with worse outcome. *Circulation.* 1999;100:1298-304.
376. Di Carli MF, Asgarzadie F, Schelbert HR, et al. Quantitative relation between myocardial viability and improvement in heart failure symptoms after revascularization in patients with ischemic cardiomyopathy. *Circulation.* 1995;92:3436-44.
377. Allman KC, Shaw LJ, Hachamovitch R, et al. Myocardial viability testing and impact of revascularization on prognosis in patients with coronary artery disease and left ventricular dysfunction: a meta-analysis. *J Am Coll Cardiol.* 2002;39:1151-8.
378. Zimmermann R, Mall G, Rauch B, et al. Residual 201TI activity in irreversible defects as a marker of myocardial viability: clinicopathological study. *Circulation.* 1995;91:1016-21.
379. Maes AF, Borgers M, Flameng W, et al. Assessment of myocardial viability in chronic coronary artery disease using technetium-99m sestamibi SPECT: correlation with histologic and positron emission tomographic studies and functional follow-up. *J Am Coll Cardiol.* 1997;29:62-8.
380. Medrano R, Lowry RW, Young JB, et al. Assessment of myocardial viability with 99mTc sestamibi in patients undergoing cardiac transplantation: a scintigraphic/pathological study. *Circulation.* 1996;94:1010-17.
381. Udelson JE, Coleman PS, Metherall J, et al. Predicting recovery of severe regional ventricular dysfunction: comparison of resting scintigraphy with 201TI and 99mTc-sestamibi. *Circulation.* 1994;89:2552-61.
382. Perrone-Filardi P, Pace L, Prastaro M, et al. Dobutamine echocardiography predicts improvement of hypoperfused dysfunctional myocardium after revascularization in patients with coronary artery disease. *Circulation.* 1995;91:2556-65.
383. Ragosta M, Beller GA, Watson DD, et al. Quantitative planar redistribution 201TI imaging in detection of myocardial viability and prediction of improvement in left ventricular function after coronary bypass surgery in patients with severely depressed left ventricular function. *Circulation.* 1993;87:1630-41.
384. Kitsiou AN, Srinivasan G, Quyyumi AA, et al. Stress-induced reversible and mild-to-moderate irreversible thallium defects: are they equally accurate for predicting recovery of regional left ventricular function after revascularization? *Circulation.* 1998;98:501-8.
385. Dilsizian V, Rocco TP, Freedman NM, et al. Enhanced detection of ischemic but viable myocardium by the reinjection of thallium after stress-redistribution imaging. *N Engl J Med.* 1990;323:141-6.
386. Kiat H, Berman DS, Maddahi J, et al. Late reversibility of tomographic myocardial thallium-201 defects: an accurate marker of myocardial viability. *J Am Coll Cardiol.* 1988;12:1456-63.
387. Mori T, Minamiji K, Kurogane H, et al. Rest-injected thallium-201 imaging for assessing viability of severe asynergic regions. *J Nucl Med.* 1991;32:1718-24.
388. Sinusas AJ, Bergin JD, Edwards NC, et al. Redistribution of 99mTc-sestamibi and 201TI in the presence of a severe coronary artery stenosis. *Circulation.* 1994;89:2332-41.
389. Kauffman GJ, Boyne TS, Watson DD, et al. Comparison of rest thallium-201 imaging and rest technetium-99m sestamibi imaging for assessment of myocardial viability in patients with coronary artery disease and severe left ventricular dysfunction. *J Am Coll Cardiol.* 1996;27:1592-7.
390. Maurea S, Cuocolo A, Soricelli A, et al. Enhanced detection of viable myocardium by technetium-99m-MIBI imaging after nitrate administration in chronic coronary artery disease. *J Nucl Med.* 1995;36:1945-52.
391. Matsunari I, Fujino S, Taki J, et al. Quantitative rest technetium-99m tetrofosmin imaging in predicting functional recovery after revascularization: comparison with rest-redistribution thallium-201. *J Am Coll Cardiol.* 1997;29:1226-33.
392. Gunning MG, Anagnostopoulos C, Knight CJ, et al. Comparison of 201TI, 99mTc-tetrofosmin, and dobutamine magnetic resonance imaging for identifying hibernating myocardium. *Circulation.* 1998;98:1869-74.
393. Levine MG, McGill CC, Ahlberg AW, et al. Functional assessment with electrocardiographic gated single-photon emission computed tomography improves the ability of technetium-99m sestamibi myocardial perfusion imaging to predict myocardial viability in patients undergoing revascularization. *Am J Cardiol.*

- 1999;83:1-5.
394. Stollfuss JC, Haas F, Matsunari I, et al. 99mTc-tetrofosmin SPECT for prediction of functional recovery defined by MRI in patients with severe left ventricular dysfunction: additional value of gated SPECT. *J Nucl Med.* 1999;40:1824-31.
395. Bax JJ, Wijns W, Cornel JH, et al. Accuracy of currently available techniques for prediction of functional recovery after revascularization in patients with left ventricular dysfunction due to chronic coronary artery disease: comparison of pooled data. *J Am Coll Cardiol.* 1997;30:1451-60.
396. Di Carli MF, Davidson M, Little R, et al. Value of metabolic imaging with positron emission tomography for evaluating prognosis in patients with coronary artery disease and left ventricular dysfunction. *Am J Cardiol.* 1994;73:527-33.
397. Gibson RS, Watson DD, Taylor GJ, et al. Prospective assessment of regional myocardial perfusion before and after coronary revascularization surgery by quantitative thallium-201 scintigraphy. *J Am Coll Cardiol.* 1983;1:804-15.
398. Acampa W, Petretta M, Florimonte L, et al. Sestamibi SPECT in the detection of myocardial viability in patients with chronic ischemic left ventricular dysfunction: comparison between visual and quantitative analysis. *J Nucl Cardiol.* 2000;7:406-13.
399. Kim RJ, Wu E, Rafael A, et al. The use of contrast-enhanced magnetic resonance imaging to identify reversible myocardial dysfunction. *N Engl J Med.* 2000;343:1445-53.
400. Wu E, Judd RM, Vargas JD, et al. Visualisation of presence, location, and transmural extent of healed Q-wave and non-Q-wave myocardial infarction. *Lancet.* 2001;357:21-8.
401. Eagle KA, Guyton RA, Davidoff R, et al. ACC/AHA guidelines for coronary artery bypass graft surgery: a report of the American College of Cardiology/American Heart Association Task Force on Practice Guidelines (Committee to Revise the 1991 Guidelines for Coronary Artery Bypass Graft Surgery). *J Am Coll Cardiol.* 1999;34:1262-347.
402. Vasan RS, Larson MG, Benjamin EJ, et al. Congestive heart failure in subjects with normal versus reduced left ventricular ejection fraction: prevalence and mortality in a population-based cohort. *J Am Coll Cardiol.* 1999;33:1948-55.
403. Alexander J, Dainiak N, Berger HJ, et al. Serial assessment of doxorubicin cardiotoxicity with quantitative radionuclide angiography. *N Engl J Med.* 1979;300:278-83.
404. Palmeri ST, Bonow RO, Myers CE, et al. Prospective evaluation of doxorubicin cardiotoxicity by rest and exercise radionuclide angiography. *Am J Cardiol.* 1986;58:607-13.
405. Schwartz RG, McKenzie WB, Alexander J, et al. Congestive heart failure and left ventricular dysfunction complicating doxorubicin therapy: seven-year experience using serial radionuclide angiography. *Am J Med.* 1987;82:1109-18.
406. Schaadt B, Kelbaek H. Age and left ventricular ejection fraction identify patients with advanced breast cancer at high risk for development of epirubicin-induced heart failure. *J Nucl Cardiol.* 1997;4:494-501.
407. Feldman AM, Lorell BH, Reis SE. Trastuzumab in the treatment of metastatic breast cancer: anticancer therapy versus cardiotoxicity. *Circulation.* 2000;102:272-4.
408. Lopez M, Vici P, Di Lauro K, et al. Randomized prospective clinical trial of high-dose epirubicin and dexrazoxane in patients with advanced breast cancer and soft tissue sarcomas. *J Clin Oncol.* 1998;16:86-92.
409. Palmeri ST, Bonow RO, Myers CE, et al. Prospective evaluation of doxorubicin cardiotoxicity by rest and exercise radionuclide angiography. *Am J Cardiol.* 1985;58:607-613.AQ
410. Lekakis J, Nanas J, Prassopoulos V, et al. Natural evolution of antimyosin scan and cardiac function in patients with acute myocarditis. *Int J Cardiol.* 1995;52:53-8.
411. Agostini D, Babatasi G, Manrique A, et al. Impairment of cardiac neuronal function in acute myocarditis: iodine-123-MIBG scintigraphy study. *J Nucl Med.* 1998;39:1841-44.
412. Dec GW, Palacios I, Yasuda T, et al. Antimyosin antibody cardiac imaging: its role in the diagnosis of myocarditis. *J Am Coll Cardiol.* 1990;16:97-104.
413. Matsuura H, Palacios IF, Dec GW, et al. Intraventricular conduction abnormalities in patients with clinically suspected myocarditis are associated with myocardial necrosis. *Am Heart J.* 1994;127:1290-7.
414. Matsumori A, Yamada T, Sasayama S. Antimyosin antibody imaging in clinical myocarditis and cardiomyopathy: principle and application. *Int J Cardiol.* 1996;54:183-90.
415. Narula J, Khaw BA, Dec GW, et al. Diagnostic accuracy of antimyosin scintigraphy in suspected myocarditis. *J Nucl Cardiol.* 1996;3:371-81.
416. Narula J, Malhotra A, Yasuda T, et al. Usefulness of antimyosin antibody imaging for the detection of active rheumatic myocarditis. *Am J Cardiol.* 1999;84:946-50, A7.
417. Morguet AJ, Munz DL, Kreuzer H, et al. Scintigraphic detection of inflammatory heart disease. *Eur J Nucl Med.* 1994;21:666-74.
418. Kuhl U, Lauer B, Souvatzoglu M, et al. Antimyosin scintigraphy and immunohistologic analysis of endomyocardial biopsy in patients with clinically suspected myocarditis—evidence of myocardial cell damage and inflammation in the absence of histologic signs of myocarditis. *J Am Coll Cardiol.* 1998;32:1371-6.
419. Khaw BA, Narula J. Non-invasive detection of myocyte necrosis in myocarditis and dilated cardiomyopathy with radiolabelled antimyosin. *Eur Heart J.* 1995;16(suppl O):119-23.
420. Taillefer R. Detection of myocardial necrosis and inflammation by nuclear cardiac imaging. *Cardiol Clin.* 1994;12:289-302.
421. Eguchi M, Tsuchihashi K, Nakata T, et al. Right ventricular abnormalities assessed by myocardial single-photon emission computed tomography using technetium-99m sestamibi/tetrofosmin in right ventricle-originated ventricular tachyarrhythmias. *J Am Coll Cardiol.* 2000;36:1767-73.
422. Frist W, Yasuda T, Segall G, et al. Noninvasive detection of human cardiac transplant rejection with indium-111 antimyosin (Fab) imaging. *Circulation.* 1987;76:V81-5.
423. Hesse B, Mortensen SA, Folke M, et al. Ability of antimyosin scintigraphy monitoring to exclude acute rejection during the first year after heart transplantation. *J Heart Lung Transplant.* 1995;14:23-31.
424. Fang JC, Rocco T, Jarcho J, et al. Noninvasive assessment of transplant-associated arteriosclerosis. *Am Heart J.* 1998;135:980-7.
425. Carlsen J, Toft JC, Mortensen SA, et al. Myocardial perfusion scintigraphy as a screening method for significant coronary artery stenosis in cardiac transplant recipients. *J Heart Lung Transplant.* 2000;19:873-8.
426. Elhendy A, Sozzi FB, van Domburg RT, et al. Accuracy of dobutamine tetrofosmin myocardial perfusion imaging for the noninvasive diagnosis of transplant coronary artery stenosis. *J Heart Lung Transplant.* 2000;19:360-6.
427. Marin-Neto JA, Bromberg-Marin G, Pazin-Filho A, et al. Cardiac autonomic impairment and early myocardial damage involving the right ventricle are independent phenomena in Chagas' disease. *Int J Cardiol.* 1998;65:261-9.
428. Simoes MV, Pintya AO, Bromberg-Marin G, et al. Relation of

- regional sympathetic denervation and myocardial perfusion disturbance to wall motion impairment in Chagas' cardiomyopathy. *Am J Cardiol.* 2000;86:975-81.
429. Eguchi M, Tsuchihashi K, Hotta D, et al. Technetium-99m sestamibi/tetrofosmin myocardial perfusion scanning in cardiac and noncardiac sarcoidosis. *Cardiology.* 2000;94:193-9.
430. Tellier P, Paycha F, Antony I, et al. Reversibility by dipyridamole of thallium-201 myocardial scan defects in patients with sarcoidosis. *Am J Med.* 1988;85:189-93.
431. Mana J. Nuclear imaging: 67Gallium, 201thallium, 18F-labeled fluoro-2-deoxy-D-glucose positron emission tomography. *Clin Chest Med.* 1997;18:799-811.
432. Hongo M, Fujii T, Hirayama J, et al. Radionuclide angiographic assessment of left ventricular diastolic filling in amyloid heart disease: a study of patients with familial amyloid polyneuropathy. *J Am Coll Cardiol.* 1989;13:48-53.
433. Tanaka M, Hongo M, Kinoshita O, et al. Iodine-123 metaiodobenzylguanidine scintigraphic assessment of myocardial sympathetic innervation in patients with familial amyloid polyneuropathy. *J Am Coll Cardiol.* 1997;29:168-74.
434. McKenna WJ, Thiene G, Nava A, et al. Diagnosis of arrhythmogenic right ventricular dysplasia/cardiomyopathy. Task Force of the Working Group Myocardial and Pericardial Disease of the European Society of Cardiology and of the Scientific Council on Cardiomyopathies of the International Society and Federation of Cardiology. *Br Heart J.* 1994;71:215-8.
435. Le Guludec D, Gauthier H, Porcher R, et al. Prognostic value of radionuclide angiography in patients with right ventricular arrhythmias. *Circulation.* 2001;103:1972-6.
436. Pohost GM, Vignola PA, McKusick KE, et al. Hypertrophic cardiomyopathy. Evaluation by gated cardiac blood pool scanning. *Circulation.* 1977;55:92-9.
437. Bulkley BH, Rouleau J, Strauss HW, et al. Idiopathic hypertrophic subaortic stenosis: detection by thallium 201 myocardial perfusion imaging. *N Engl J Med.* 1975;293:1113-6.
438. Ito Y, Hasegawa S, Yamaguchi H, et al. Relation between thallium-201/iodine 123-BMIPP subtraction and fluorine 18 deoxyglucose polar maps in patients with hypertrophic cardiomyopathy. *J Nucl Cardiol.* 2000;7:16-22.
439. Yamada M, Elliott PM, Kaski JC, et al. Dipyridamole stress thallium-201 perfusion abnormalities in patients with hypertrophic cardiomyopathy: relationship to clinical presentation and outcome. *Eur Heart J.* 1998;19:500-7.
440. O'Gara PT, Bonow RO, Maron BJ, et al. Myocardial perfusion abnormalities in patients with hypertrophic cardiomyopathy: assessment with thallium-201 emission computed tomography. *Circulation.* 1987;76:1214-23.
441. Choudhury L, Rosen SD, Patel D, et al. Coronary vasodilator reserve in primary and secondary left ventricular hypertrophy: a study with positron emission tomography. *Eur Heart J.* 1997;18:108-16.
442. Houghton JL, Frank MJ, Carr AA, et al. Relations among impaired coronary flow reserve, left ventricular hypertrophy and thallium perfusion defects in hypertensive patients without obstructive coronary artery disease. *J Am Coll Cardiol.* 1990;15:43-51.
443. Houghton JL, Carr AA, Prisant LM, et al. Morphologic, hemodynamic and coronary perfusion characteristics in severe left ventricular hypertrophy secondary to systemic hypertension and evidence for nonatherosclerotic myocardial ischemia. *Am J Cardiol.* 1992;69:219-24.
444. Bonow RO, Rosing DR, Bacharach SL, et al. Effects of verapamil on left ventricular systolic function and diastolic filling in patients with hypertrophic cardiomyopathy. *Circulation.* 1981;64:787-96.
445. Udelson JE, Bonow RO, O'Gara PT, et al. Verapamil prevents silent myocardial perfusion abnormalities during exercise in asymptomatic patients with hypertrophic cardiomyopathy. *Circulation.* 1989;79:1052-60.
446. Li ST, Tack CJ, Fananapazir L, et al. Myocardial perfusion and sympathetic innervation in patients with hypertrophic cardiomyopathy. *J Am Coll Cardiol.* 2000;35:1867-73.
447. Dilsizian V, Bonow RO, Epstein SE, et al. Myocardial ischemia detected by thallium scintigraphy is frequently related to cardiac arrest and syncope in young patients with hypertrophic cardiomyopathy. *J Am Coll Cardiol.* 1993;22:796-804.
448. Merlet P, Valette H, Dubois-Rande JL, et al. Iodine 123-labeled metaiodobenzylguanidine imaging in heart disease. *J Nucl Cardiol.* 1994;1:S79-S85.
449. Cuocolo A, Sax FL, Brush JE, et al. Left ventricular hypertrophy and impaired diastolic filling in essential hypertension: diastolic mechanisms for systolic dysfunction during exercise. *Circulation.* 1990;81:978-86.
450. Vasan RS, Benjamin EJ, Levy D. Prevalence, clinical features and prognosis of diastolic heart failure: an epidemiologic perspective. *J Am Coll Cardiol.* 1995;26:1565-74.
451. Wasserman AG, Katz RJ, Varghese PJ, et al. Exercise radionuclide ventriculographic responses in hypertensive patients with chest pain. *N Engl J Med.* 1984;311:1276-80.
452. Brush JE Jr, Cannon RO III, Schenke WH, et al. Angina due to coronary microvascular disease in hypertensive patients without left ventricular hypertrophy. *N Engl J Med.* 1988;319:1302-7.
453. Houghton JL, Smith VE, Strogatz DS, et al. Effect of African-American race and hypertensive left ventricular hypertrophy on coronary vascular reactivity and endothelial function. *Hypertension.* 1997;29:706-14.
454. Kuwahara T, Hamada M, Hiwada K. Direct evidence of impaired cardiac sympathetic innervation in essential hypertensive patients with left ventricular hypertrophy. *J Nucl Med.* 1998;39:1486-91.
455. Schulman DS, Francis CK, Black HR, et al. Thallium-201 stress imaging in hypertensive patients. *Hypertension.* 1987;10:16-21.
456. Christian TF, Zinsmeister AR, Miller TD, et al. Left ventricular systolic response to exercise in patients with systemic hypertension without left ventricular hypertrophy. *Am J Cardiol.* 1990;65:1204-8.
457. Alshami AA, Jolly SR, Smith FL, et al. Exercise testing in patients with electrocardiographic evidence of left ventricular hypertrophy. *Clin Nucl Med.* 1994;19:904-9.
458. Vaduganathan P, He ZX, Mahmarian JJ, et al. Diagnostic accuracy of stress thallium-201 tomography in patients with left ventricular hypertrophy. *Am J Cardiol.* 1998;81:1205-7.
459. Otto CM, Kuusisto J, Reichenbach DD, et al. Characterization of the early lesion of 'degenerative' valvular aortic stenosis: histological and immunohistochemical studies. *Circulation.* 1994;90:844-53.
460. Vandeplass A, Willems JL, Piessens J, et al. Frequency of angina pectoris and coronary artery disease in severe isolated valvular aortic stenosis. *Am J Cardiol.* 1988;62:117-20.
461. Garcia-Rubira JC, Lopez V, Cubero J. Coronary arterial disease in patients with severe isolated aortic stenosis. *Int J Cardiol.* 1992;35:121-2.
462. Mullany CJ, Elveback LR, Frye RL, et al. Coronary artery disease and its management: influence on survival in patients undergoing aortic valve replacement. *J Am Coll Cardiol.* 1987;10:66-72.
463. Lund O, Nielsen TT, Pilegaard HK, et al. The influence of coro-

- nary artery disease and bypass grafting on early and late survival after valve replacement for aortic stenosis. *J Thorac Cardiovasc Surg.* 1990;100:327-37.
464. Czer LS, Gray RJ, Stewart ME, et al. Reduction in sudden late death by concomitant revascularization with aortic valve replacement. *J Thorac Cardiovasc Surg.* 1988;95:390-401.
465. Alexopoulos D, Kolovou G, Kyriakidis M, et al. Angina and coronary artery disease in patients with aortic valve disease. *Angiology.* 1993;44:707-11.
466. Green SJ, Pizzarello RA, Padmanabhan VT, et al. Relation of angina pectoris to coronary artery disease in aortic valve stenosis. *Am J Cardiol.* 1985;55:1063-5.
467. Patsilinaikos SP, Kranidis AI, Antonelis IP, et al. Detection of coronary artery disease in patients with severe aortic stenosis with noninvasive methods. *Angiology.* 1999;50:309-17.
468. Kupari M, Virtanen KS, Turto H, et al. Exclusion of coronary artery disease by exercise thallium-201 tomography in patients with aortic valve stenosis. *Am J Cardiol.* 1992;70:635-40.
469. Samuels B, Kiat H, Friedman JD, et al. Adenosine pharmacologic stress myocardial perfusion tomographic imaging in patients with significant aortic stenosis: diagnostic efficacy and comparison of clinical, hemodynamic and electrocardiographic variables with 100 age-matched control subjects. *J Am Coll Cardiol.* 1995; 25:99-106.
470. Kettunen R, Huikuri HV, Heikkila J, et al. Preoperative diagnosis of coronary artery disease in patients with valvular heart disease using technetium-99m isonitrile tomographic imaging together with high-dose dipyridamole and handgrip exercise. *Am J Cardiol.* 1992;69:1442-5.
471. Rask LP, Karp KH, Eriksson NP, et al. Dipyridamole thallium-201 single-photon emission tomography in aortic stenosis: gender differences. *Eur J Nucl Med.* 1995;22:1155-62.
472. Borer JS, Bacharach SL, Green MV, et al. Exercise-induced left ventricular dysfunction in symptomatic and asymptomatic patients with aortic regurgitation: assessment by radionuclide cineangiography. *Am J Cardiol.* 1979;42:351-7.
473. Dehmer GJ, Firth BG, Hillis LD, et al. Alterations in left ventricular volumes and ejection fraction at rest and during exercise in patients with aortic regurgitation. *Am J Cardiol.* 1981;48:17-27.
474. Bonow RO, Lakatos E, Maron BJ, et al. Serial long-term assessment of the natural history of asymptomatic patients with chronic aortic regurgitation and normal left ventricular systolic function. *Circulation.* 1991;84:1625-35.
475. Henry WL, Bonow RO, Borer JS, et al. Observations on the optimum time for operative intervention for aortic regurgitation, I: evaluation of the results of aortic valve replacement in symptomatic patients. *Circulation.* 1980;61:471-83.
476. Hochreiter C, Niles N, Devereux RB, et al. Mitral regurgitation: relationship of noninvasive descriptors of right and left ventricular performance to clinical and hemodynamic findings and to prognosis in medically and surgically treated patients. *Circulation.* 1986;73:900-12.
477. Schuler G, Peterson KL, Johnson A, et al. Temporal response of left ventricular performance to mitral valve surgery. *Circulation.* 1979;59:1218-31.
478. Enriquez-Sarano M, Tajik AJ, Schaff HV, et al. Echocardiographic prediction of survival after surgical correction of organic mitral regurgitation. *Circulation.* 1994;90:830-7.
479. Zile MR, Gaasch WH, Carroll JD, et al. Chronic mitral regurgitation: predictive value of preoperative echocardiographic indexes of left ventricular function and wall stress. *J Am Coll Cardiol.* 1984;3:235-42.
480. Wisenbaugh T, Skudicky D, Sareli P. Prediction of outcome after valve replacement for rheumatic mitral regurgitation in the era of chordal preservation. *Circulation.* 1994;89:191-7.
481. Malcic I, Senecic I, Tezak S, et al. Radioangioscintigraphy and Doppler echocardiography in the quantification of left-to-right shunt. *Pediatr Cardiol.* 2000;21:240-3.
482. Treves S. Detection and quantitation of cardiovascular shunts with commonly available radionuclides. *Semin Nucl Med.* 1980;10:16-26.
483. Pruckmayer M, Zacherl S, Salzer-Muhar U, et al. Scintigraphic assessment of pulmonary and whole-body blood flow patterns after surgical intervention in congenital heart disease. *J Nucl Med.* 1999;40:1477-83.
484. Blumgart HL, Yens OC. Velocity of blood flow, I: the method utilized. *J Clin Invest.* 1926;4:1-13.
485. American Society of Nuclear Cardiology. Updated imaging guidelines for nuclear cardiology procedures, part 1. *J Nucl Cardiol.* 2001;8:G5-G58.
486. American Society of Nuclear Cardiology. Imaging guidelines for nuclear cardiology procedures, part 2. *J Nucl Cardiol.* 1999;6: G47-G84.
487. American Society of Nuclear Cardiology. Imaging guidelines for nuclear cardiology procedures: instrumentation quality assurance and performance. *J Nucl Cardiol.* 1996;3:G5-G10.
488. American Society of Nuclear Cardiology. Imaging guidelines for nuclear cardiology procedures: equilibrium gated blood pool imaging protocols. *J Nucl Cardiol.* 1996;3:G26-G29.
489. American Society of Nuclear Cardiology. Imaging guidelines for nuclear cardiology procedures: myocardial perfusion planar protocols. *J Nucl Cardiol.* 1996;3:G30-G34.
490. American Society of Nuclear Cardiology. Imaging guidelines for nuclear cardiology procedures. First-pass radionuclide angiography (FPRNA). *J Nucl Cardiol.* 1996;3:G16-G25.
491. American Society of Nuclear Cardiology. Imaging guidelines for nuclear cardiology procedures. Myocardial perfusion stress protocols. *J Nucl Cardiol.* 1996;3:G11-G15.
492. Cramer MJ, Verzijlbergen JF, van der Wall EE, et al. Comparison of adenosine and high-dose dipyridamole both combined with low-level exercise stress for 99Tcm-MIBI SPET myocardial perfusion imaging. *Nucl Med Commun.* 1996;17:97-104.
493. Esquerre JP, Coca FJ, Martinez SJ, et al. Prone decubitus: a solution to inferior wall attenuation in thallium-201 myocardial tomography. *J Nucl Med.* 1989;30:398-401.
494. Segall GM, Davis MJ. Prone versus supine thallium myocardial SPECT: a method to decrease artifactual inferior wall defects. *J Nucl Med.* 1989;30:548-55.
- 494a. Cerqueira MD, Weissman, NJ, Dilsizian V, et al. Standardized myocardial segmentation and nomenclature for tomographic imaging of the heart: a statement for healthcare professionals from the Cardiac Imaging Committee of the Council on Clinical Cardiology of the American Heart Association. *Circulation.* 2002;105:539-42.
495. Esquivel L, Pollock SG, Beller GA, et al. Effect of the degree of effort on the sensitivity of the exercise thallium-201 stress test in symptomatic coronary artery disease. *Am J Cardiol.* 1989;63:160-5.
496. Pennell DJ, Underwood SR, Swanton RH, et al. Dobutamine thallium myocardial perfusion tomography. *J Am Coll Cardiol.* 1991; 18:1471-9.
497. Mertes H, Sawada SG, Ryan T, et al. Symptoms, adverse effects, and complications associated with dobutamine stress echocardiography: experience in 1118 patients. *Circulation.* 1993;88:15-9.

498. Hiro J, Hiro T, Reid CL, et al. Safety and results of dobutamine stress echocardiography in women versus men and in patients older and younger than 75 years of age. *Am J Cardiol.* 1997;80:1014-20.
499. Steele P, Sklar J, Kirch D, et al. Thallium-201 myocardial imaging during maximal and submaximal exercise: comparison of submaximal exercise with propranolol. *Am Heart J.* 1983;106:1353-7.
500. Hockings B, Saltissi S, Croft DN, et al. Effect of beta adrenergic blockade on thallium-201 myocardial perfusion imaging. *Br Heart J.* 1983;49:83-9.
501. Martin GJ, Henkin RE, Scanlon PJ. Beta blockers and the sensitivity of the thallium treadmill test. *Chest.* 1987;92:486-7.
502. Zacca NM, Verani MS, Chahine RA, et al. Effect of nifedipine on exercise-induced left ventricular dysfunction and myocardial hypoperfusion in stable angina. *Am J Cardiol.* 1982;50:689-95.
503. Aoki M, Sakai K, Koyanagi S, et al. Effect of nitroglycerin on coronary collateral function during exercise evaluated by quantitative analysis of thallium-201 single photon emission computed tomography. *Am Heart J.* 1991;121:1361-6.
504. Goller V, Clausen M, Henze E, et al. Reduction of exercise-induced myocardial perfusion defects by isosorbide-5-nitrate: assessment using quantitative Tc-99m-MIBI-SPECT. *Coron Artery Dis.* 1995;6:245-9.
505. Vanzetto G, Glover DK, Ruiz M, et al. 99mTc-N-NOET myocardial uptake reflects myocardial blood flow and not viability in dogs with reperfused acute myocardial infarction. *Circulation.* 2000;101:2424-30.
506. Williams KA, Taillon LA. Gated planar technetium 99m-labeled sestamibi myocardial perfusion image inversion for quantitative scintigraphic assessment of left ventricular function. *J Nucl Cardiol.* 1995;2:285-95.
507. Boonyaprapa S, Ekmahachai M, Thanachaikun N, et al. Measurement of left ventricular ejection fraction from gated technetium-99m sestamibi myocardial images. *Eur J Nucl Med.* 1995;22:528-31.
508. DePuey EG, Nichols K, Dobrinsky C. Left ventricular ejection fraction assessed from gated technetium-99m-sestamibi SPECT. *J Nucl Med.* 1993;34:1871-6.
509. Williams KA, Taillon LA. Left ventricular function in patients with coronary artery disease assessed by gated tomographic myocardial perfusion images: comparison with assessment by contrast ventriculography and first-pass radionuclide angiography. *J Am Coll Cardiol.* 1996;27:173-81.
510. Germano G, Erel J, Kiat H, et al. Quantitative LVEF and qualitative regional function from gated thallium-201 perfusion SPECT. *J Nucl Med.* 1997;38:749-54.
511. Smith WH, Kastner RJ, Calnon DA, et al. Quantitative gated single photon emission computed tomography imaging: a counts-based method for display and measurement of regional and global ventricular systolic function. *J Nucl Cardiol.* 1997;4:451-63.
512. Arheden H, Holmqvist C, Thilen U, et al. Left-to-right cardiac shunts: comparison of measurements obtained with MR velocity mapping and with radionuclide angiography. *Radiology.* 1999;211:453-8.
513. Iskandrian AE, Germano G, VanDecker W, et al. Validation of left ventricular volume measurements by gated SPECT 99mTc-labeled sestamibi imaging. *J Nucl Cardiol.* 1998;5:574-8.
514. Johnson LL, Lawson MA, Blackwell GG, et al. Optimizing the method to calculate right ventricular ejection fraction from first-pass data acquired with a multicrystal camera. *J Nucl Cardiol.* 1995;2:372-9.
515. Massardo T, Gal RA, Grenier RP, et al. Left ventricular volume calculation using a count-based ratio method applied to multigated radionuclide angiography. *J Nucl Med.* 1990;31:450-6.
516. Williams KA, Bryant TA, Taillon LA. First-pass radionuclide angiographic analysis with two regions of interest to improve left ventricular ejection fraction accuracy. *J Nucl Med.* 1998;39:1857-61.
517. Nichols K, Dorbala S, DePuey EG, et al. Influence of arrhythmias on gated SPECT myocardial perfusion and function quantification. *J Nucl Med.* 1999;40:924-34.
518. Hyun IY, Kwan J, Park KS, et al. Reproducibility of Tl-201 and Tc-99m sestamibi gated myocardial perfusion SPECT measurement of myocardial function. *J Nucl Cardiol.* 2001;8:182-7.
519. Maunoury C, Chen CC, Chua KB, et al. Quantification of left ven-